Improving Mean-Field Theory for Bosons in Optical Lattices via Degenerate Perturbation Theory

Diplomarbeit in Biophysik

durchgeführt von

Martin Kübler

am Fachbereich Physik der TU Kaiserslautern

unter Anleitung von

Prof. Dr. Sebastian Eggert

September 2016

Zusammenfassung

Das Ziel dieser Diplomarbeit besteht darin, den Quantenphasenübergang zwischen dem Mott-Isolator und der superfluiden Phase eines homogenen Bose-Gases im optischen Gitter zu beschreiben. In bisherigen Arbeiten wurde dafür die Rayleigh-Schrödinger Störungstheorie verwendet, die allerdings teilweise unphysikalische Ergebnisse liefert, da die Entartung zwischen zwei benachbarten Mott-Bereichen nicht berücksichtigt wird. Deshalb wird in dieser Arbeit die Brillouin-Wigner Störungstheorie angewandt, die formal zwischen der nicht-entarteten und der entarteten Störungstheorie interpoliert.

Um analytisch rechnen zu können, wird die Molekularfeld-Näherung eingeführt. Es werden detaillierte Rechnungen präsentiert, wie die Brillouin-Wigner-Theorie anzuwenden ist, genauso wie ein graphischer Ansatz, der es erlaubt, die jeweiligen analytischen Terme effizient zu erfassen. Um die Gültigkeit der Berechnungen zu beweisen, werden die Ergebnisse mit anderen Arbeiten verglichen.

Neben dem analytischen Berechnen der Phasengrenze zwischen dem Mott-Isolator und der superfluiden Phase wird noch die Kondensatdichte berechnet. Dies wird durch simultanes Lösen von zwei algebraischen Gleichungen erreicht. Die analytischen und numerischen Ergebnisse sind physikalisch sinnvoll und können einen Bereich der Systemparameter abdecken, der bisher noch unzugänglich war.

Unsere Ergebnisse sind insbesondere von Interesse, wenn eine harmonische Falle zu den bisherigen Rechnungen im homogenen System hinzugefügt wird, wie sie im Experiment vorliegt. Daher stellt die Diplomarbeit eine essentielle Vorbereitung dar, um die experimentell beobachtete Hochzeitstorten-Struktur der Teilchendichte zu bestimmen.

Abstract

The objective of this diploma thesis is the theoretical description of the Mott-insulator to superfluid quantum phase transition of a homogeneous Bose gas in an optical lattice. In former works, the Rayleigh-Schrödinger perturbation theory was used, which yields partially unphysical results, since the degeneracy of two adjacent Mott lobes is not taken into account. Therefore, in this work the Brillouin-Wigner perturbation theory is applied, which formally interpolates between non-degenerate and degenerate perturbation theory.
In order to perform the analytic calculations, the mean-field approximation is introduced. Detailed calculations of how to apply the Brillouin-Wigner theory are presented including a graphical approach which allows to efficiently keep track of the respective analytic terms. To prove the validity of this computation, the results are compared with other works.
Besides of the analytic calculation of the phase boundary from the Mott-insulator to the superfluid phase, the condensate density is determined. This is done by simultaneously solving two algebraic equations. The analytical and numerical results turn out to be physically meaningful and can cover a region of system parameters, which was inaccessible up to now.
Our results are of particular interest provided a harmonic trap is added to the former calculations in a homogeneous system, in view of describing an experiment. Thus, the diploma thesis represents an essential preparatory work for determining the experimentally observed wedding-cake structure of the particle density.

Contents

1 Introduction

Since the very beginning of quantum mechanics at the start of the 20^{th} century, scientists all over the world have worked on this topic to refine this theory. And although many inventions like the laser could be explained with the help of quantum mechanics, still many phenomena remain challenging in the theoretical description, like the macroscopic quantum phenomena of Bose-Einstein condensation, quantum Hall effect or high temperature superconductivity. Therefore, as modern physics of the 21^{st} century has, equally in experiment and theory, a strong focus on these macroscopic quantum phenomena, their application is of great interest, so they all need a microscopic quantum theory to be explained and understood to their full extent.
But every major theory needs to predict experimental results over a large range of system parameters, whose obtainments are often a challenging task due to the unattainability of many of them. For instance, you cannot just turn a knob to change the interatomic spacing in your superconductor. Therefore, a new simulation system is sought after, which yields just the same physical behaviour as the original system, but this time with parameters that are easier to tune. Some examples for such simulation systems are trapped ions, photonic systems or ultracold quantum gases [1], while the latter one can be realized by fermions, bosons or different fractional mixtures of both. Besides of the confining trap, an optical lattice can be added with different lattice geometries, or even external driving. And it's particularly these three features that endow the ultracold quantum gases with such astounding properties, which all find their counterparts in solid-state physics. The confining trap represents the macroscopic dimension of a crystal, while the optical lattice reproduces the crystal lattice with all the properties like unit cell spacing or interaction strength. Finally, impurities in the crystal can be modelled by mixing atoms from another species into an ultracold quantum gas.
For bosons, it is possible to cool down the ultracold quantum gas under a certain critical temperature, and obtain a Bose-Einstein condensate, i.e. a macroscopically occupied ground state. This gives rise to a versatility of applications, since a Bose-Einstein condensate is much more dense than the thermal dilute ultracold quantum gases.
In this work, we focus on a purely bosonic Bose-Einstein condensate in an optical lattice, which is predestined to serve as a simulation system for superconductors. In this sense, the bosons correspond to the bosonic Cooper pairs and the optical lattice corresponds to the crystalline structure. A special focus is put on the quantum phase transition of the Bose-Einstein condensate from the Mott-insulator to the superfluid phase, which simulates the transition from an isolating material to a superconductor.
Thus, the guiding idea of this diploma thesis is the theoretical description of this quantum simulator in the sense of Feynman's words: "Nature isn't classical, dammit, and if you want to make a simulation of nature, you'd better make it quantum mechanical, and by golly it's a wonderful problem, because it doesn't look so easy." [2].

1.1 Bose-Einstein Condensate

A Bose-Einstein condensate is a state of matter at very low temperature close to zero, so that thermal effects can be neglected and quantum effects become dominant. The particles forming the Bose-Einstein condensate enter on a large scale the lowest quantum state. Therefore, the quantum behaviour of atoms, molecules or even photons [3] can be directly observed and measured, which is at least very difficult in other states of matter and thus makes Bose-Einstein condensates the perfect testing ground for almost all of quantum physics. For the better understanding of this, we take a look at the thermal de Broglie wavelength

$$\lambda_{\mathrm{th}} = \frac{h}{\sqrt{2\pi m k_{\mathrm{B}} T}}\,, \tag{1.1}$$

with $h \approx 6.63 \times 10^{-34}\,\mathrm{Js}$ the Planck constant, m the mass of the condensing particle, $k_{\mathrm{B}} \approx 1.38 \times 10^{-23}\,\mathrm{J/K}$ the Boltzmann constant, and T the temperature. For high temperature, λ_{th} becomes very small and therefore particles can be approximated as point sized objects. This picture breaks down the lower the temperature gets, as the de Broglie wavelength λ_{th} increases. At some point, λ_{th} is larger than the interatomic spacing, and therefore the particle waves start to overlap. This is when Bose-Einstein condensation begins. This actual situation is represented in FIG. 1.1.

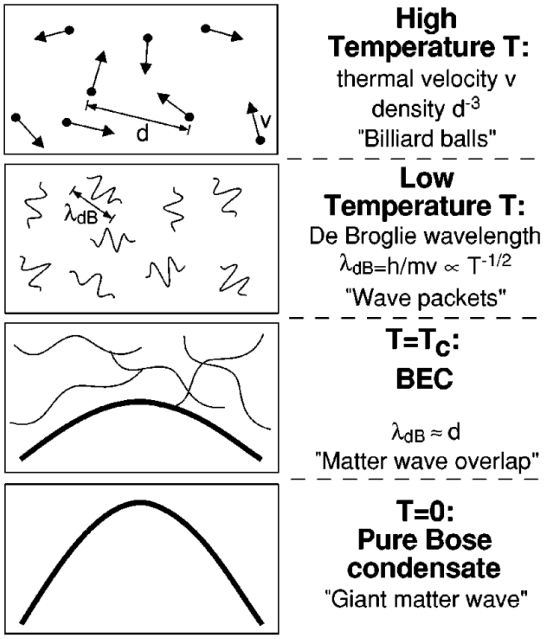

FIG. 1.1: Schematic illustration of atoms during cooling process down to Bose-Einstein condensation [4].

The first theoretical prediction of the existence of a Bose-Einstein condensate was done by Albert Einstein in 1925 [5], who extended the bosonic statistics for massless bosons like photons found by Satyendra Nath Bose to matter [6]. Already back then, Einstein supposed a close connection between Bose-Einstein condensation and superconductivity [5]. After this, it took 70 years up to 1995 until the first experimental realization of a Bose-Einstein condensate by Eric Allin Cornell with Carl Edwin Wieman [7] and Wolfgang Ketterle [8]. While Cornell and Wieman produced a Bose-Einstein condensate of $\sim 2 \times 10^3$ atoms of rubidium-87, Ketterle generated a Bose-Einstein condensate of $\sim 5 \times 10^5$ atoms of sodium-23.

The main barrier, which rendered any previous attempt futile, was to achieve the needed temperature of several nano Kelvin for the Bose-Einstein condensation to happen at all. The key technology utterly required for this and any other ultracold experiment is the laser cooling, which was mainly developed by Steven Chu [9], Claude Cohen-Tannoudji, and William Daniel Phillips [10].

Without going into details, the rough idea of laser cooling is to use a near resonant laser, which only interacts with the atoms when they move in the opposite direction of the wave vector of photons emitted by a laser, which results in the atom being slowed down by the light. The thereby absorbed energy is emitted randomly over space and therefore cannot sum up to a

directional, transversal acceleration. Although there are recent results by Florian Schreck of achieving Bose-Einstein condensation just by laser cooling [11], in most experiments not only laser cooling is used. A second cooling is applied afterwards, namely evaporative cooling. This cooling mechanism exploits the facts that the heat distribution of the atoms in a sample follows the Maxwell–Boltzmann distribution, Thus, taking away the hottest atoms causes the rest of the sample to rearrange again accordingly to the Maxwell–Boltzmann distribution, resulting in effectively lowering the temperature of the sample. Of course, this evaporative cooling mechanism yields a loss of particles, which is one of the main reasons why Bose-Einstein condensates of large particle numbers are very difficult to obtain. Once the critical temperature of few nano Kelvins is reached, the ultracold atoms collapse to a Bose-Einstein condensate.
An intuitive approach for the critical temperature takes the de Broglie wavelength to be of the order of the interatomic spacing

$$\lambda_{\mathrm{th}} \approx n^{-\frac{1}{3}}\,, \tag{1.2}$$

which is depicted in FIG. 1.1 and is one necessary condition for Bose-Einstein condensation. Formula (1.2) inserted in (1.1) yields

$$T \approx \frac{h^2 n^{\frac{2}{3}}}{2\pi m k_{\mathrm{B}}}\,. \tag{1.3}$$

This formula gives already the right qualitative behaviour with $T \sim n^{\frac{2}{3}}$, but the quantitative coefficients are not yet sufficient. The exact value of the critical temperature T_{c} for the phase transition to a Bose-Einstein condensate can be calculated for a homogeneous Bose gas via [12]

$$T_{\mathrm{c}} = \frac{2\pi\hbar^2}{m k_{\mathrm{B}}} \left[\frac{n}{\zeta\left(\frac{3}{2}\right)}\right]^{\frac{2}{3}}\,, \tag{1.4}$$

with $\hbar \approx 1.05 \times 10^{-34}\,\mathrm{Js}$ the reduced Planck constant, n the particle density, and $\zeta\left(\frac{3}{2}\right) \approx 2.61$ the Riemann zeta function. The critical temperature T_{c} rises with increasing the particle density n, therefore high particle densities are eligible but hard to achieve due to the evaporative cooling. In order to get some quantitative idea of the accuracy of the formula, we set in the values of the group of Wolfgang Ketterle [8]. The mass of the sodium-23 atom is $m_{\mathrm{Na}} = 3.82 \times 10^{-26}\,\mathrm{kg}$, the used density is $n_{\mathrm{Na}} = 10^{20}\,\mathrm{m}^{-3}$, which yields after (1.4) as $T_{\mathrm{c,Na}} = 1.51 \times 10^{-6}\,\mathrm{K}$. The measured critical temperature 2 μK is close to this predicted value.

1.2 Optical Lattices

An optical lattice is made out of counter-propagating laser beams, forming a standing wave. This is either achieved by two lasers pointing at each other or one laser being reflected at a mirror.

The laser beams of such an optical lattice induce electric dipole moments in the particles, and the resulting force pushes them back to the well or the top, depending of the detuning, much like in optical tweezers [13], see FIG. 1.2..

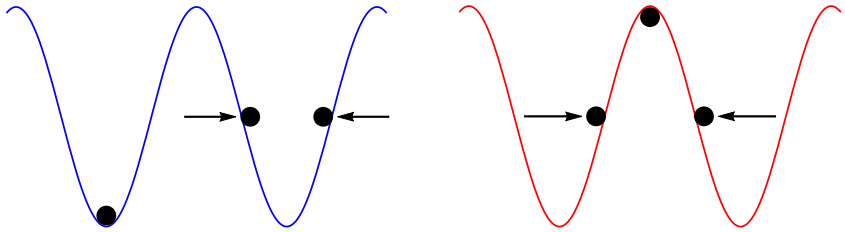

FIG. 1.2: The blue detuned laser (a) locks the particles at the wells, therefore the first particle from the left feels no force from the lasers. The red detuned laser (b) locks the particles at the top, the force from the laser on the particle pushes them in the opposite direction, compared with the blue detuned laser. The arrows point in the direction of the force on the particles by the laser beams.

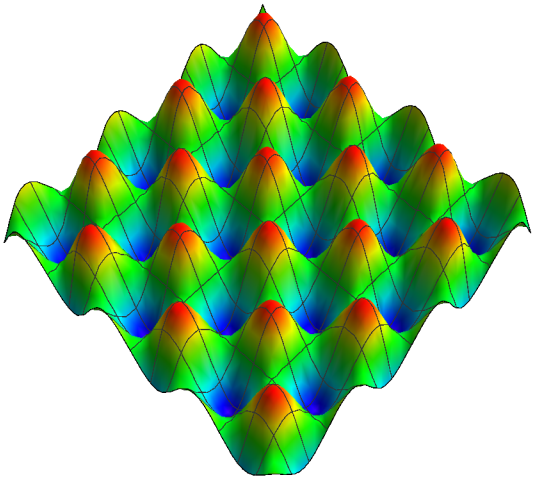

FIG. 1.3: A two-dimensional optical lattice. The particles are locked either in the red tops or in the blue wells.

This idea can now be expanded to two and three dimensions, resulting in a planar (see FIG. 1.3) or a cubic optical lattice. Therefore, many other lattice geometries can be designed, each one with unique characteristics. Some of them are shown in FIG. 1.4. Sketch (a) is the cubic lattice in three dimensions, where the particles can move in all directions with the same probability, thus the Hamiltonian of this system has a kinetic term which is spatial isotropic. This reduces the complexity a lot. In sketch (b) a linear, quasi-one dimensional lattice, the particles can move only in two directions.
The lattices in pictures (c) and (d) are two-dimensional lattices, where the first one is a triangular lattice, while the latter one represents a Kagome lattice. In these two-dimensional lattices, the kinetic terms are more difficult to handle. Therefore, their experimental realization is much more difficult than of a cubic lattice, but was nevertheless done in the recent years. The triangular

lattice was realized by the group of Klaus Sengstock [14], while the Kagome lattice was done by the group of Dan M. Stamper-Kurn [15].
Note that these lattices can be found in real solid-state systems, like sodium chloride crystals (a), carbon nano tubes (b), magnesium crystals (c), and herbertsmithite (d).

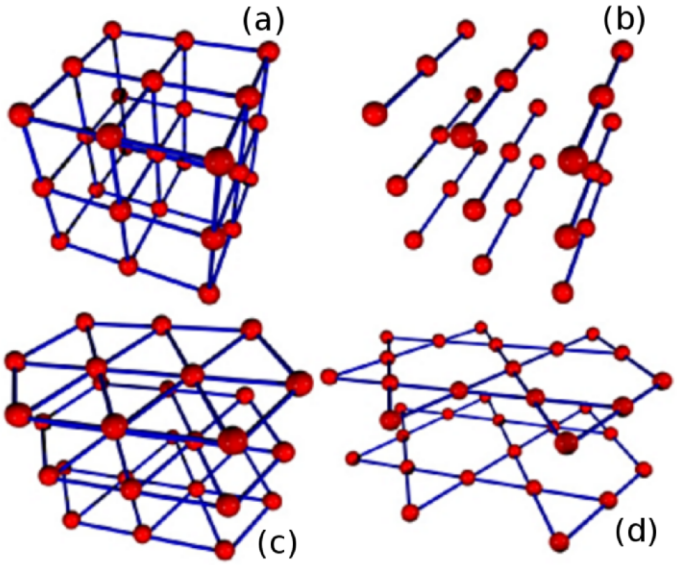

FIG. 1.4: Different optical lattices, the red dots mark the position of the particles [16].

Because the particles in an optical lattice are at defined positions with fixed distances between each other, they yield a physical behaviour very similar to crystals or other condensed matter systems, which allows to transfer many results achieved in optical lattices to condensed matter physics. Changing a parameter like the distance between two lattice sites is quite easy, since all the laser settings are tunable, whereas changing these parameters in a crystal happens to be much more difficult. Therefore, optical lattices grant great support for almost all condensed matter problems. But there are some important differences between optical lattices and real solid-state systems, for instance there are no phonons in optical lattices.

1.3 Phase Transitions

A phase transition represents a thermodynamic phenomenon, which causes a material to change its phase. To trigger this changing, a state variable has to go beyond a specific, critical value. For example, the material water evaporates if the state variable temperature passes the critical value of 373.15 K. According to the Ehrenfest classification [17], the entire diversity of phase transitions can be categorized by the number of derivatives of the free energy which reveals the first discontinuity.
A first-order phase transition appears if the first derivatives of the free energy are discontinuous. This process requires a latent heat, therefore energy is absorbed by the material just to make the phase transition happen, without changing its actual temperature. These first-order phase transitions are widely spread in nature, like water will absorb the heat of vaporization of 40.8 kJ/mol while evaporation. This energy does not change the inner energy of the system, but

increases the entropy, i. e. the disorder.
If all first derivatives of the free energy are continuous, but one of the second derivatives is discontinuous, a second-order phase transition takes place. They are also called continuous phase transitions. There are many examples of second-order phase transitions, like the ferromagnetic transition or the superconducting transition. Even the system we work with in this thesis, namely bosons in an optical lattice show a second-order phase transition, namely from the Mott insulator to the superfluid phase. The Bose-Einstein condensate exists only in the superfluid phase, which is characterized by zero viscosity and thence high mobility of the particles. Furthermore, the spatial uncertainty is large, while the momentum uncertainty is small, just as explained in FIG. 1.5. For the Mott insulator it is the opposite way, since the particles are locked down at the respective lattice sites. Thus, the space uncertainty is small, while the momentum uncertainty is big.

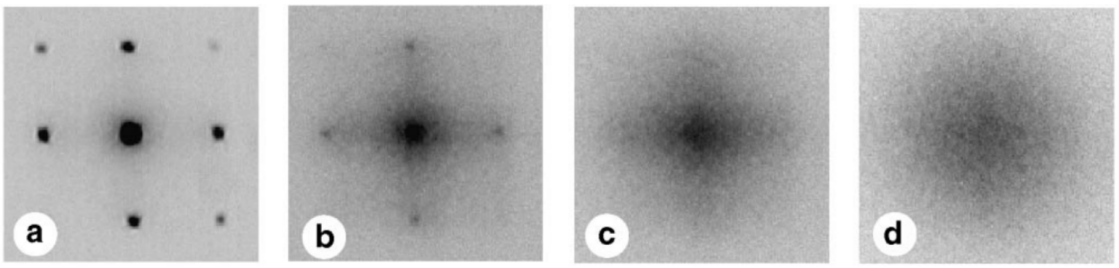

FIG. 1.5: Time-of-flight pictures from [18]. Since these are pictures of momentum space, the momentum uncertainty increases from (a) to (d). According to Heisenberg's uncertainty principle [19], the state in (a) is uncertain in space, and therefore has to be the superfluid phase. The state in (d) is obviously in a localized phase, which is called the Mott insulator.

But since the Bose gas is at $T = 0$, we cannot have a classical, thermally driven phase transition [20, 21]. Therefore, this is a second-order quantum phase transition [22], which happens not due to varying the temperature, but due to varying the depth of the wells. In our case, the amplitude of the laser is changed to make this quantum phase transition happen. A Bose gas in a deep optical lattice is localized at the lattice sites, which is a state called Mott insulator. By tuning the lasers in such a way that the lattice sites become more shallow, the probability for the particles to hop from one site to a neighbouring one increases. At some point, the Bose gas will undergo a phase transition of second order [23] from the Mott insulating Bose gas to a Bose-Einstein condensate in the superfluid phase, which can be detected by tilting the lattice: if the particles stay in the lattice sites, it is in the Mott insulator phase, if it flows according to the tilt, then it is in the superfluid phase.
This thesis focuses on this quantum phase transition between Mott insulator and superfluid, which bears many physical properties with superconductors. At a critical temperature, superconductors undergo a phase transition of second order from their normal phase to the superconducting phase by their electrons forming bosonic Cooper pairs which can move without friction. This is analogous to the Bose gas in the Mott insulator phase losing its friction when becoming a superfluid Bose-Einstein condensate at a critical lattice site depth.

1.4 Outline of Thesis

The diploma thesis proceeds from here on according to the following steps.

Chapter 2: Theoretical Basis
In chapter 2 we introduce the theoretical basis which is needed for elaborating the further thesis. First we discuss the one-band Bose-Hubbard model, which describes bosons in an optical lattice at zero temperature. With the Landau theory we introduce the condensate density $\Psi^*\Psi$, where Ψ^*, Ψ denote the order parameter. In order to treat the Hamiltonian analytically, we simplify the Bose-Hubbard model by applying the mean-field approximation, which means we neglect quantum fluctuations. This makes the kinetic term directly proportional to the order parameter Ψ^*, Ψ, which is supposedly small in the vicinity of the phase boundary and can therefore be treated perturbatively. Afterwards we follow the literature and apply the Rayleigh-Schrödinger perturbation theory in order to determine both the phase boundary and the order parameter. Although we obtain the correct mean-field phase boundary, an energetic degeneracy between every two neighbouring lobes does occur. Therefore, the order parameter turns out to be incorrect in the vicinity of this degeneracy, which warrants another improved approach.

Chapter 3: Perturbation Theory
In chapter 3 the Brillouin-Wigner perturbation theory is derived in detail. In order to handle the infinite Hilbert space, we split it into two subspaces, one being finite and the other one being infinite. Eliminating the infinitely large subspace leads to an effective Hamiltonian, which describes our system with the finite subspace and takes with every perturbative order more and more of the infinite subspace into account. This effective Hamiltonian can describe a finite subsystem containing just one state, but we can also expand this to two states by arranging the effective Hamiltonian as elements of a 2×2-matrix. In this way we show that Brillouin-Wigner perturbation theory contains both the non-degenerate perturbation theory of Rayleigh-Schrödinger as well as the degenerate perturbation theory as special cases.

Chapter 4: Approximative Solutions
In chapter 4 we apply the Brillouin-Wigner theory to the Bose-Hubbard mean-field theory, which allows us to reproduce some well-established results from other works and therefore proof the validity of our calculations. First, we linearize our two-state approach to reproduce the results from Ref. [24], which yields a proper order parameter, but not a valid phase boundary. While in a second calculation we transform our one-state approach into a fourth-order Rayleigh-Schrödinger perturbation theory to reproduce the results from Ref. [23], which gives a good phase boundary but an unphysical order parameter.

Chapter 5: Graphical Approach
In chapter 5 we introduce a graphical approach, which allows to systematically keep track of the lengthy analytic calculations in terms of simple graphs. With this graphical approach we are able to write down all formulas of the Brillouin-Wigner perturbation theory up to the eighth perturbative order.

Chapter 6: Mean-Field Phase Boundary
In chapter 6 we calculate the correct mean-field phase boundary within our Brillouin-Wigner approach. We show that it is sufficient for this to go up to second order in the Brillouin-Wigner

perturbation theory with respect to the kinetic term. Higher order terms turn out to not contribute to the mean-field phase boundary.

Chapter 7: Order Parameter

In chapter 7 we perform calculations within the Brillouin-Wigner theory to determine the condensate density $n_0 = \Psi^*\Psi$. We start with presenting some basic considerations, which are necessary in order to calculate the order parameter out of the Brillouin-Wigner perturbation theory. Based on this, we calculate the order parameter both from the one-state approach and from the two-state approach, where the latter two-state approach turns out to be superior. By choosing these two states as two neighbouring Mott-lobes, we can include the degeneracy correctly.

Chapter 8: Conclusion and Outlook

In chapter 8 we sum up the previous chapters and the obtained results. As an outlook we suggest to extend our results via Thomas-Fermi approximation in order to include a harmonic trapping potential. This would allow to calculate the experimentally observed wedding-cake structure for the particle density. Furthermore, we state that our results can be improved by systematically expanding the mean-field theory to a full Landau theory.

2 Theoretical Basis

In this chapter we describe the theoretical basis needed for the further calculations in this work. First we present the Bose-Hubbard model to describe bosons in an optical lattice. Then we use the Landau theory to introduce the order parameter for the condensate density $\Psi^*\Psi$. Afterwards, we apply the mean-field theory to get an approximate formula, which can be treated analytically. The analytical treatment is actually done by perturbation theory, which is described in the last section. There we get formulas for the phase boundary and the order parameter, where the latter turns out to be physically incorrect and thus we need another approach.

2.1 Bose-Hubbard Model

The Bose-Hubbard model, first published in 1963 by H. A. Gersch and G. C. Knollman [25], is a bosons adapted version of the Hubbard model, which was published by J. Hubbard earlier in 1963 [26]. The most noticeable difference is that the Bose-Hubbard model describes bosons instead of the fermionic electrons in the Hubbard model. Two main assumptions are made for the Bose-Hubbard model. The first one is that the temperature is so low, that it is sufficient to take into account only the lowest energy band. The second assumption is to neglect any long-range interaction and long-range hopping. Since we do our calculation at $T = 0$, these assumptions are justified. The Hamilton operator for the Bose-Hubbard model reads

$$\hat{H} = \frac{1}{2}U \sum_i \hat{a}_i^\dagger \hat{a}_i^\dagger \hat{a}_i \hat{a}_i - J \sum_{\langle i,j \rangle} \hat{a}_i^\dagger \hat{a}_j - \mu \sum_i \hat{a}_i^\dagger \hat{a}_i \,, \tag{2.1}$$

with U scaling the on-site interaction for $U > 0$ repulsive and $U < 0$ attractive, whereas $\hat{a}_i^\dagger$ and $\hat{a}_i$ are the bosonic creation and annihilation operators at site i with the canonical commutation relations

$$\begin{aligned} \left[\hat{a}_i, \hat{a}_j^\dagger\right]_- &= \delta_{i,j} \,, \\ \left[\hat{a}_i^\dagger, \hat{a}_j^\dagger\right]_- &= 0 \,, \\ \left[\hat{a}_i, \hat{a}_j\right]_- &= 0 \,, \end{aligned} \tag{2.2}$$

with $\delta_{i,j}$ being the Kronecker-delta and the commutator

$$[A, B]_- = AB - BA\,. \tag{2.3}$$

For the following, we introduce the particle number operator as

$$\hat{n}_i = \hat{a}_i^\dagger \hat{a}_i\,, \tag{2.4}$$

which defines the occupation number representation via

$$\begin{aligned}
\hat{n}_i|\, n_i \,\rangle &= n_i|\, n_i \,\rangle\,, \\
\hat{a}_i|\, n_i \,\rangle &= \sqrt{n_i}|\, n_i - 1 \,\rangle\,, \\
\hat{a}_i^\dagger|\, n_i \,\rangle &= \sqrt{n_i + 1}|\, n_i + 1 \,\rangle\,.
\end{aligned} \tag{2.5}$$

Furthermore, J represents the kinetic term of the Hamiltonian, which is in the Bose-Hubbard model for optical lattices the hopping energy and namely describes the energy gain ($J > 0$) or loss ($J < 0$) from tunnelling from one lattice site to another. The summation indices $\langle i, j\rangle$ are nearest neighbouring lattice sites. Finally, μ is the chemical potential, determining the energy difference for a boson in the optical lattice in comparison with a free boson without external influences.

2.2 Landau Theory

For further treatment of our system, we choose to apply the Landau theory [27] by introducing the order parameter, which is in our case the condensate density $\Psi^*\Psi$. In the Mott-phase, we have $\Psi^*\Psi = 0$, while in the superfluid phase, we have $\Psi^*\Psi > 0$.
We start with the grand potential

$$\mathcal{F} = U - TS - \mu N\,, \tag{2.6}$$

with U the internal energy, T the temperature, S the entropy, μ the chemical potential, and N the number of particles. In this thesis, we calculate at $T = 0$ and thus (2.6) reduces to

$$\mathcal{F} = U - \mu N\,, \tag{2.7}$$

which we name the energy of our system. According to the Landau theory [27], we can represent the energy $\mathcal{F}$ of our system as a function of Ψ^* and Ψ, therefore $\mathcal{F} = \mathcal{F}(\Psi^*, \Psi)$, but because of the $U(1)$-symmetry of the Bose-Hubbard model (2.1), this reduces to $\mathcal{F} = \mathcal{F}(\Psi^*\Psi)$. Thus we can write the energy of our system as a Taylor expansion

$$\mathcal{F} = a_0 + a_2\Psi^*\Psi + a_4\Psi^{*2}\Psi^2 + \dots . \tag{2.8}$$

Since we want to minimize the energy $\mathcal{F}$, we find the extrema by differentiation

$$\frac{\partial \mathcal{F}}{\partial \Psi^*} = \Psi\left(a_2 + 2a_4\Psi^*\Psi + ...\right) . \tag{2.9}$$

With $\partial\mathcal{F}/\partial\Psi^* = 0$, this gives two possible solutions for the condensate density $\Psi^*\Psi$, either we have

$$\Psi^*\Psi = 0 \tag{2.10}$$

or

$$\Psi^*\Psi = -\frac{a_2}{2a_4} + \dots . \tag{2.11}$$

For the Mott insulator, we have no condensate density, and thus (2.10) describes the Mott insulator phase. This yields the energy of the Mott-insulator according to (2.8) as

$$\mathcal{F}_{\text{Mott}} = a_0 . \tag{2.12}$$

In order to verify the existence of a superfluid phase with a positive order parameter, we have to insert (2.11) into (2.8) and get

$$\mathcal{F}_{\text{Superfluid}} = a_0 - \frac{a_2^2}{4a_4} . \tag{2.13}$$

In a phase transition of first order, we have $a_4 < 0$. In our case, we have a phase transition of second order, and thus $a_4 > 0$, thence $\mathcal{F}_{\text{Superfluid}} < a_0$ for $\Psi^*\Psi > 0$. Therefore, in order for the energy to be minimized, we have (2.11) in the superfluid phase. Out of this we conclude, that we are at the phase boundary for $a_2 = 0$.

2.3 Mean-Field Approximation

The energy $\mathcal{F}$ can be calculated via a field-theoretic method, where a Legendre transform of the grand-canonical free energy gives very precise results [16, 28]. Another way is to apply the mean-field approximation, which is quantitatively less correct, but gives a good qualitative insight. Furthermore, the calculations are less complex and thus much faster to compute with high precision. In order to apply the mean-field approximation, we start with rewriting (2.1) with (2.2) and (2.4) to

$$\hat{H} = \frac{1}{2}U \sum_i \hat{n}_i \left(\hat{n}_i - 1\right) - J \sum_{\langle i,j \rangle} \hat{a}_i^\dagger \hat{a}_j - \mu \sum_i \hat{n}_i \,, \tag{2.14}$$

which leaves only the kinetic term non-local, since the creation and annihilation operator act on different sites. In order to get approximately rid of this non-local term, we perform a Bogoliubov decomposition for these operators

$$\begin{aligned} \hat{a}_i^\dagger &= \Psi^* + \delta\hat{a}_i^\dagger \\ \hat{a}_i &= \Psi + \delta\hat{a}_i \,, \end{aligned} \tag{2.15}$$

where Ψ^*, Ψ represents the mean field with $n_0 = \Psi^*\Psi$ being the condensate density, whereas $\delta\hat{a}_i^\dagger$, $\delta\hat{a}_i$ devote fluctuation corrections. Within the mean-field approximation one neglects all quadratic fluctuations in the kinetic term of the Hamiltonian. Thus, we have

$$0 \approx \left(\Psi^* - \hat{a}_i^\dagger\right)\left(\Psi - \hat{a}_j\right) \,, \tag{2.16}$$

which can be rewritten as

$$\hat{a}_i^\dagger \hat{a}_j \approx \Psi^* \hat{a}_j + \Psi \hat{a}_i^\dagger - \Psi^*\Psi \,. \tag{2.17}$$

Now we insert (2.17) into the kinetic term of (2.14) and get the Bose-Hubbard mean-field Hamiltonian

$$\hat{H}_{\mathrm{MF}} = \frac{1}{2}U \sum_i \hat{n}_i \left(\hat{n}_i - 1\right) - Jz \sum_i \left(\Psi^* \hat{a}_i + \Psi \hat{a}_i^\dagger - \Psi^*\Psi\right) - \mu \sum_i \hat{n}_i \,. \tag{2.18}$$

Here z devotes the number of nearest neighbours. Since (2.18) is local, we can restrict us to one lattice site. Thus, we get the mean-field Bose-Hubbard Hamiltonian

$$\hat{H}_{\mathrm{MF}} = \frac{1}{2}U\hat{n}\left(\hat{n}-1\right) - Jz\left(\Psi^*\hat{a} + \Psi\hat{a}^\dagger - \Psi^*\Psi\right) - \mu\hat{n}\,. \tag{2.19}$$

Note that the kinetic term of this Hamiltonian is proportional to the order parameter Ψ^*, Ψ.

2.4 Perturbation Theory

Since the condensate density $\Psi^*\Psi$ is zero in the Mott-insulator and positive in the superfluid phase, we can assume that the order parameter is small as long as we stay in the superfluid phase close to the phase boundary. Since the kinetic term is proportional to the order parameter Ψ^*, Ψ, we can calculate it with a perturbative approach.
In order to do so, we do the primal splitting of the Hamiltonian into a unperturbed ground state energy and a small perturbation with λ being a smallness parameter. One way to do so is

$$\begin{aligned}
\hat{H} &= \hat{\mathcal{H}}^{(0)} + \lambda\hat{\mathcal{V}}\,,\\
\hat{\mathcal{H}}^{(0)} &= \frac{1}{2}U\hat{n}\left(\hat{n}-1\right) - \mu\hat{n} + Jz\Psi^*\Psi\,,\\
\hat{\mathcal{V}} &= -Jz\left(\Psi^*\hat{a} + \Psi\hat{a}^\dagger\right)\,,
\end{aligned} \tag{2.20}$$

with the unperturbed ground-state energy

$$\mathcal{E}_n^{(0)} = E_n^{(0)} + Jz\Psi^*\Psi = \frac{1}{2}Un\left(n-1\right) - \mu n + Jz\Psi^*\Psi\,, \tag{2.21}$$

which is used in [23]. Another way to split (2.19) is

$$\begin{aligned}
\hat{H} &= \hat{H}^{(0)} + \lambda\hat{V}\,,\\
\hat{H}^{(0)} &= \frac{1}{2}U\hat{n}\left(\hat{n}-1\right) - \mu\hat{n}\,,\\
\hat{V} &= -Jz\left(\Psi^*\hat{a} + \Psi\hat{a}^\dagger - \Psi^*\Psi\right)\,,
\end{aligned} \tag{2.22}$$

with the unperturbed ground-state energy

$$E_n^{(0)} = \frac{1}{2} U n\,(n-1) - \mu n\,, \tag{2.23}$$

which is used in [24].
The advantage of (2.20) is that the perturbative term $\hat{\mathcal{V}}$ consists of only two summands instead of three summands in $\hat{V}$ as in (2.22), simplifying an actual evaluation of this term a lot. The advantage of (2.22) is the independency of $\hat{H}^{(0)}$ from $\Psi^*\Psi$, therefore $\partial E_n^{(0)}/\partial\Psi^* = 0$, which is a derivation needed to receive the order parameter out of the energy. However, since both systems (2.20) and (2.22) have the same Hamiltonian, the results obtained by one are equivalent to the results from the other. Therefore, we are free to choose the primal split which facilitates our calculations the most.

For the calculations in this chapter, we decide for the primal split according to (2.20). Thus, we apply the Rayleigh-Schrödinger perturbation theory according to [23, 29] and get for the eigenstate and the eigenvalue

$$|\,\Psi_n\,\rangle = \sum_{i=0}^{\infty} J^i |\,\Psi_n^{(i)}\,\rangle\,, \tag{2.24}$$

$$E(n) = \sum_{i=0}^{\infty} J^i \mathcal{E}_n^{(i)}\,. \tag{2.25}$$

With the Schrödinger equation we get for the correction terms

$$\mathcal{E}_n^{(p)} = \langle\,\Psi_n^{(0)}\,|\hat{\mathcal{V}}|\,\Psi_n^{(p-1)}\,\rangle\,, \tag{2.26}$$

$$|\,\Psi_n^{(p)}\,\rangle = \sum_{m\neq n} |\,\Psi_m^{(0)}\,\rangle \frac{\langle\,\Psi_m^{(0)}\,|\hat{\mathcal{V}}|\,\Psi_n^{(p-1)}\,\rangle}{\mathcal{E}_n^{(0)} - \mathcal{E}_m^{(0)}} - \sum_{j=1}^{p} \mathcal{E}_n^{(j)} \sum_{m\neq n} |\,\Psi_m^{(0)}\,\rangle \frac{\langle\,\Psi_m^{(0)}\,|\,\Psi_n^{(p-j)}\,\rangle}{\mathcal{E}_n^{(0)} - \mathcal{E}_m^{(0)}}\,, \tag{2.27}$$

with the initial value for these recursion formulas

$$|\,\Psi_n^{(0)}\,\rangle = |\,n\,\rangle \tag{2.28}$$

and

$$\mathcal{E}_n^{(0)} = \frac{U}{2} n\,(n-1) - \mu n + Jz\Psi^*\Psi\,. \tag{2.29}$$

With these formulas, we can get the energy in the Landau representation up to the fourth order as [23, (3.39)]

$$E(n) = a_0 + a_2\Psi^*\Psi + a_4\Psi^{*2}\Psi^2 + \ldots\,, \tag{2.30}$$

with the Landau coefficients

$$a_0 = E_n^{(0)} = \frac{U}{2} n\,(n-1) - \mu n\,, \tag{2.31}$$

$$a_2 = Jz + J^2z^2\left(\frac{n+1}{E_n^{(0)} - E_{n+1}^{(0)}} + \frac{n}{E_n^{(0)} - E_{n-1}^{(0)}}\right)\,, \tag{2.32}$$

and

$$\begin{aligned} a_4 =& J^4z^4\left[\frac{n+1}{\left(E_n^{(0)} - E_{n+1}^{(0)}\right)^2}\left(\frac{n+2}{E_n^{(0)} - E_{n+2}^{(0)}} - \frac{n}{E_n^{(0)} - E_{n-1}^{(0)}} - \frac{n+1}{E_n^{(0)} - E_{n+1}^{(0)}}\right)\right. \\ &\left. + \frac{n}{\left(E_n^{(0)} - E_{n-1}^{(0)}\right)^2}\left(\frac{n-1}{E_n^{(0)} - E_{n-2}^{(0)}} - \frac{n+1}{E_n^{(0)} - E_{n+1}^{(0)}} - \frac{n}{E_n^{(0)} - E_{n-1}^{(0)}}\right)\right]\,. \end{aligned} \tag{2.33}$$

In order to get the phase boundary, we calculate $\partial E(n)/\partial\Psi^* = 0$, set $\Psi^*\Psi = 0$ and solve with respect to Jz/U to get the mean-field phase boundary (2.34) as in Ref. [30], which is shown in FIG. 2.1:

$$\frac{Jz}{U} = -\frac{\left(E_n^{(0)} - E_{n+1}^{(0)}\right)\left(E_n^{(0)} - E_{n-1}^{(0)}\right)}{U\left[E_n^{(0)} - E_{n-1}^{(0)} + 2nE_n^{(0)} - n\left(E_{n+1}^{(0)} + E_{n-1}^{(0)}\right)\right]}\,. \tag{2.34}$$

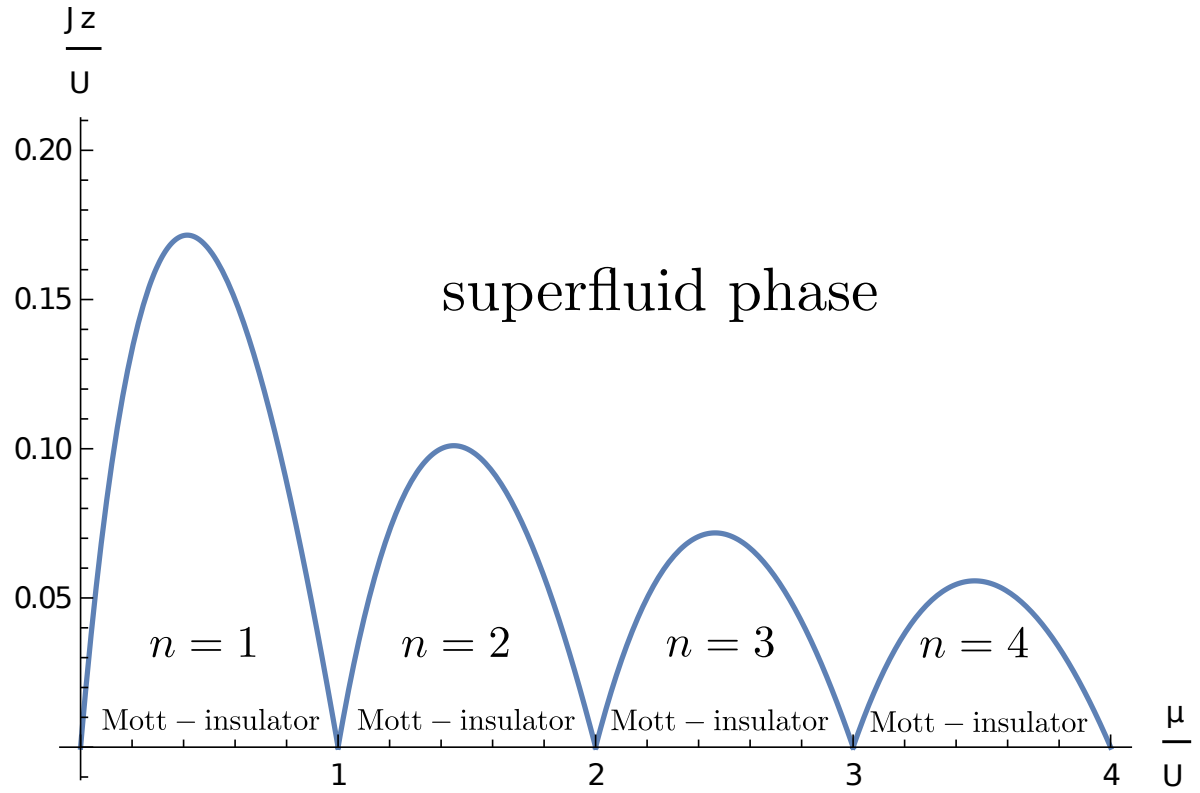

FIG. 2.1: Phase boundary plot, obtained by Rayleigh-Schrödinger perturbation theory. Inside of the lobes we are in the Mott-insulator phase, while outside of the lobes we are in the superfluid phase. The number of particles n increases from the left to the right by one per lobe.

It is obvious that for large $\frac{Jz}{U}$, we are in the superfluid phase, far away from the phase boundary, since the Mott-insulator needs low hopping probabilities. Since all of our theory is based on the assumption of being close to the phase boundary, we can't obtain reliable results for big $\frac{Jz}{U}$ deep in the superfluid phase. Nevertheless, for $\frac{Jz}{U} \lesssim 0.20$, we assume our model to be valid. While for $\frac{Jz}{U} = 0$, we have no superfluid phase and only Mott-insulator, we always reach the superfluid phase by increasing $\frac{Jz}{U}$. Another way to get from the Mott-insulator to the superfluid phase is the tuning of $\frac{\mu}{U}$ at $\frac{Jz}{U} > 0$. If we start in the first Mott-lobe and increase $\frac{\mu}{U}$, the ordered structure breaks down at some point and the superfluid phase is energetically more favourable and thus realized.
After obtaining the phase boundary, we take a closer look at the lowest energies for increasing n. In the plot of the energies (2.31) in FIG. 2.2, we see that the lowest energies have a degeneracy at integer values of μ/U. Like in between the lobes for $n = 1$ (red) and $n = 2$ (blue) at $\frac{\mu}{U} = 1$, at this point, it is $E_1^{(0)} = E_2^{(0)}$ and therefore $\mu = Un$. Analogous formula are valid between every two neighbouring lobes. It is exactly this degeneracy which makes every algebraic treatment of this system quite complex, but since we have only two degenerate energies, a solution can be found.

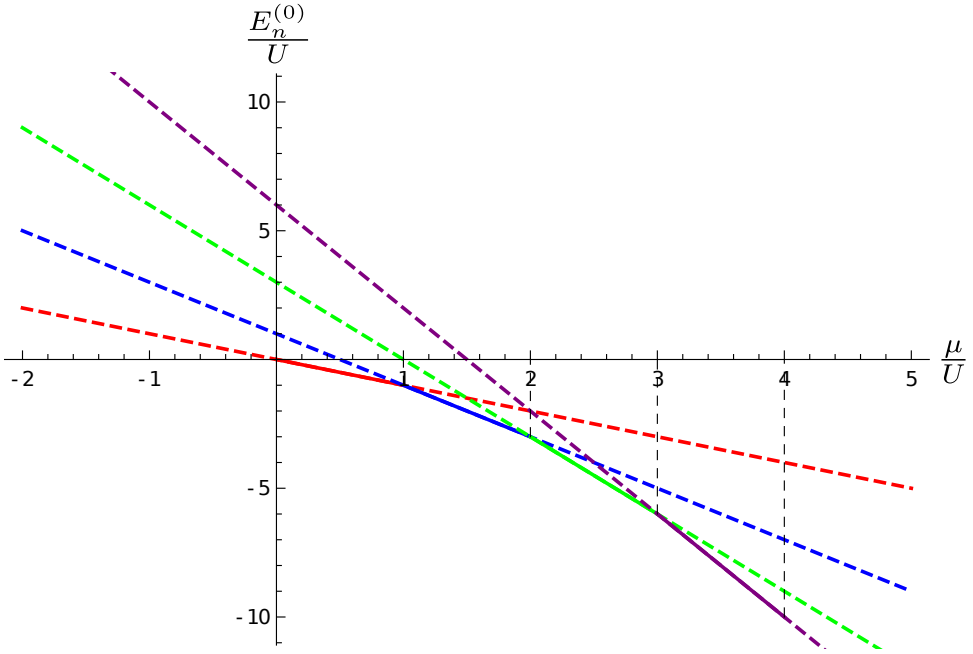

FIG. 2.2: The different lines correspond to different values for n with $n = 1$ (red), $n = 2$ (blue), $n = 3$ (green), and $n = 4$ (purple). The vertical, dashed, black lines correspond to the points of degeneracy. The solid coloured lines are the realized, lowest energy, while the dashed coloured lines indicate the continuation of the energy line.

With this degeneracy in mind, we draw our attention to the order parameter. First, we plot (2.11) with (2.32) and (2.33). Since a_4 approaches infinity for $\mu = Un$, where we have $E_n^{(0)} = E_{n+1}^{(0)}$ according to (2.31), the condensate density $\Psi^*\Psi$ tends to zero at the degeneracy between two adjacent lobes, which indicates a phase boundary there, although there is none. This unphysical behaviour is depicted in FIG. 2.3.

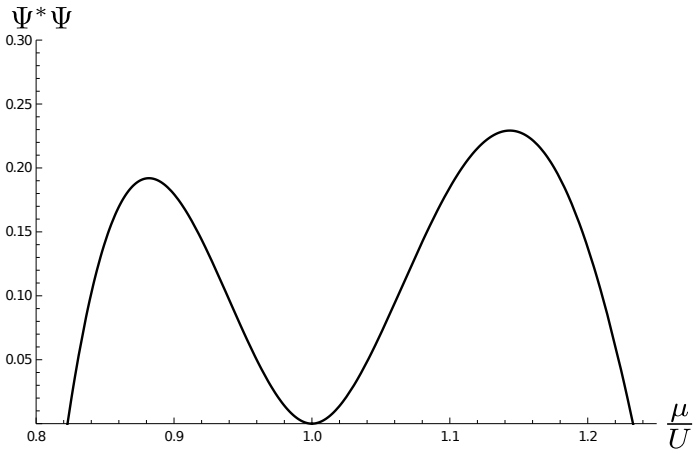

FIG. 2.3: The order parameter from [23], using (2.11) with (2.32) and (2.33). For this plot is $\frac{Jz}{U} = 0.08$. The left part origins from $n = 1$ and the right part from $n = 2$. The order parameter is zero at the phase boundary and shows a physical behaviour close to the phase boundary. In the vicinity of the degeneracy, the Rayleigh-Schrödinger result breaks down. The value $\Psi^*\Psi = 0$ at $\frac{\mu}{U} = 1$ implies a false phase boundary there.

Therefore, we need another approach. We stay in a perturbative picture, which already succeeded in reproducing the phase boundary, but in order to get the order parameter as well, we will not apply the well-known Rayleigh-Schrödinger perturbation theory, but the less common Brillouin-Wigner perturbation theory.

3 Perturbation Theory

The best known perturbation theory is the Rayleigh-Schrödinger perturbation theory. More precisely, there is the normal Rayleigh-Schrödinger perturbation theory and the degenerate Rayleigh-Schrödinger perturbation theory. If a parameter ranges over degenerate parts and non-degenerate parts, both perturbation theories are needed.
In contrast to that the less known Brillouin-Wigner perturbation theory describes degenerate parts as well as non-degenerate parts with one and the same approach. In case of the Bose-Hubbard model we do have a degeneracy between every two adjacent Mott lobes, but want smooth parameters over the entire regime of all lobes.
Thus, we will use the Brillouin-Wigner perturbation theory in this work, which is derived and discussed in this chapter. By doing this, we show how to get the well-known Rayleigh-Schrödinger perturbation theory out of the Brillouin-Wigner perturbation approach.

3.1 Basic Considerations and Projection Operator Formalism

Before we start with the real derivation of the Brillouin-Wigner perturbation theory, we have to take a look at the basic, required structures of our Hamilton operator and our Hilbert space. We will find projection operators as a crafty way to handle both in one formalism.
In order to do any kind of perturbation theory, we choose our Hamilton operator is such a way, that it can be split as follows:

$$\hat{H} = \hat{H}^{(0)} + \lambda \hat{V} \,. \tag{3.1}$$

Here $\hat{H}$ denotes the Hamilton operator of the whole, perturbed system, $\hat{H}^{(0)}$ represents the unperturbed Hamilton operator, and $\hat{V}$ stands for the operator of the perturbation. Furthermore, we have introduced λ as a smallness parameter, thus the perturbation is considered to be small in comparison with the unperturbed Hamilton operator.

3.1.1 Unperturbed Hamilton Operator and Energy States

The time-independent Schrödinger equation represents the eigenvalue problem of the unperturbed Hamilton operator $\hat{H}^{(0)}$ and involves the unperturbed energy eigenvalues $E_n^{(0)}$ as well as the unperturbed energy states $|\,\Psi_n^{(0)}\,\rangle$:

$$\hat{H}^{(0)}|\,\Psi_n^{(0)}\,\rangle = E_n^{(0)}|\,\Psi_n^{(0)}\,\rangle\,. \tag{3.2}$$

Here the quantum number n enumerates all states of the system, which are assumed to be discrete without loss of generality. Furthermore, the unperturbed energy states obey the completeness relation

$$\sum_n |\,\Psi_n^{(0)}\,\rangle\langle\,\Psi_n^{(0)}\,| = \mathbb{1} \tag{3.3}$$

and the orthonormality relation

$$\langle\Psi_n^{(0)}|\,\Psi_m^{(0)}\,\rangle = \delta_{n,m}\,, \tag{3.4}$$

where $\delta_{n,m}$ represents the Kronecker delta.
Now we introduce projection operators for the respective unperturbed energy states:

$$\hat{P}_n = |\,\Psi_n^{(0)}\,\rangle\langle\,\Psi_n^{(0)}\,|\,. \tag{3.5}$$

Due to (3.4) they fulfil the property

$$\hat{P}_n\hat{P}_{n'} = \delta_{n,n'}\hat{P}_n\,. \tag{3.6}$$

This means that for $n \neq n'$ two projector operators project into different subspaces, whereas for $n = n'$ (3.6) represents the idempotent property of a projection operator. With (3.5) the unperturbed Hamilton operator can be written as

$$\hat{H}^{(0)} = \sum_n E_n^{(0)}\hat{P}_n \tag{3.7}$$

in accordance with (3.2).

3.1.2 Hilbert Space

We split the underlying Hilbert space into two parts by using the projection operators $\hat{P}$ and $\hat{Q}$:

$$\hat{Q} + \hat{P} = \mathbb{1} \,. \tag{3.8}$$

Here we assume that $\hat{P}$ is given by:

$$\hat{P} = \sum_{k \in N} \hat{P}_k \tag{3.9}$$

for some set N of quantum numbers. Thus, we conclude from (3.8) and (3.9)

$$\hat{Q} = \mathbb{1} - \sum_{k \in N} \hat{P}_k \,, \tag{3.10}$$

which can be summarized as

$$\hat{Q} = \sum_{k \in \tilde{N}} \hat{P}_k \tag{3.11}$$

with $\tilde{N}$ being the complement of N.
With this we obtain from (3.6) and (3.9) that $\hat{P}$ fulfils, indeed, the idempotent property of a projection operator

$$\hat{P}^2 = \hat{P} \,, \tag{3.12}$$

which is also valid for $\hat{Q}$ due to (3.10)

$$\hat{Q}^2 = \hat{Q} \,. \tag{3.13}$$

Furthermore, we conclude

$$\hat{P}\hat{Q} = \hat{Q}\hat{P} = 0\,, \tag{3.14}$$

which states that $\hat{P}$ and $\hat{Q}$ project into disjunct subspaces of the Hilbert space.
With this, we calculate that the commutator between $\hat{H}^{(0)}$ and $\hat{P}$

$$\left[\hat{H}^{(0)}, \hat{P}\right]_- = \hat{H}^{(0)}\hat{P} - \hat{P}\hat{H}^{(0)} \tag{3.15}$$

vanishes due to (3.6), (3.7), and (3.9):

$$\begin{aligned}\left[\hat{H}^{(0)}, \hat{P}\right]_- =& \hat{H}^{(0)}\hat{P} - \hat{P}\hat{H}^{(0)} = \sum_n E_n^{(0)}\hat{P}_n \sum_{k\in N}\hat{P}_k - \sum_{k\in N}\hat{P}_k \sum_n E_n^{(0)}\hat{P}_n \\ &= \sum_n \sum_{k\in N} E_n^{(0)}\left(\hat{P}_n\hat{P}_k - \hat{P}_k\hat{P}_n\right) \\ &= 0\,. \end{aligned} \tag{3.16}$$

Taking into account (3.10) then yields

$$\left[\hat{H}^{(0)}, \hat{Q}\right]_- = 0\,. \tag{3.17}$$

From (3.14), (3.16), and (3.17) we also conclude

$$\hat{P}\hat{H}^{(0)}\hat{Q} = \hat{Q}\hat{H}^{(0)}\hat{P} = 0\,. \tag{3.18}$$

3.2 General Derivation

In the following, we derive an effective Hamiltonian for the Hilbert subspace, which is characterized by the projection operator $\hat{P}$. To this end we have to eliminate the complementary Hilbert subspace, which is characterized by the projection operator $\hat{Q}$.

3.2.1 Schrödinger Equation with Projection Operators

Since we have now the two projection operators $\hat{P}$ and $\hat{Q}$, we need two conditions to define the respective Hilbert subspaces. For this, we start with reformulating the full time-independent Schrödinger equation

$$\hat{H}|\,\Psi_n\,\rangle = E_n|\,\Psi_n\,\rangle \tag{3.19}$$

with the help of the projection operators. To this end we insert the unity operator $\mathbb{1}$ and get

$$\hat{H}\mathbb{1}|\,\Psi_n\,\rangle = E_n\mathbb{1}|\,\Psi_n\,\rangle\,. \tag{3.20}$$

Applying (3.8) leads to

$$\hat{H}\left(\hat{P}+\hat{Q}\right)|\,\Psi_n\,\rangle = E_n\left(\hat{P}+\hat{Q}\right)|\,\Psi_n\,\rangle\,, \tag{3.21}$$

which yields

$$\hat{H}\hat{P}|\,\Psi_n\,\rangle + \hat{H}\hat{Q}|\,\Psi_n\,\rangle = E_n\hat{P}|\,\Psi_n\,\rangle + E_n\hat{Q}|\,\Psi_n\,\rangle\,. \tag{3.22}$$

Multiplying (3.22) from the left with $\hat{P}$ and using both (3.12) and (3.14) gives then

$$\hat{P}\hat{H}\hat{P}|\,\Psi_n\,\rangle + \hat{P}\hat{H}\hat{Q}|\,\Psi_n\,\rangle = E_n\hat{P}|\,\Psi_n\,\rangle\,. \tag{3.23}$$

Correspondingly multiplying (3.22) from the left with $\hat{Q}$ and using (3.13) and (3.14), we obtain

$$\hat{Q}\hat{H}\hat{P}|\,\Psi_n\,\rangle + \hat{Q}\hat{H}\hat{Q}|\,\Psi_n\,\rangle = E_n\hat{Q}|\,\Psi_n\,\rangle\,. \tag{3.24}$$

3.2.2 Eliminating a Subspace

Now we try to find a single equation for $\hat{P}|\,\Psi_n\,\rangle$ in a shape similar to the time-independent Schrödinger-equation, which necessitates eliminating $\hat{Q}|\,\Psi_n\,\rangle$ from (3.23). To this end, we start with (3.24) and use (3.13):

$$\hat{Q}\hat{H}\hat{P}|\,\Psi_n\,\rangle + \hat{Q}\hat{H}\hat{Q}^2|\,\Psi_n\,\rangle = E_n\hat{Q}|\,\Psi_n\,\rangle\,. \tag{3.25}$$

From rearranging and factoring out follows:

$$\hat{Q}\hat{H}\hat{P}|\,\Psi_n\,\rangle = \left(E_n - \hat{Q}\hat{H}\hat{Q}\right)\hat{Q}|\,\Psi_n\,\rangle\,. \tag{3.26}$$

Thus, a formal solution with respect to $\hat{Q}|\,\Psi_n\,\rangle$ yields

$$\hat{Q}|\,\Psi_n\,\rangle = \left(E_n - \hat{Q}\hat{H}\hat{Q}\right)^{-1}\hat{Q}\hat{H}\hat{P}|\,\Psi_n\,\rangle\,. \tag{3.27}$$

A further multiplication with $\hat{Q}$ from the left gives then with (3.13)

$$\hat{Q}|\,\Psi_n\,\rangle = \hat{Q}\left(E_n - \hat{Q}\hat{H}\hat{Q}\right)^{-1}\hat{Q}\hat{H}\hat{P}|\,\Psi_n\,\rangle\,. \tag{3.28}$$

Inserting (3.28) in (3.23), we get a single equation for $\hat{P}|\,\Psi_n\,\rangle$:

$$\hat{P}\hat{H}\hat{P}|\,\Psi_n\,\rangle + \hat{P}\hat{H}\hat{Q}\left(E_n - \hat{Q}\hat{H}\hat{Q}\right)^{-1}\hat{Q}\hat{H}\hat{P}|\,\Psi_n\,\rangle = E_n\hat{P}|\,\Psi_n\,\rangle\,. \tag{3.29}$$

Using (3.1) allows to rewrite (3.29) according to

$$\hat{P}\hat{H}\hat{P}|\,\Psi_n\,\rangle + \hat{P}\left(\hat{H}^{(0)} + \lambda\hat{V}\right)\hat{Q}\left(E_n - \hat{Q}\hat{H}\hat{Q}\right)^{-1}\hat{Q}\left(\hat{H}^{(0)} + \lambda\hat{V}\right)\hat{P}|\,\Psi_n\,\rangle = E_n\hat{P}|\,\Psi_n\,\rangle\,. \tag{3.30}$$

At first we expand only the first bracket:

$$
\begin{aligned}
&\hat{P}\hat{H}\hat{P}|\,\Psi_n\,\rangle \\
&+\hat{P}\hat{H}^{(0)}\hat{Q}\left(E_n-\hat{Q}\hat{H}\hat{Q}\right)^{-1}\hat{Q}\left(\hat{H}^{(0)}+\lambda\hat{V}\right)\hat{P}|\,\Psi_n\,\rangle \\
&+\hat{P}\lambda\hat{V}\hat{Q}\left(E_n-\hat{Q}\hat{H}\hat{Q}\right)^{-1}\hat{Q}\left(\hat{H}^{(0)}+\lambda\hat{V}\right)\hat{P}|\,\Psi_n\,\rangle = E_n\hat{P}|\,\Psi_n\,\rangle\,.
\end{aligned}
\tag{3.31}
$$

By using (3.18), the second line vanishes and we expand the last bracket:

$$
\begin{aligned}
&\hat{P}\hat{H}\hat{P}|\,\Psi_n\,\rangle \\
&+\hat{P}\lambda\hat{V}\hat{Q}\left(E_n-\hat{Q}\hat{H}\hat{Q}\right)^{-1}\hat{Q}\hat{H}^{(0)}\hat{P}|\,\Psi_n\,\rangle \\
&+\hat{P}\lambda\hat{V}\hat{Q}\left(E_n-\hat{Q}\hat{H}\hat{Q}\right)^{-1}\hat{Q}\lambda\hat{V}\hat{P}|\,\Psi_n\,\rangle = E_n\hat{P}|\,\Psi_n\,\rangle\,.
\end{aligned}
\tag{3.32}
$$

We use again (3.18), so that the second line vanishes, and get finally

$$
\hat{P}\hat{H}\hat{P}|\,\Psi_n\,\rangle+\hat{P}\lambda\hat{V}\hat{Q}\left(E_n-\hat{Q}\hat{H}\hat{Q}\right)^{-1}\hat{Q}\lambda\hat{V}\hat{P}|\,\Psi_n\,\rangle = E_n\hat{P}|\,\Psi_n\,\rangle\,. \tag{3.33}
$$

A subsequent reordering yields

$$
\hat{P}\left[\hat{H}+\lambda\hat{V}\hat{Q}\left(E_n-\hat{Q}\hat{H}\hat{Q}\right)^{-1}\hat{Q}\lambda\hat{V}\right]\hat{P}|\,\Psi_n\,\rangle = E_n\hat{P}|\,\Psi_n\,\rangle\,. \tag{3.34}
$$

This represents a single equation for $\hat{P}|\,\Psi_n\,\rangle$, which is the basis for the Brillouin-Wigner perturbation theory.

3.3 Brillouin-Wigner Perturbation Theory

Now we reformulate (3.34) in terms of a matrix representation within the Hilbert subspace defined by the projection operator $\hat{P}$. Afterwards, we specialize to the cases that $\hat{P}$ consists of one and two states, respectively.

3.3.1 Resolvent

The resulting equation (3.34) for $\hat{P}|\,\Psi_n\,\rangle$ is of the form of a time-independent Schrödinger-equation

$$\hat{P}\hat{H}_{\text{eff}}\hat{P}|\,\Psi_n\,\rangle = E_n\hat{P}|\,\Psi_n\,\rangle\,, \tag{3.35}$$

where we have introduced the effective Hamiltonian

$$\hat{H}_{\text{eff}} = \hat{H} + \lambda^2\hat{V}\hat{Q}\left(E_n - \hat{Q}\hat{H}\hat{Q}\right)^{-1}\hat{Q}\hat{V}\,. \tag{3.36}$$

Since $\hat{H}_{\text{eff}}$ is sandwiched by $\hat{P}$, everything that goes in or out of $\hat{H}_{\text{eff}}$ must involve the Hilbert subspace $\hat{P}$ projects into. However, $\hat{H}_{\text{eff}}$ contains also the projection operator $\hat{Q}$, so one has to go beyond the Hilbert subspace $\hat{P}$ projects into.
Another way to represent $\hat{H}_{\text{eff}}$ is by inserting (3.1) into (3.36), so we obtain

$$\hat{H}_{\text{eff}} = \hat{H}^{(0)} + \lambda\hat{V} + \lambda^2\hat{V}\hat{Q}\left(E_n - \hat{Q}\hat{H}^{(0)}\hat{Q} - \lambda\hat{Q}\hat{V}\hat{Q}\right)^{-1}\hat{Q}\hat{V}\,. \tag{3.37}$$

Here the resolvent

$$\hat{R}(E_n) = \left(E_n - \hat{Q}\hat{H}^{(0)}\hat{Q} - \lambda\hat{Q}\hat{V}\hat{Q}\right)^{-1} = \left[E_n - \hat{Q}\left(\hat{H}^{(0)} + \lambda\hat{V}\right)\hat{Q}\right]^{-1} \tag{3.38}$$

can be expanded in a Taylor series with respect to λ with the help of a geometric series:

$$\hat{R}(E_n) = \left(E_n - \hat{Q}\hat{H}^{(0)}\hat{Q}\right)^{-1}\sum_{s=0}^{\infty}\left[\lambda\hat{Q}\hat{V}\hat{Q}\left(E_n - \hat{Q}\hat{H}^{(0)}\hat{Q}\right)^{-1}\right]^s\,. \tag{3.39}$$

Note the crucial property of (3.39) that it contains the full energy eigenvalue E_n, and not just the unperturbed energy eigenvalue $E_n^{(0)}$.
We can now insert (3.38) in (3.37):

$$\hat{H}_{\text{eff}} = \hat{H}^{(0)} + \lambda\hat{V} + \lambda^2\hat{V}\hat{Q}\hat{R}(E_n)\hat{Q}\hat{V}\,. \tag{3.40}$$

In the limit $\lambda \to 0$ this reproduces the unperturbed Schrödinger equation (3.2). The essential property of (3.40) is, however, the non-linear appearance of E_n in the resolvent $\hat{R}(E_n)$ from (3.38).
Take heed of the first perturbative order $\lambda\hat{V}$ in (3.40), which is not contained by the resolvent

$\hat{R}(E_n)$, but directly emanates from the perturbed Hamilton operator $\hat{H}$ in (3.1). In contrast to that all higher orders in (3.40) originate from the resolvent term, more precisely $s = 0$ gives the second perturbative order, $s = 1$ goes up to the third perturbative order, $s = 2$ goes up to the fourth perturbative order, and so on. Thus, the perturbative order is always twice larger than s.
This fundamental difference of origin of perturbative orders is already evident in (3.22), where the term $\hat{H}\hat{P}$ gives rise to the zeroth and the first perturbative order, and the term $\hat{H}\hat{Q}$ gives rise to all higher orders. In other words, the zeroth and the first perturbative order are within the Hilbert subspace $\hat{P}$ projects into, whilst for all higher orders, the Hilbert subspace $\hat{Q}$ projects into must be taken into account.
Now we calculate exemplarily all correction terms of the effective Hamiltonian up to λ^4. To do so, we take the sum over s in the resolvent (3.39) up to $s = 2$ and insert this into (3.40)

$$\begin{aligned}\hat{H}_{\text{eff}} =& \hat{H}^{(0)} + \lambda\hat{V} \\ &+ \lambda^2\hat{V}\hat{Q}\hat{R}^{(0)}(E_n)\hat{Q}\hat{V} \\ &+ \lambda^3\hat{V}\hat{Q}\hat{R}^{(0)}(E_n)\hat{Q}\hat{V}\hat{Q}\hat{R}^{(0)}(E_n)\hat{Q}\hat{V} \\ &+ \lambda^4\hat{V}\hat{Q}\hat{R}^{(0)}(E_n)\hat{Q}\hat{V}\hat{Q}\hat{R}^{(0)}(E_n)\hat{Q}\hat{V}\hat{Q}\hat{R}^{(0)}(E_n)\hat{Q}\hat{V}\,. \end{aligned} \tag{3.41}$$

Here we have introduced the resolvent with the perturbed energy

$$\hat{R}^{(0)}(E_n) = \left(E_n - \hat{Q}\hat{H}^{(0)}\hat{Q}\right)^{-1}\,, \tag{3.42}$$

which allows us to rewrite $\hat{H}_{\text{eff}}$ by index shifting (3.39) according to

$$\hat{H}_{\text{eff}} = \hat{H}^{(0)} + \lambda\hat{V}\sum_{s=-1}^{\infty}\left[\lambda\hat{Q}\hat{R}^{(0)}(E_n)\hat{Q}\hat{V}\right]^{s+1}\,. \tag{3.43}$$

Now we specialize to the respective projection operators $\hat{P}$ and $\hat{Q}$ given by (3.9) and (3.11). With this we show that the matrix element of the resolvent (3.42) yields

$$\frac{1}{E_n - E_l^{(0)}} = \langle\, \Psi_l^{(0)} \,|\hat{R}^{(0)}(E_n)|\, \Psi_l^{(0)} \,\rangle\,, \tag{3.44}$$

with $l \in \tilde{N}$ and $n \in N$.
In order to proof this, we start with multiplying (3.42) from the left with $\langle\, \Psi_l^{(0)} \,|\left(E_n - \hat{Q}\hat{H}^{(0)}\hat{Q}\right)$ and from the right with $|\, \Psi_\ell^{(0)} \,\rangle$, which gives due to (3.4)

$$\langle\, \Psi_l^{(0)} \,|\, \Big(E_n - \hat{Q}\hat{H}^{(0)}\hat{Q}\Big)\, \hat{R}^{(0)}(E_n) |\, \Psi_\ell^{(0)} \,\rangle = \langle\, \Psi_l^{(0)} \,|\, \Psi_\ell^{(0)} \,\rangle = \delta_{l,\ell}\,, \tag{3.45}$$

which yields after an expansion

$$E_n \langle\, \Psi_l^{(0)} \,|\hat{R}^{(0)}(E_n)|\, \Psi_\ell^{(0)} \,\rangle - \langle\, \Psi_l^{(0)} \,|\hat{Q}\hat{H}^{(0)}\hat{Q}\hat{R}^{(0)}(E_n)|\, \Psi_\ell^{(0)} \,\rangle = \delta_{l,\ell}\,. \tag{3.46}$$

Now we insert (3.11)

$$\begin{aligned} &E_n \langle\, \Psi_l^{(0)} \,|\hat{R}^{(0)}(E_n)|\, \Psi_\ell^{(0)} \,\rangle \\ &\quad - \langle\, \Psi_l^{(0)} \,|\, \sum_{l' \in \tilde{N}} |\, \Psi_{l'}^{(0)} \,\rangle \langle\, \Psi_{l'}^{(0)} \,|\hat{H}^{(0)} \sum_{l'' \in \tilde{N}} |\, \Psi_{l''}^{(0)} \,\rangle \langle\, \Psi_{l''}^{(0)} \,|\hat{R}^{(0)}(E_n)|\, \Psi_\ell^{(0)} \,\rangle = \delta_{l,\ell}\,, \end{aligned} \tag{3.47}$$

and gives after reordering the sums

$$\begin{aligned} &E_n \langle\, \Psi_l^{(0)} \,|\hat{R}^{(0)}(E_n)|\, \Psi_\ell^{(0)} \,\rangle \\ &\quad - \sum_{l',l'' \in \tilde{N}} \langle\, \Psi_l^{(0)} \,|\, \Psi_{l'}^{(0)} \,\rangle \langle\, \Psi_{l'}^{(0)} \,|\hat{H}^{(0)}|\, \Psi_{l''}^{(0)} \,\rangle \langle\, \Psi_{l''}^{(0)} \,|\hat{R}^{(0)}(E_n)|\, \Psi_\ell^{(0)} \,\rangle = \delta_{l,\ell}\,. \end{aligned} \tag{3.48}$$

Due to the orthonormality (3.4) and the eigenvalue problem (3.2) we get

$$E_n \langle\, \Psi_l^{(0)} \,|\hat{R}^{(0)}(E_n)|\, \Psi_\ell^{(0)} \,\rangle - \sum_{l',l'' \in \tilde{N}} \delta_{l,l'}\delta_{l',l''} E_{l''}^{(0)} \langle\, \Psi_{l''}^{(0)} \,|\hat{R}^{(0)}(E_n)|\, \Psi_\ell^{(0)} \,\rangle = \delta_{l,\ell}\,. \tag{3.49}$$

Evaluating the Kronecker symbol yields due to $\ell \in \tilde{N}$

$$E_n \langle\, \Psi_l^{(0)} \,|\hat{R}^{(0)}(E_n)|\, \Psi_\ell^{(0)} \,\rangle - E_l^{(0)} \langle\, \Psi_l^{(0)} \,|\hat{R}^{(0)}(E_n)|\, \Psi_\ell^{(0)} \,\rangle = \delta_{l,\ell}\,. \tag{3.50}$$

We factor out and obtain

$$\Big(E_n - E_l^{(0)}\Big) \langle\, \Psi_l^{(0)} \,|\hat{R}^{(0)}(E_n)|\, \Psi_\ell^{(0)} \,\rangle = \delta_{l,\ell}\,, \tag{3.51}$$

so dividing by $\left(E_n - E_l^{(0)}\right)$ yields, indeed, the final result (3.44).

Taking into account (3.11) and (3.44) in (3.41), we obtain for $n \in N$

$$\begin{aligned}\hat{H}_{\text{eff}} =& \hat{H}^{(0)} + \lambda \hat{V} \\ &+ \lambda^2 \sum_{l \in \tilde{N}} \frac{\hat{V} |\, \Psi_l^{(0)} \,\rangle\langle\, \Psi_l^{(0)} \,| \hat{V}}{E_n - E_l^{(0)}} \\ &+ \lambda^3 \sum_{l,l' \in \tilde{N}} \frac{\hat{V} |\, \Psi_l^{(0)} \,\rangle\langle\, \Psi_l^{(0)} \,| \hat{V} |\, \Psi_{l'}^{(0)} \,\rangle\langle\, \Psi_{l'}^{(0)} \,| \hat{V}}{\left(E_n - E_l^{(0)}\right)\left(E_n - E_{l'}^{(0)}\right)} \\ &+ \lambda^4 \sum_{l,l',l'' \in \tilde{N}} \frac{\hat{V} |\, \Psi_l^{(0)} \,\rangle\langle\, \Psi_l^{(0)} \,| \hat{V} |\, \Psi_{l'}^{(0)} \,\rangle\langle\, \Psi_{l'}^{(0)} \,| \hat{V} |\, \Psi_{l''}^{(0)} \,\rangle\langle\, \Psi_{l''}^{(0)} \,| \hat{V}}{\left(E_n - E_l^{(0)}\right)\left(E_n - E_{l'}^{(0)}\right)\left(E_n - E_{l''}^{(0)}\right)} + \dots . \end{aligned} \tag{3.52}$$

This representation of the effective Hamiltonian $\hat{H}_{\text{eff}}$ has no operators anymore in the denominators, and thus can be used for further calculations.

3.3.2 Matrix Representation

Now we determine an equation for determining the perturbed ground-state energy E_m. To this end, we choose $n, n' \in N$ and reformulate (3.35) with (3.9) to

$$\sum_{n,n' \in N} |\, \Psi_n^{(0)} \,\rangle\langle\, \Psi_n^{(0)} \,| \hat{H}_{\text{eff}} |\, \Psi_{n'}^{(0)} \,\rangle\langle\, \Psi_{n'}^{(0)} \,|\, \Psi_m \,\rangle = E_m \sum_{n' \in N} |\, \Psi_{n'}^{(0)} \,\rangle\langle\, \Psi_{n'}^{(0)} \,|\, \Psi_m \,\rangle . \tag{3.53}$$

Now we multiply from the left with $\langle\, \Psi_n^{(0)} \,|$

$$\sum_{n,n' \in N} \langle\, \Psi_n^{(0)} \,| \hat{H}_{\text{eff}} |\, \Psi_{n'}^{(0)} \,\rangle\langle\, \Psi_{n'}^{(0)} \,|\, \Psi_m \,\rangle = E_m \sum_{n,n' \in N} \langle\, \Psi_n^{(0)} \,|\, \Psi_{n'}^{(0)} \,\rangle\langle\, \Psi_{n'}^{(0)} \,|\, \Psi_m \,\rangle , \tag{3.54}$$

which gives

$$\langle\, \Psi_{n'}^{(0)} \,|\, \Psi_m \,\rangle \sum_{n,n' \in N} \left(\langle\, \Psi_n^{(0)} \,| \hat{H}_{\text{eff}} |\, \Psi_{n'}^{(0)} \,\rangle - E_m \delta_{n,n'} \right) = 0 . \tag{3.55}$$

In order to obtain a non-trivial solution $\langle \Psi_{n'}^{(0)} \,|\, \Psi_m \rangle \neq 0$ from (3.55), we conclude:

$$\mathrm{Det}\left(\langle \Psi_n^{(0)} \,|\hat{\mathrm{H}}_{\mathrm{eff}}|\, \Psi_{n'}^{(0)} \rangle - \mathrm{E}_m \delta_{n,n'} \right) = 0\,. \tag{3.56}$$

Note that the determinant in (3.56) has to be performed with respect to $n, n' \in N$.

3.3.3 One State

We consider now the special case that $\hat{P}$ contains only one state, namely

$$\hat{P} = \hat{P}_n\,. \tag{3.57}$$

With this, (3.56) simplifies with $n = n' = m$

$$E_n = \langle \Psi_n^{(0)} \,|\hat{H}_{\mathrm{eff}}|\, \Psi_n^{(0)} \rangle\,. \tag{3.58}$$

Inserting (3.52) in (3.58) we get

$$\begin{aligned} E_n =& \langle \Psi_n^{(0)} \,|\hat{H}^{(0)}|\, \Psi_n^{(0)} \rangle + \lambda \langle \Psi_n^{(0)} \,|\hat{V}|\, \Psi_n^{(0)} \rangle \\ &+ \lambda^2 \sum_{l \in \tilde{N}} \langle \Psi_n^{(0)} \,| \frac{\hat{V}|\, \Psi_l^{(0)} \rangle \langle \Psi_l^{(0)} \,|\hat{V}}{E_n - E_l^{(0)}} |\, \Psi_n^{(0)} \rangle \\ &+ \lambda^3 \sum_{l,l' \in \tilde{N}} \langle \Psi_n^{(0)} \,| \frac{\hat{V}|\, \Psi_l^{(0)} \rangle \langle \Psi_l^{(0)} \,|\hat{V}|\, \Psi_{l'}^{(0)} \rangle \langle \Psi_{l'}^{(0)} \,|\hat{V}}{\left(E_n - E_l^{(0)}\right)\left(E_n - E_{l'}^{(0)}\right)} |\, \Psi_n^{(0)} \rangle \\ &+ \lambda^4 \sum_{l,l',l'' \in \tilde{N}} \langle \Psi_n^{(0)} \,| \frac{\hat{V}|\, \Psi_l^{(0)} \rangle \langle \Psi_l^{(0)} \,|\hat{V}|\, \Psi_{l'}^{(0)} \rangle \langle \Psi_{l'}^{(0)} \,|\hat{V}|\, \Psi_{l''}^{(0)} \rangle \langle \Psi_{l''}^{(0)} \,|\hat{V}}{\left(E_n - E_l^{(0)}\right)\left(E_n - E_{l'}^{(0)}\right)\left(E_n - E_{l''}^{(0)}\right)} |\, \Psi_n^{(0)} \rangle + \dots\,. \end{aligned} \tag{3.59}$$

Due to (3.2) and (3.4) we have

$$E_n^{(0)} = \langle \Psi_n^{(0)} \,|\hat{H}^{(0)}|\, \Psi_n^{(0)} \rangle\,. \tag{3.60}$$

Furthermore, we define the matrix element of the perturbed part of the Hamiltonian

$$V_{n,m} = \langle \Psi_n^{(0)} | \hat{V} | \Psi_m^{(0)} \rangle . \tag{3.61}$$

With (3.60) and (3.61) we rewrite (3.59) as

$$\begin{aligned} E_n =& E_n^{(0)} + \lambda V_{n,n} \\ &+ \lambda^2 \sum_{l \in \tilde{N}} \frac{V_{n,l} V_{l,n}}{E_n - E_l^{(0)}} \\ &+ \lambda^3 \sum_{l,l' \in \tilde{N}} \frac{V_{n,l} V_{l,l'} V_{l',n}}{\left(E_n - E_l^{(0)}\right)\left(E_n - E_{l'}^{(0)}\right)} \\ &+ \lambda^4 \sum_{l,l',l'' \in \tilde{N}} \frac{V_{n,l} V_{l,l'} V_{l',l''} V_{l'',n}}{\left(E_n - E_l^{(0)}\right)\left(E_n - E_{l'}^{(0)}\right)\left(E_n - E_{l''}^{(0)}\right)} + \dots . \end{aligned} \tag{3.62}$$

Note that, due to the non-linearity in E_n, equation (3.62) represents a self-consistency equation for the energy eigenvalue E_n. Furthermore, we observe up to fourth that every order in λ consists of only one single term. Since we have $n \neq l, l', l''$, the denominator is never zero and thence no divergency occurs in this perturbative expansion of the perturbed ground-state Energy E_n.

3.3.4 Two States

Now we consider the case that $\hat{P}$ consists of two states, namely

$$\hat{P} = \hat{P}_n + \hat{P}_{n'} . \tag{3.63}$$

We insert this into (3.35):

$$\left(\hat{P}_n + \hat{P}_{n'}\right) \hat{H}_{\text{eff}} \left(\hat{P}_n + \hat{P}_{n'}\right) | \Psi_m \rangle = E_m \left(\hat{P}_n + \hat{P}_{n'}\right) | \Psi_m \rangle . \tag{3.64}$$

Expanding yields

$$\left(\hat{P}_n \hat{H}_{\text{eff}} \hat{P}_n + \hat{P}_n \hat{H}_{\text{eff}} \hat{P}_{n'} + \hat{P}_{n'} \hat{H}_{\text{eff}} \hat{P}_n + \hat{P}_{n'} \hat{H}_{\text{eff}} \hat{P}_{n'}\right) | \Psi_m \rangle = \left(E_m \hat{P}_n + E_m \hat{P}_{n'}\right) | \Psi_m \rangle . \tag{3.65}$$

We multiply from the left with $\langle \Psi_n^{(0)} |$ and expand

$$\langle\,\Psi_n^{(0)}\,|\hat{P}_n\hat{H}_{\rm eff}\hat{P}_n|\,\Psi_m\,\rangle + \langle\,\Psi_n^{(0)}\,|\hat{P}_n\hat{H}_{\rm eff}\hat{P}_{n'}|\,\Psi_m\,\rangle + \langle\,\Psi_n^{(0)}\,|\hat{P}_{n'}\hat{H}_{\rm eff}\hat{P}_n|\,\Psi_m\,\rangle$$
$$+\,\langle\,\Psi_n^{(0)}\,|\hat{P}_{n'}\hat{H}_{\rm eff}\hat{P}_{n'}|\,\Psi_m\,\rangle = \langle\,\Psi_n^{(0)}\,|E_m\hat{P}_n|\,\Psi_m\,\rangle + \langle\,\Psi_n^{(0)}\,|E_m\hat{P}_{n'}|\,\Psi_m\,\rangle\,. \tag{3.66}$$

Taking into account (3.4)–(3.6) this reduces to

$$\langle\,\Psi_n^{(0)}\,|\hat{H}_{\rm eff}|\,\Psi_n^{(0)}\,\rangle\langle\,\Psi_n^{(0)}\,|\,\Psi_m\,\rangle + \langle\,\Psi_n^{(0)}\,|\hat{H}_{\rm eff}|\,\Psi_{n'}^{(0)}\,\rangle\langle\,\Psi_{n'}^{(0)}\,|\,\Psi_m\,\rangle = E_m\langle\,\Psi_n^{(0)}\,|\,\Psi_m\,\rangle\,. \tag{3.67}$$

With defining the matrix elements

$$H_{{\rm eff},n,n'} = \langle\,\Psi_n^{(0)}\,|\hat{H}_{\rm eff}|\,\Psi_{n'}^{(0)}\,\rangle\,, \tag{3.68}$$

(3.67) reduces to

$$H_{{\rm eff},n,n}\langle\,\Psi_n^{(0)}\,|\,\Psi_m\,\rangle + H_{{\rm eff},n,n'}\langle\,\Psi_{n'}^{(0)}\,|\,\Psi_m\,\rangle = E_m\langle\,\Psi_n^{(0)}\,|\,\Psi_m\,\rangle\,. \tag{3.69}$$

Now we multiply (3.65) from the left with $\langle\,\Psi_{n'}^{(0)}\,|$ and obtain, correspondingly

$$\langle\,\Psi_{n'}^{(0)}\,|\hat{H}_{\rm eff}|\,\Psi_n^{(0)}\,\rangle\langle\,\Psi_n^{(0)}\,|\,\Psi_m\,\rangle + \langle\,\Psi_{n'}^{(0)}\,|\hat{H}_{\rm eff}|\,\Psi_{n'}^{(0)}\,\rangle\langle\,\Psi_{n'}^{(0)}\,|\,\Psi_m\,\rangle = E_m\langle\,\Psi_{n'}^{(0)}\,|\,\Psi_m\,\rangle\,. \tag{3.70}$$

which reduces with (3.68) to

$$H_{{\rm eff},n',n}\langle\,\Psi_n^{(0)}\,|\,\Psi_m\,\rangle + H_{{\rm eff},n',n'}\langle\,\Psi_{n'}^{(0)}\,|\,\Psi_m\,\rangle = E_m\langle\,\Psi_{n'}^{(0)}\,|\,\Psi_m\,\rangle\,. \tag{3.71}$$

We combine (3.69) and (3.71) in form of

$$\begin{pmatrix} H_{{\rm eff},n,n}\langle\,\Psi_n^{(0)}\,|\,\Psi_m\,\rangle & H_{{\rm eff},n,n'}\langle\,\Psi_{n'}^{(0)}\,|\,\Psi_m\,\rangle \\ H_{{\rm eff},n',n}\langle\,\Psi_n^{(0)}\,|\,\Psi_m\,\rangle & H_{{\rm eff},n',n'}\langle\,\Psi_{n'}^{(0)}\,|\,\Psi_m\,\rangle \end{pmatrix} = E_m \begin{pmatrix} \langle\,\Psi_n^{(0)}\,|\,\Psi_m\,\rangle \\ \langle\,\Psi_{n'}^{(0)}\,|\,\Psi_m\,\rangle \end{pmatrix}. \tag{3.72}$$

In matrix notation this gives

$$\begin{pmatrix} H_{\text{eff},n,n} & H_{\text{eff},n,n'} \\ H_{\text{eff},n',n} & H_{\text{eff},n',n'} \end{pmatrix} \begin{pmatrix} \langle\, \Psi_n^{(0)} \,|\, \Psi_m \,\rangle \\ \langle\, \Psi_{n'}^{(0)} \,|\, \Psi_m \,\rangle \end{pmatrix} = E_m \begin{pmatrix} \langle\, \Psi_n^{(0)} \,|\, \Psi_m \,\rangle \\ \langle\, \Psi_{n'}^{(0)} \,|\, \Psi_m \,\rangle \end{pmatrix} , \tag{3.73}$$

which corresponds to

$$\left[\begin{pmatrix} H_{\text{eff},n,n} & H_{\text{eff},n,n'} \\ H_{\text{eff},n',n} & H_{\text{eff},n',n'} \end{pmatrix} - \mathbb{1} E_m \right] \begin{pmatrix} \langle\, \Psi_n^{(0)} \,|\, \Psi_m \,\rangle \\ \langle\, \Psi_{n'}^{(0)} \,|\, \Psi_m \,\rangle \end{pmatrix} = 0 \,. \tag{3.74}$$

As the vector in (3.74) is supposed to be non-zero, we conclude

$$\text{Det} \begin{pmatrix} H_{\text{eff},n,n} - E_m & H_{\text{eff},n,n'} \\ H_{\text{eff},n',n} & H_{\text{eff},n',n'} - E_m \end{pmatrix} = 0 \,. \tag{3.75}$$

Note that

$$\Gamma = \begin{pmatrix} H_{\text{eff},n,n} & H_{\text{eff},n,n'} \\ H_{\text{eff},n',n} & H_{\text{eff},n',n'} \end{pmatrix} = \begin{pmatrix} A & B \\ C & D \end{pmatrix} \tag{3.76}$$

represents a 2×2 matrix, since the projection operator $\hat{P}$ in (3.63) consists of two states. The elements A, B, C and D of the matrix Γ can be calculated up to any order in λ, just as in subsection 2.3.1.

3.4 Rayleigh-Schrödinger Perturbation Theory

In this section, we show how to get the well-known Rayleigh-Schrödinger perturbation theory out of the Brillouin-Wigner perturbation theory. We will do this first for the non-degenerate case, and then for the degenerate case.

3.4.1 Non-Degenerate Case

We obtain the non-degenerate Rayleigh-Schrödinger perturbation theory from the Brillouin-Wigner perturbation theory by performing a Taylor expansion in λ for the energy eigenvalue E_n. We do this explicitly for the one-state example of equation (3.62). We start with the Taylor expansion of the full energy eigenvalue

$$E_n = \sum_{\sigma} \lambda^{\sigma} E_n^{(\sigma)} \,. \tag{3.77}$$

Since we have in (3.62) evaluated the energy eigenvalue up to fourth order in λ, i. e. the resolvent up to second order in λ, we do not get any reliable correction terms if we now go to any higher order in λ than 4. Therefore, we insert the expansion (3.77) up to the second order in λ in (3.62) with $\tilde{N} = n$, thus no degeneracy is considered

$$\begin{aligned}
E_n =& E_n^{(0)} + \lambda V_{n,n} \\
&+ \lambda^2 \sum_{l \neq n} \left[V_{n,l} V_{l,n} \left(E_n^{(0)} + \lambda E_n^{(1)} + \lambda^2 E_n^{(2)} - E_l^{(0)} \right)^{-1} \right] \\
&+ \lambda^3 \sum_{l,l' \neq n} \Big\{ V_{n,l} V_{l,l'} V_{l',n} \left[\left(E_n^{(0)} + \lambda E_n^{(1)} + \lambda^2 E_n^{(2)} - E_l^{(0)} \right) \right. \\
&\left. \times \left(E_n^{(0)} + \lambda E_n^{(1)} + \lambda^2 E_n^{(2)} - E_{l'}^{(0)} \right) \right]^{-1} \Big\} \\
&+ \lambda^4 \sum_{l,l',l'' \neq n} \Big\{ V_{n,l} V_{l,l'} V_{l',l''} V_{l'',n} \left[\left(E_n^{(0)} + \lambda E_n^{(1)} + \lambda^2 E_n^{(2)} - E_l^{(0)} \right) \right. \\
&\left. \times \left(E_n^{(0)} + \lambda E_n^{(1)} + \lambda^2 E_n^{(2)} - E_{l'}^{(0)} \right) \left(E_n^{(0)} + \lambda E_n^{(1)} + \lambda^2 E_n^{(2)} - E_{l''}^{(0)} \right) \right]^{-1} \Big\} + \dots \,.
\end{aligned} \tag{3.78}$$

We simplify now the denominators by neglecting all terms, which lead to higher orders in λ than 4:

$$\begin{aligned}
E_n =& E_n^{(0)} + \lambda V_{n,n} \\
&+ \lambda^2 \sum_{l \neq n} \frac{V_{n,l} V_{l,n}}{E_n^{(0)} - E_l^{(0)} + \lambda E_n^{(1)} + \lambda^2 E_n^{(2)}} \\
&+ \lambda^3 \sum_{l,l' \neq n} \frac{V_{n,l} V_{l,l'} V_{l',n}}{\left(E_n^{(0)} - E_l^{(0)} \right) \left(E_n^{(0)} - E_{l'}^{(0)} \right) + \lambda E_n^{(1)} \left(2E_n^{(0)} - E_l^{(0)} - E_{l'}^{(0)} \right)} \\
&+ \lambda^4 \sum_{l,l',l'' \neq n} \frac{V_{n,l} V_{l,l'} V_{l',l''} V_{l'',n}}{\left(E_n^{(0)} - E_l^{(0)} \right) \left(E_n^{(0)} - E_{l'}^{(0)} \right) \left(E_n^{(0)} - E_{l''}^{(0)} \right)} \,.
\end{aligned} \tag{3.79}$$

We can now extract the respective corrections for the energy term. To do so, we have to sort the correction terms in orders of λ, for which we have to get the λ out of the denominator into the numerator. So we do a Taylor approximation according to

$$\begin{aligned}
E_n =& E_n^{(0)} + \lambda V_{n,n} \\
&+ \lambda^2 \sum_{l \neq n} \frac{V_{n,l} V_{l,n}}{E_n^{(0)} - E_l^{(0)}} \frac{1}{1 + \lambda \frac{E_n^{(1)}}{E_n^{(0)} - E_l^{(0)}} + \lambda^2 \frac{E_n^{(2)}}{E_n^{(0)} - E_l^{(0)}}} \\
&+ \lambda^3 \sum_{l,l' \neq n} \frac{V_{n,l} V_{l,l'} V_{l',n}}{\left(E_n^{(0)} - E_l^{(0)}\right)\left(E_n^{(0)} - E_{l'}^{(0)}\right)} \frac{1}{1 + \lambda \frac{E_n^{(1)}\left(2E_n^{(0)} - E_l^{(0)} - E_{l'}^{(0)}\right)}{\left(E_n^{(0)} - E_l^{(0)}\right)\left(E_n^{(0)} - E_{l'}^{(0)}\right)}} \\
&+ \lambda^4 \sum_{l,l',l'' \neq n} \frac{V_{n,l} V_{l,l'} V_{l',l''} V_{l'',n}}{\left(E_n^{(0)} - E_l^{(0)}\right)\left(E_n^{(0)} - E_{l'}^{(0)}\right)\left(E_n^{(0)} - E_{l''}^{(0)}\right)} + \dots ,
\end{aligned} \tag{3.80}$$

which yields

$$\begin{aligned}
E_n =& E_n^{(0)} + \lambda V_{n,n} \\
&+ \lambda^2 \sum_{l \neq n} \frac{V_{n,l} V_{l,n}}{E_n^{(0)} - E_l^{(0)}} \left\{ 1 - \lambda \frac{E_n^{(1)}}{E_n^{(0)} - E_l^{(0)}} + \lambda^2 \left[\left(\frac{E_n^{(1)}}{E_n^{(0)} - E_l^{(0)}} \right)^2 - \frac{E_n^{(2)}}{E_n^{(0)} - E_l^{(0)}} \right] \right\} \\
&+ \lambda^3 \sum_{l,l' \neq n} \frac{V_{n,l} V_{l,l'} V_{l',n}}{\left(E_n^{(0)} - E_l^{(0)}\right)\left(E_n^{(0)} - E_{l'}^{(0)}\right)} \left[1 - \lambda \frac{E_n^{(1)}\left(2E_n^{(0)} - E_l^{(0)} - E_{l'}^{(0)}\right)}{\left(E_n^{(0)} - E_l^{(0)}\right)\left(E_n^{(0)} - E_{l'}^{(0)}\right)} \right] \\
&+ \lambda^4 \sum_{l,l',l'' \neq n} \frac{V_{n,l} V_{l,l'} V_{l',l''} V_{l'',n}}{\left(E_n^{(0)} - E_l^{(0)}\right)\left(E_n^{(0)} - E_{l'}^{(0)}\right)\left(E_n^{(0)} - E_{l''}^{(0)}\right)} + \dots .
\end{aligned} \tag{3.81}$$

From this we can read off the first-order correction

$$E_n^{(1)} = V_{n,n} , \tag{3.82}$$

the second-order term

$$E_n^{(2)} = \sum_{l \neq n} \frac{V_{n,l} V_{l,n}}{E_n^{(0)} - E_l^{(0)}} , \tag{3.83}$$

as well as the third order

$$E_n^{(3)} = \sum_{l,l' \neq n} \frac{V_{n,l} V_{l,l'} V_{l',n}}{\left(E_n^{(0)} - E_l^{(0)}\right)\left(E_n^{(0)} - E_{l'}^{(0)}\right)} - \sum_{l \neq n} \frac{V_{n,l} V_{l,n} V_{n,n}}{\left(E_n^{(0)} - E_l^{(0)}\right)^2} \,. \tag{3.84}$$

Note that (3.82)–(3.84) agree with [31, (3.516)]. Corresponding, the fourth-order result reads

$$\begin{aligned} E_n^{(4)} = & \sum_{l,l',l'' \neq n} \frac{V_{n,l} V_{l,l'} V_{l',l''} V_{l'',n}}{\left(E_n^{(0)} - E_l^{(0)}\right)\left(E_n^{(0)} - E_{l'}^{(0)}\right)\left(E_n^{(0)} - E_{l''}^{(0)}\right)} \\ & - \sum_{l,l' \neq n} \frac{V_{n,l} V_{l,l'} V_{l',n} V_{n,n} \left(2E_n^{(0)} - E_l^{(0)} - E_{l'}^{(0)}\right)}{\left(E_n^{(0)} - E_l^{(0)}\right)^2 \left(E_n^{(0)} - E_{l'}^{(0)}\right)^2} \\ & + \sum_{l \neq n} \frac{V_{n,l} V_{l,n}}{E_n^{(0)} - E_l^{(0)}} \left[\left(\frac{V_{n,n}}{E_n^{(0)} - E_l^{(0)}} \right)^2 - \frac{V_{n,l} V_{l,n}}{\left(E_n^{(0)} - E_l^{(0)}\right)^2} \right] , \end{aligned} \tag{3.85}$$

which coincides with [32]. Note that we have more terms here than in the Brillouin-Wigner perturbation theory up to the same order in λ.

3.4.2 Degenerate Case

In this subsection, we derive the energy correction terms of the degenerate Rayleigh-Schrödinger perturbation theory up to first order. For this, we start with the two-state matrix (3.76) and take every entry up to first order in λ

$$\Gamma^{(1)} = \begin{pmatrix} \langle\, n \,| E_n^{(0)} + \lambda \hat{V} |\, n \,\rangle & \langle\, n \,| E_{n+1}^{(0)} + \lambda \hat{V} |\, n+1 \,\rangle \\ \langle\, n+1 \,| E_n^{(0)} + \lambda \hat{V} |\, n \,\rangle & \langle\, n+1 \,| E_{n+1}^{(0)} + \lambda \hat{V} |\, n+1 \,\rangle \end{pmatrix} = \begin{pmatrix} E_n^{(0)} & \lambda V_{n,n+1} \\ \lambda V_{n+1,n} & E_{n+1}^{(0)} \end{pmatrix} . \tag{3.86}$$

Out of this matrix, obtained by Brillouin-Wigner perturbation theory, the same results can be calculated as from degenerate Rayleigh-Schrödinger perturbation theory.

4 Approximative Solutions

The perturbed ground-state energy E_n obtained by Brillouin-Wigner perturbation theory, cannot be solved explicitly for E_n, and therefore numerical methods are needed for further calculations. Another approach is to apply approximations, like the two presented in this chapter.
The first approximation is a linearization of the two-state approach, which reproduces [24]. This gives a good qualitative insight into the condensate density $\Psi^*\Psi$, but the phase boundary is quite imprecise.
The second approximation is based on applying a Taylor series on the fourth-order Brillouin-Wigner perturbation theory for the two-state approach, which gives the fourth-order Rayleigh-Schrödinger perturbation theory, just as shown in the previous section. This reproduces [23], which yields the phase-boundary in the mean-field approximation, but gives a non-physical order parameter like in FIG. 2.3.
However, these approximations allow us to reproduce with our theory two established results, which indicates that our theory is right.

4.1 Linearized Approach

In this section, the problem, that the perturbed ground-state Energy E_n is only obtained self-consistently in Brillouin-Wigner perturbation theory, is simplified a lot by linearization. This allows to maintain a fully analytical solution, which bears some astounding qualitative insights, but is, however, quantitatively quite inaccurate.

We start within the two-state approach by taking the matrix Γ from (3.76), and calculate its entries up to the first order. To do so, we consider λ being small, so that all orders in λ^2 or higher can be neglected. This leads to the linearized matrix

$$\Gamma^{(1)} = \begin{pmatrix} A & B \\ \\ C & D \end{pmatrix}, \tag{4.1}$$

where the matrix entries are calculated from the effective Hamiltonian. For the diagonal matrix element $H_{\text{eff},n,n}$ according to (3.68), we obtain by using the primal split (2.20)

$$A = H_{\text{eff},n,n} = \langle\, n\,|\hat{\mathcal{H}}^{(0)}|\, n\,\rangle + \lambda\langle\, n\,|\hat{\mathcal{V}}|\, n\,\rangle$$
$$= \mathcal{E}_n^{(0)} - \lambda J z \Psi^* \langle\, n\,|\hat{a}|\, n\,\rangle - \lambda J z \Psi \langle\, n\,|\hat{a}^\dagger|\, n\,\rangle\,. \tag{4.2}$$

Note that the algebraic relations from (2.5) prescribe how the operators $\hat{a}$ and $\hat{a}^\dagger$ are applied to the state $|\, n\,\rangle$. With the orthonormality relation $\langle\, m\,|\, n\,\rangle = \delta_{m,n}$ the formula is simplified, and since $m \neq n$, the final result is obtained

$$A = \mathcal{E}_n^{(0)} = E_n^{(0)} + J z \lambda \Psi^* \Psi\,. \tag{4.3}$$

A similar calculation yields for D

$$D = H_{\text{eff},n+1,n+1} = E_{n+1}^{(0)} + J z \lambda \Psi^* \Psi\,. \tag{4.4}$$

For the off-diagonal matrix elements, we calculate

$$B = H_{\text{eff},n,n+1} = -\lambda J z \Psi^* \sqrt{n+1}\,, \tag{4.5}$$

while a similar calculation yields for C

$$C = H_{\text{eff},n+1,n} = -\lambda J z \Psi \sqrt{n+1}\,. \tag{4.6}$$

We insert these results in (3.75) with $m = n$ to get

$$\text{Det}\begin{pmatrix} E_n^{(0)} + J z \lambda \Psi^* \Psi - E_n & -\lambda J z \Psi^* \sqrt{n+1} \\ -\lambda J z \Psi \sqrt{n+1} & E_{n+1}^{(0)} + J z \lambda \Psi^* \Psi - E_n \end{pmatrix} = 0\,. \tag{4.7}$$

Now we calculate the determinant and bring the result in a polynomial shape

$$E_n^2 + E_n \left(-E_n^{(0)} - E_{n+1}^{(0)} - 2 J z \lambda \Psi^* \Psi\right) + E_n^{(0)} \left(E_{n+1}^{(0)} + J z \lambda \Psi^* \Psi\right)$$
$$+ J z \lambda \Psi^* \Psi \left[E_{n+1}^{(0)} + J z \lambda \left(\Psi^* \Psi - n - 1\right)\right] = 0\,, \tag{4.8}$$

which yields with inserting $E_n^{(0)} = \frac{1}{2}Un\,(n-1) - \mu n$ and $E_{n+1}^{(0)} = \frac{1}{2}Un\,(n+1) - \mu\,(n+1)$ the solutions

$$\begin{aligned} E_{n\pm} =& \lambda J z \Psi^* \Psi + \frac{1}{2}\left[\frac{1}{2}Un\,(n-1) - \mu n + \frac{1}{2}Un\,(n+1) - \mu\,(n+1)\right] \\ & \pm \frac{1}{2}\sqrt{(\mu - Un)^2 + 4\lambda^2 J^2 z^2 \Psi^* \Psi\,(n+1)}\,. \end{aligned} \tag{4.9}$$

Now we extremize the energy (4.9) with respect to the condensate density $\Psi^*\Psi$ by applying $\frac{1}{\Psi}\frac{\partial}{\partial \Psi^*}$, while taking into account $\frac{\partial E_n}{\partial \Psi^*} = 0$ and yield

$$0 = \lambda J z \pm \frac{\lambda^2 J^2 z^2\,(n+1)}{\sqrt{(\mu - Un)^2 + 4\lambda^2 J^2 z^2 \Psi^* \Psi\,(n+1)}}\,. \tag{4.10}$$

Solving with respect to $\Psi^*\Psi$ we get

$$\Psi^* \Psi = \frac{\lambda^2 J^2 z^2\,(n+1)^2 - (\mu - Un)^2}{4\lambda^2 J^2 z^2\,(n+1)} = \frac{(n+1)}{4} - \frac{(\mu - Un)^2}{4\lambda^2 J^2 z^2\,(n+1)}\,, \tag{4.11}$$

which turns out to coincide with the formula of Ref. [24].

At the degeneracy we have $J = 0$, which would lead to a quadratic divergent term in (4.11). But since for the degeneracy $E_n^{(0)} = E_{n+1}^{(0)}$, we get $\mu - Un = 0$, which appears as well in the numerator in second order in (4.11). Thus we have no divergence problems here. Since $\mu = Un$ is only valid for the exactly degenerate case, we expand this to $\mu = Un + \varepsilon$ the nearly-degenerate case. If $\varepsilon = 0$, we are at the degeneracy, for positive and negative small ε, we are nearly degenerate and can describe the direct vicinity of the degeneracy like in [24] with

$$\Psi^* \Psi = \frac{(n+1)}{4} - \frac{\varepsilon^2}{4\lambda^2 J^2 z^2\,(n+1)}\,. \tag{4.12}$$

4.2 Fourth-Order Rayleigh-Schrödinger Approach

In this section, we will first go up to the fourth order in the Brillouin-Wigner perturbation theory for the two-state approach, and then perform a Taylor series expansion, which brings us effectively back to the Rayleigh-Schrödinger result of fourth order.

To do so, we have to calculate $H_{\text{eff},n,n}$, $H_{\text{eff},n,n'}$, $H_{\text{eff},n',n}$ and $H_{\text{eff},n',n'}$ up to the fourth order in λ. We use the primal split of the Hamiltonian according to (2.20). For the first matrix element, we have to evaluate

$$\begin{aligned} H_{\text{eff},n,n} = \langle\, n\,|\hat{H}_{\text{eff}}|\, n\,\rangle =& \langle\, n\,|\mathcal{E}_n^{(0)}|\, n\,\rangle + \lambda\langle\, n\,|\hat{\mathcal{V}}|\, n\,\rangle + \lambda^2 \sum_{l\in\tilde{N}} \frac{\langle\, n\,|\hat{\mathcal{V}}|\, l\,\rangle\langle\, l\,|\hat{\mathcal{V}}|\, n\,\rangle}{E_n - \mathcal{E}_l^{(0)}} \\ &+ \lambda^3 \sum_{l,l'\in\tilde{N}} \frac{\langle\, n\,|\hat{\mathcal{V}}|\, l\,\rangle\langle\, l\,|\hat{\mathcal{V}}|\, l'\,\rangle\langle\, l'\,|\hat{\mathcal{V}}|\, n\,\rangle}{\left(E_n - \mathcal{E}_l^{(0)}\right)\left(E_n - \mathcal{E}_{l'}^{(0)}\right)} \\ &+ \lambda^4 \sum_{l,l',l''\in\tilde{N}} \frac{\langle\, n\,|\hat{\mathcal{V}}|\, l\,\rangle\langle\, l\,|\hat{\mathcal{V}}|\, l'\,\rangle\langle\, l'\,|\hat{\mathcal{V}}|\, l''\,\rangle\langle\, l''\,|\hat{\mathcal{V}}|\, n\,\rangle}{\left(E_n - \mathcal{E}_l^{(0)}\right)\left(E_n - \mathcal{E}_{l'}^{(0)}\right)\left(E_n - \mathcal{E}_{l''}^{(0)}\right)}\,. \end{aligned} \tag{4.13}$$

Here the matrix elements read

$$\langle\, l\,|\hat{\mathcal{V}}|\, n\,\rangle = -Jz\left(\Psi^*\sqrt{n}\,\delta_{l,n-1} + \Psi\sqrt{n+1}\,\delta_{l,n+1}\right)\,. \tag{4.14}$$

Since the sum takes only $l \in \tilde{N}$ into account, and thus $l \neq n, n+1$, we can simplify (4.14) to

$$\langle\, l\,|\hat{\mathcal{V}}|\, n\,\rangle = -Jz\Psi^*\sqrt{n}\,\delta_{l,n-1}\,, \tag{4.15}$$

which necessitates for a non-zero solution $l = n-1$. By consecutively applying this procedure to (4.13), we get for the respective matrix elements

$$H_{\text{eff},n,n} = \mathcal{E}_n^{(0)} + \lambda^2 \frac{J^2 z^2 \Psi^* \Psi n}{E_n - \mathcal{E}_{n-1}^{(0)}} + \lambda^4 \frac{J^4 z^4 \Psi^{*2} \Psi^2 (n-1)\, n}{\left(E_n - \mathcal{E}_{n-1}^{(0)}\right)^2 \left(E_n - \mathcal{E}_{n-2}^{(0)}\right)}\,, \tag{4.16}$$

$$H_{\text{eff},n,n'} = -\lambda J z \Psi^* \sqrt{n+1}\,, \tag{4.17}$$

$$H_{\text{eff},n',n} = -\lambda J z \Psi \sqrt{n+1}\,, \tag{4.18}$$

$$H_{\text{eff},n',n'} = \mathcal{E}_{n+1}^{(0)} + \lambda^2 \frac{J^2 z^2 \Psi^* \Psi\,(n+2)}{E_n - \mathcal{E}_{n+2}^{(0)}} + \lambda^4 \frac{J^4 z^4 \Psi^{*2} \Psi^2\,(n+2)\,(n+3)}{\left(E_n - \mathcal{E}_{n+2}^{(0)}\right)^2 \left(E_n - \mathcal{E}_{n+3}^{(0)}\right)}\,. \tag{4.19}$$

We evaluate now the determinant (3.75) with $m = n$

$$\mathrm{Det}\begin{pmatrix} H_{\mathrm{eff},n,n} - E_n & H_{\mathrm{eff},n,n'} \\ H_{\mathrm{eff},n',n} & H_{\mathrm{eff},n',n'} - E_n \end{pmatrix} = 0\,, \tag{4.20}$$

which is

$$\left(H_{\mathrm{eff},n,n} - E_n\right)\left(H_{\mathrm{eff},n',n'} - E_n\right) - H_{\mathrm{eff},n',n}H_{\mathrm{eff},n,n'} = 0\,, \tag{4.21}$$

and leads to the polynomial

$$E_n^2 - E_n\left(H_{\mathrm{eff},n,n} + H_{\mathrm{eff},n',n'}\right) + H_{\mathrm{eff},n,n}H_{\mathrm{eff},n',n'} - H_{\mathrm{eff},n',n}H_{\mathrm{eff},n,n'} = 0\,. \tag{4.22}$$

By inserting the respective matrix elements of the effective Hamiltonians (4.16)–(4.19) we get

$$\begin{aligned}
&E_n^2 - E_n\left[\mathcal{E}_n^{(0)} + \lambda^2\frac{J^2z^2\Psi^*\Psi n}{E_n - \mathcal{E}_{n-1}^{(0)}} + \lambda^4\frac{J^4z^4\Psi^{*2}\Psi^2\,(n-1)\,n}{\left(E_n - \mathcal{E}_{n-1}^{(0)}\right)^2\left(E_n - \mathcal{E}_{n-2}^{(0)}\right)}\right.\\
&\left.+\mathcal{E}_{n+1}^{(0)} + \lambda^2\frac{J^2z^2\Psi^*\Psi\,(n+2)}{E_n - \mathcal{E}_{n+2}^{(0)}} + \lambda^4\frac{J^4z^4\Psi^{*2}\Psi^2\,(n+2)\,(n+3)}{\left(E_n - \mathcal{E}_{n+2}^{(0)}\right)^2\left(E_n - \mathcal{E}_{n+3}^{(0)}\right)}\right]\\
&+\left[\mathcal{E}_n^{(0)} + \lambda^2\frac{J^2z^2\Psi^*\Psi n}{E_n - \mathcal{E}_{n-1}^{(0)}} + \lambda^4\frac{J^4z^4\Psi^{*2}\Psi^2\,(n-1)\,n}{\left(E_n - \mathcal{E}_{n-1}^{(0)}\right)^2\left(E_n - \mathcal{E}_{n-2}^{(0)}\right)}\right]\\
&\times\left[\mathcal{E}_{n+1}^{(0)} + \lambda^2\frac{J^2z^2\Psi^*\Psi\,(n+2)}{E_n - \mathcal{E}_{n+2}^{(0)}} + \lambda^4\frac{J^4z^4\Psi^{*2}\Psi^2\,(n+2)\,(n+3)}{\left(E_n - \mathcal{E}_{n+2}^{(0)}\right)^2\left(E_n - \mathcal{E}_{n+3}^{(0)}\right)}\right]\\
&-\left(-\lambda Jz\Psi\sqrt{n+1}\right)\left(-\lambda Jz\Psi^*\sqrt{n+1}\right) = 0\,.
\end{aligned} \tag{4.23}$$

We simplify by taking into account that we only have to consider orders of λ up to four

$$
\begin{aligned}
&E_n^2 - E_n\mathcal{E}_n^{(0)} - \lambda^2 E_n \frac{J^2 z^2 \Psi^* \Psi n}{E_n - \mathcal{E}_{n-1}^{(0)}} - \lambda^4 E_n \frac{J^4 z^4 \Psi^{*2} \Psi^2 \left(n-1\right) n}{\left(E_n - \mathcal{E}_{n-1}^{(0)}\right)^2 \left(E_n - \mathcal{E}_{n-2}^{(0)}\right)} \\
&- E_n\mathcal{E}_{n+1}^{(0)} - \lambda^2 E_n \frac{J^2 z^2 \Psi^* \Psi \left(n+2\right)}{E_n - \mathcal{E}_{n+2}^{(0)}} - \lambda^4 E_n \frac{J^4 z^4 \Psi^{*2} \Psi^2 \left(n+2\right)\left(n+3\right)}{\left(E_n - \mathcal{E}_{n+2}^{(0)}\right)^2 \left(E_n - \mathcal{E}_{n+3}^{(0)}\right)} \\
&+ \mathcal{E}_n^{(0)}\mathcal{E}_{n+1}^{(0)} + \lambda^2 \mathcal{E}_n^{(0)} \frac{J^2 z^2 \Psi^* \Psi \left(n+2\right)}{E_n - \mathcal{E}_{n+2}^{(0)}} + \lambda^4 \mathcal{E}_n^{(0)} \frac{J^4 z^4 \Psi^{*2} \Psi^2 \left(n+2\right)\left(n+3\right)}{\left(E_n - \mathcal{E}_{n+2}^{(0)}\right)^2 \left(E_n - \mathcal{E}_{n+3}^{(0)}\right)} \\
&+ \lambda^2 \mathcal{E}_{n+1}^{(0)} \frac{J^2 z^2 \Psi^* \Psi n}{E_n - \mathcal{E}_{n-1}^{(0)}} + \lambda^4 \frac{J^4 z^4 \Psi^{*2} \Psi^2 n \left(n+2\right)}{\left(E_n - \mathcal{E}_{n-1}^{(0)}\right)\left(E_n - \mathcal{E}_{n+2}^{(0)}\right)} \\
&+ \lambda^4 \mathcal{E}_{n+1}^{(0)} \frac{J^4 z^4 \Psi^{*2} \Psi^2 \left(n-1\right) n}{\left(E_n - \mathcal{E}_{n-1}^{(0)}\right)^2 \left(E_n - \mathcal{E}_{n-2}^{(0)}\right)} - \lambda^2 J^2 z^2 \Psi\Psi^* \left(n+1\right) = 0\,. \qquad (4.24)
\end{aligned}
$$

In this formula, λ turns out to appear only in the power two and four. This motivates to perform a corresponding Taylor series for E_n as

$$
E_n \approx \mathcal{E}_n^{(0)} + \lambda^2 E_n^{(2)} + \lambda^4 E_n^{(4)}\,, \qquad (4.25)
$$

and therefore follows

$$
\frac{1}{E_n - \mathcal{E}_{n-1}^{(0)}} \approx \frac{1}{\mathcal{E}_n^{(0)} - \mathcal{E}_{n-1}^{(0)}} - \frac{\lambda^2 E_n^{(2)}}{\left(\mathcal{E}_n^{(0)} - \mathcal{E}_{n-1}^{(0)}\right)^2} \qquad (4.26)
$$

and

$$
\frac{1}{E_n - \mathcal{E}_{n+2}^{(0)}} \approx \frac{1}{\mathcal{E}_n^{(0)} - \mathcal{E}_{n+2}^{(0)}} - \frac{\lambda^2 E_n^{(2)}}{\left(\mathcal{E}_n^{(0)} - \mathcal{E}_{n+2}^{(0)}\right)^2}\,. \qquad (4.27)
$$

We insert (4.25)–(4.27) into (4.24) and neglect again all terms of λ higher than four.

$$
\begin{aligned}
&\left(\mathcal{E}_n^{(0)}+\lambda^2E_n^{(2)}+\lambda^4E_n^{(4)}\right)^2-\left(\mathcal{E}_n^{(0)}+\lambda^2E_n^{(2)}+\lambda^4E_n^{(4)}\right)\mathcal{E}_n^{(0)}\\
&-\lambda^2\left(\mathcal{E}_n^{(0)}+\lambda^2E_n^{(2)}\right)J^2z^2\Psi^*\Psi n\left[\frac{1}{\mathcal{E}_n^{(0)}-\mathcal{E}_{n-1}^{(0)}}-\frac{\lambda^2E_n^{(2)}}{\left(\mathcal{E}_n^{(0)}-\mathcal{E}_{n-1}^{(0)}\right)^2}\right]\\
&-\lambda^4\mathcal{E}_n^{(0)}\frac{J^4z^4\Psi^{*2}\Psi^2\left(n-1\right)n}{\left(\mathcal{E}_n^{(0)}-\mathcal{E}_{n-1}^{(0)}\right)^2\left(\mathcal{E}_n^{(0)}-\mathcal{E}_{n-2}^{(0)}\right)}-\left(\mathcal{E}_n^{(0)}+\lambda^2E_n^{(2)}+\lambda^4E_n^{(4)}\right)\mathcal{E}_{n+1}^{(0)}\\
&-\lambda^2\left(\mathcal{E}_n^{(0)}+\lambda^2E_n^{(2)}\right)J^2z^2\Psi^*\Psi\left(n+2\right)\left[\frac{1}{\mathcal{E}_n^{(0)}-\mathcal{E}_{n+2}^{(0)}}-\frac{\lambda^2E_n^{(2)}}{\left(\mathcal{E}_n^{(0)}-\mathcal{E}_{n+2}^{(0)}\right)^2}\right]\\
&-\lambda^4\mathcal{E}_n^{(0)}\frac{J^4z^4\Psi^{*2}\Psi^2\left(n+2\right)\left(n+3\right)}{\left(\mathcal{E}_n^{(0)}-\mathcal{E}_{n+2}^{(0)}\right)^2\left(\mathcal{E}_n^{(0)}-\mathcal{E}_{n+3}^{(0)}\right)}+\mathcal{E}_n^{(0)}\mathcal{E}_{n+1}^{(0)}\\
&+\lambda^2\mathcal{E}_n^{(0)}J^2z^2\Psi^*\Psi\left(n+2\right)\left[\frac{1}{\mathcal{E}_n^{(0)}-\mathcal{E}_{n+2}^{(0)}}-\frac{\lambda^2E_n^{(2)}}{\left(\mathcal{E}_n^{(0)}-\mathcal{E}_{n+2}^{(0)}\right)^2}\right]\\
&+\lambda^4\mathcal{E}_n^{(0)}\frac{J^4z^4\Psi^{*2}\Psi^2\left(n+2\right)\left(n+3\right)}{\left(\mathcal{E}_n^{(0)}-\mathcal{E}_{n+2}^{(0)}\right)^2\left(\mathcal{E}_n^{(0)}-\mathcal{E}_{n+3}^{(0)}\right)}+\lambda^4\frac{J^4z^4\Psi^{*2}\Psi^2n\left(n+2\right)}{\left(\mathcal{E}_n^{(0)}-\mathcal{E}_{n-1}^{(0)}\right)\left(\mathcal{E}_n^{(0)}-\mathcal{E}_{n+2}^{(0)}\right)}\\
&+\lambda^2\mathcal{E}_{n+1}^{(0)}J^2z^2\Psi^*\Psi n\left[\frac{1}{\mathcal{E}_n^{(0)}-\mathcal{E}_{n-1}^{(0)}}-\frac{\lambda^2E_n^{(2)}}{\left(\mathcal{E}_n^{(0)}-\mathcal{E}_{n-1}^{(0)}\right)^2}\right]\\
&+\lambda^4\mathcal{E}_{n+1}^{(0)}\frac{J^4z^4\Psi^{*2}\Psi^2\left(n-1\right)n}{\left(\mathcal{E}_n^{(0)}-\mathcal{E}_{n-1}^{(0)}\right)^2\left(\mathcal{E}_n^{(0)}-\mathcal{E}_{n-2}^{(0)}\right)}-\lambda^2J^2z^2\Psi\Psi^*\left(n+1\right)=0\,.
\end{aligned}
\tag{4.28}
$$

We expand, neglecting orders of λ higher than four

$$
\begin{aligned}
&\mathcal{E}_n^{(0)2}+\lambda^4E_n^{(2)2}+2\lambda^2\mathcal{E}_n^{(0)}E_n^{(2)}+2\lambda^4\mathcal{E}_n^{(0)}E_n^{(4)}-\mathcal{E}_n^{(0)2}-\lambda^2E_n^{(2)}\mathcal{E}_n^{(0)}-\lambda^4\mathcal{E}_n^{(0)}E_n^{(4)}\\
&-\lambda^2\frac{J^2z^2\Psi^*\Psi n\mathcal{E}_n^{(0)}}{\mathcal{E}_n^{(0)}-\mathcal{E}_{n-1}^{(0)}}-\lambda^4\frac{J^2z^2\Psi^*\Psi nE_n^{(2)}}{\mathcal{E}_n^{(0)}-\mathcal{E}_{n-1}^{(0)}}+\lambda^4\frac{J^2z^2\Psi^*\Psi nE_n^{(2)}\mathcal{E}_n^{(0)}}{\left(\mathcal{E}_n^{(0)}-\mathcal{E}_{n-1}^{(0)}\right)^2}\\
&-\lambda^4\mathcal{E}_n^{(0)}\frac{J^4z^4\Psi^{*2}\Psi^2\left(n-1\right)n}{\left(\mathcal{E}_n^{(0)}-\mathcal{E}_{n-1}^{(0)}\right)^2\left(\mathcal{E}_n^{(0)}-\mathcal{E}_{n-2}^{(0)}\right)}-\mathcal{E}_n^{(0)}\mathcal{E}_{n+1}^{(0)}-\lambda^2\mathcal{E}_{n+1}^{(0)}E_n^{(2)}-\lambda^4\mathcal{E}_{n+1}^{(0)}E_n^{(4)}\\
&-\lambda^2\frac{J^2z^2\Psi^*\Psi\left(n+2\right)\mathcal{E}_n^{(0)}}{\mathcal{E}_n^{(0)}-\mathcal{E}_{n+2}^{(0)}}-\lambda^4\frac{J^2z^2\Psi^*\Psi\left(n+2\right)E_n^{(2)}}{\mathcal{E}_n^{(0)}-\mathcal{E}_{n+2}^{(0)}}+\lambda^4\frac{J^2z^2\Psi^*\Psi\left(n+2\right)E_n^{(2)}\mathcal{E}_n^{(0)}}{\left(\mathcal{E}_n^{(0)}-\mathcal{E}_{n+2}^{(0)}\right)^2}\\
&-\lambda^4\mathcal{E}_n^{(0)}\frac{J^4z^4\Psi^{*2}\Psi^2\left(n+2\right)\left(n+3\right)}{\left(\mathcal{E}_n^{(0)}-\mathcal{E}_{n+2}^{(0)}\right)^2\left(\mathcal{E}_n^{(0)}-\mathcal{E}_{n+3}^{(0)}\right)}+\mathcal{E}_n^{(0)}\mathcal{E}_{n+1}^{(0)}\\
&+\lambda^2\frac{\mathcal{E}_n^{(0)}J^2z^2\Psi^*\Psi\left(n+2\right)}{\mathcal{E}_n^{(0)}-\mathcal{E}_{n+2}^{(0)}}-\lambda^4\frac{\mathcal{E}_n^{(0)}E_n^{(2)}J^2z^2\Psi^*\Psi\left(n+2\right)}{\left(\mathcal{E}_n^{(0)}-\mathcal{E}_{n+2}^{(0)}\right)^2}\\
&+\lambda^4\mathcal{E}_n^{(0)}\frac{J^4z^4\Psi^{*2}\Psi^2\left(n+2\right)\left(n+3\right)}{\left(\mathcal{E}_n^{(0)}-\mathcal{E}_{n+2}^{(0)}\right)^2\left(\mathcal{E}_n^{(0)}-\mathcal{E}_{n+3}^{(0)}\right)}+\lambda^4\frac{J^4z^4\Psi^{*2}\Psi^2n\left(n+2\right)}{\left(\mathcal{E}_n^{(0)}-\mathcal{E}_{n-1}^{(0)}\right)\left(\mathcal{E}_n^{(0)}-\mathcal{E}_{n+2}^{(0)}\right)}\\
&+\lambda^2\frac{\mathcal{E}_{n+1}^{(0)}J^2z^2\Psi^*\Psi n}{\mathcal{E}_n^{(0)}-\mathcal{E}_{n-1}^{(0)}}-\lambda^4\frac{\mathcal{E}_{n+1}^{(0)}E_n^{(2)}J^2z^2\Psi^*\Psi n}{\left(\mathcal{E}_n^{(0)}-\mathcal{E}_{n-1}^{(0)}\right)^2}\\
&+\lambda^4\mathcal{E}_{n+1}^{(0)}\frac{J^4z^4\Psi^{*2}\Psi^2\left(n-1\right)n}{\left(\mathcal{E}_n^{(0)}-\mathcal{E}_{n-1}^{(0)}\right)^2\left(\mathcal{E}_n^{(0)}-\mathcal{E}_{n-2}^{(0)}\right)}-\lambda^2J^2z^2\Psi\Psi^*\left(n+1\right)=0\,.
\end{aligned}
\tag{4.29}
$$

We simplify and reorder

$$
\begin{aligned}
&\lambda^2\left[\mathcal{E}_n^{(0)}E_n^{(2)}-\mathcal{E}_{n+1}^{(0)}E_n^{(2)}-J^2z^2\Psi\Psi^*\left(n+1\right)-\frac{J^2z^2\Psi^*\Psi n\mathcal{E}_n^{(0)}}{\mathcal{E}_n^{(0)}-\mathcal{E}_{n-1}^{(0)}}+\frac{\mathcal{E}_{n+1}^{(0)}J^2z^2\Psi^*\Psi n}{\mathcal{E}_n^{(0)}-\mathcal{E}_{n-1}^{(0)}}\right]\\
&+\lambda^4\left[E_n^{(2)2}+\mathcal{E}_n^{(0)}E_n^{(4)}-\mathcal{E}_{n+1}^{(0)}E_n^{(4)}-\frac{J^2z^2\Psi^*\Psi nE_n^{(2)}}{\mathcal{E}_n^{(0)}-\mathcal{E}_{n-1}^{(0)}}+\frac{J^2z^2\Psi^*\Psi nE_n^{(2)}\mathcal{E}_n^{(0)}}{\left(\mathcal{E}_n^{(0)}-\mathcal{E}_{n-1}^{(0)}\right)^2}\right.\\
&-\mathcal{E}_n^{(0)}\frac{J^4z^4\Psi^{*2}\Psi^2\left(n-1\right)n}{\left(\mathcal{E}_n^{(0)}-\mathcal{E}_{n-1}^{(0)}\right)^2\left(\mathcal{E}_n^{(0)}-\mathcal{E}_{n-2}^{(0)}\right)}-\frac{J^2z^2\Psi^*\Psi\left(n+2\right)E_n^{(2)}}{\mathcal{E}_n^{(0)}-\mathcal{E}_{n+2}^{(0)}}\\
&-\frac{\mathcal{E}_{n+1}^{(0)}E_n^{(2)}J^2z^2\Psi^*\Psi n}{\left(\mathcal{E}_n^{(0)}-\mathcal{E}_{n-1}^{(0)}\right)^2}+\frac{J^4z^4\Psi^{*2}\Psi^2n\left(n+2\right)}{\left(\mathcal{E}_n^{(0)}-\mathcal{E}_{n-1}^{(0)}\right)\left(\mathcal{E}_n^{(0)}-\mathcal{E}_{n+2}^{(0)}\right)}\\
&\left.+\mathcal{E}_{n+1}^{(0)}\frac{J^4z^4\Psi^{*2}\Psi^2\left(n-1\right)n}{\left(\mathcal{E}_n^{(0)}-\mathcal{E}_{n-1}^{(0)}\right)^2\left(\mathcal{E}_n^{(0)}-\mathcal{E}_{n-2}^{(0)}\right)}\right]=0\,.
\end{aligned}
\tag{4.30}
$$

In order for this to be zero, each bracket has to be zero. From the vanishing of the first bracket in (4.30) we extract $E_n^{(2)}$:

$$E_n^{(2)} = \frac{J^2 z^2 \Psi\Psi^* (n+1)}{\mathcal{E}_n^{(0)} - \mathcal{E}_{n+1}^{(0)}} + \frac{J^2 z^2 \Psi^*\Psi n}{\mathcal{E}_n^{(0)} - \mathcal{E}_{n-1}^{(0)}} = \frac{J^2 z^2 \Psi\Psi^* (n+1)}{E_n^{(0)} - E_{n+1}^{(0)}} + \frac{J^2 z^2 \Psi^*\Psi n}{E_n^{(0)} - E_{n-1}^{(0)}} \,. \tag{4.31}$$

Note that we used here that the denominators only contain differences of energies, so we can simplify e.g.

$$\mathcal{E}_n^{(0)} - \mathcal{E}_{n+1}^{(0)} = E_n^{(0)} + \lambda J z \Psi^*\Psi - E_{n+1}^{(0)} - \lambda J z \Psi^*\Psi = E_n^{(0)} - E_{n+1}^{(0)} \,. \tag{4.32}$$

In the very same way, we get $E_n^{(4)}$ from the vanishing of the second bracket in (4.30):

$$\begin{aligned} E_n^{(4)} = &- \frac{E_n^{(2)2}}{\left(\mathcal{E}_n^{(0)} - \mathcal{E}_{n+1}^{(0)}\right)} + \frac{J^2 z^2 \Psi^*\Psi n E_n^{(2)}}{\left(\mathcal{E}_n^{(0)} - \mathcal{E}_{n-1}^{(0)}\right)\left(\mathcal{E}_n^{(0)} - \mathcal{E}_{n+1}^{(0)}\right)} - \frac{J^2 z^2 \Psi^*\Psi n E_n^{(2)} \mathcal{E}_n^{(0)}}{\left(\mathcal{E}_n^{(0)} - \mathcal{E}_{n-1}^{(0)}\right)^2\left(\mathcal{E}_n^{(0)} - \mathcal{E}_{n+1}^{(0)}\right)} \\ &+ \mathcal{E}_n^{(0)} \frac{J^4 z^4 \Psi^{*2}\Psi^2 (n-1) n}{\left(\mathcal{E}_n^{(0)} - \mathcal{E}_{n-1}^{(0)}\right)^2\left(\mathcal{E}_n^{(0)} - \mathcal{E}_{n-2}^{(0)}\right)\left(\mathcal{E}_n^{(0)} - \mathcal{E}_{n+1}^{(0)}\right)} + \frac{J^2 z^2 \Psi^*\Psi (n+2) E_n^{(2)}}{\left(\mathcal{E}_n^{(0)} - \mathcal{E}_{n+2}^{(0)}\right)\left(\mathcal{E}_n^{(0)} - \mathcal{E}_{n+1}^{(0)}\right)} \\ &+ \frac{\mathcal{E}_{n+1}^{(0)} E_n^{(2)} J^2 z^2 \Psi^*\Psi n}{\left(\mathcal{E}_n^{(0)} - \mathcal{E}_{n-1}^{(0)}\right)^2\left(\mathcal{E}_n^{(0)} - \mathcal{E}_{n+1}^{(0)}\right)} - \frac{J^4 z^4 \Psi^{*2}\Psi^2 n (n+2)}{\left(\mathcal{E}_n^{(0)} - \mathcal{E}_{n-1}^{(0)}\right)\left(\mathcal{E}_n^{(0)} - \mathcal{E}_{n+2}^{(0)}\right)\left(\mathcal{E}_n^{(0)} - \mathcal{E}_{n+1}^{(0)}\right)} \\ &- \mathcal{E}_{n+1}^{(0)} \frac{J^4 z^4 \Psi^{*2}\Psi^2 (n-1) n}{\left(\mathcal{E}_n^{(0)} - \mathcal{E}_{n-1}^{(0)}\right)^2\left(\mathcal{E}_n^{(0)} - \mathcal{E}_{n-2}^{(0)}\right)\left(\mathcal{E}_n^{(0)} - \mathcal{E}_{n+1}^{(0)}\right)} \,. \end{aligned} \tag{4.33}$$

Inserting $E_n^{(2)}$ from (4.31) into (4.33) yields after expanding

$$\begin{aligned} E_n^{(4)} = &- \frac{J^4 z^4 \Psi^2\Psi^{*2} (n+1)^2}{\left(E_n^{(0)} - E_{n+1}^{(0)}\right)^3} - \frac{J^4 z^4 \Psi^2\Psi^{*2} n (n+1)}{\left(E_n^{(0)} - E_{n+1}^{(0)}\right)^2\left(E_n^{(0)} - E_{n-1}^{(0)}\right)} \\ &+ \frac{J^4 z^4 \Psi^{*2}\Psi^2 (n+1)(n+2)}{\left(E_n^{(0)} - E_{n+2}^{(0)}\right)\left(E_n^{(0)} - E_{n+1}^{(0)}\right)^2} - \frac{J^4 z^4 \Psi^2\Psi^{*2} (n+1) n}{\left(E_n^{(0)} - E_{n-1}^{(0)}\right)^2\left(E_n^{(0)} - E_{n+1}^{(0)}\right)} \\ &- \frac{J^4 z^4 \Psi^{*2}\Psi^2 n^2}{\left(E_n^{(0)} - E_{n-1}^{(0)}\right)^3} + \frac{J^4 z^4 \Psi^{*2}\Psi^2 (n-1) n}{\left(E_n^{(0)} - E_{n-1}^{(0)}\right)^2\left(E_n^{(0)} - E_{n-2}^{(0)}\right)} \,. \end{aligned} \tag{4.34}$$

Thus, we conclude from (4.25), (4.31), and (4.34) together with (2.29) that we reproduce the result (2.30) with the Landau coefficient (2.31)–(2.33). Note that the derivation in section

2.4 used the Rayleigh-Schrödinger perturbation theory, whereas here we applied the Brillouin-Wigner perturbation theory.

5 Graphical Approach

In this chapter a graphical approach is presented which allows us to get much faster the corresponding correction terms for higher orders of λ in the matrix (3.76). The first case uses the primal split (2.20) and gives only few terms, which implicitly depend on $\Psi^*\Psi$. In contrast to this, the second case uses the primal split (2.22), gives rise to many more terms, but they only explicitly depend on $\Psi^*\Psi$.

5.1 Implicit Case

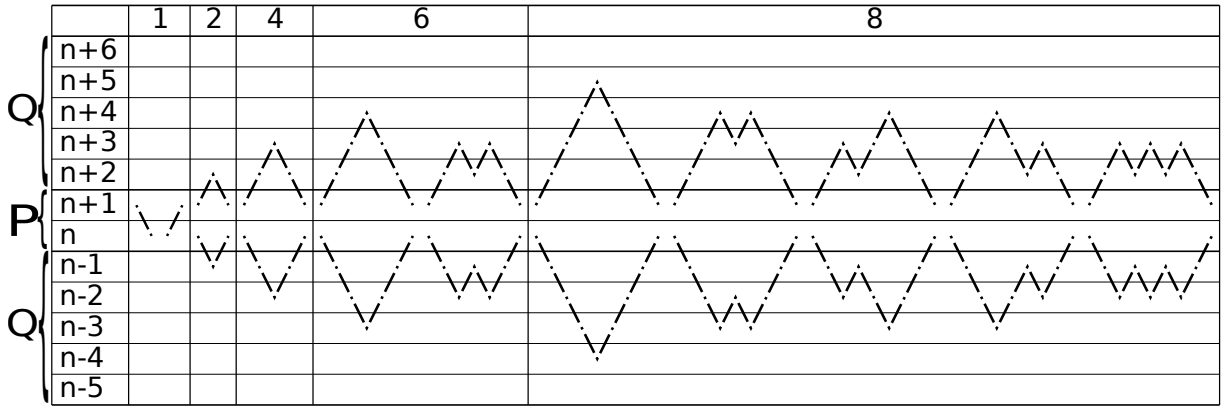

FIG. 5.1: This is the implicit graphical approach for the matix elements up to eighth order of the two-state approach. It uses the primal split (2.20).

In the first row of FIG. 5.1, we have the orders of λ for the respective correction terms. In the first column, we have the different states, here from $n-5$ up to $n+6$. Within the two-state matrix approach, we choose $\hat{P}$ to be n and $n+1$, just as in the previous chapters. Note that the columns for uneven λ give the off-diagonal matrix elements, while the columns for even λ give the diagonal matrix elements. As long as $\hat{P}$ consists of only two states, the only off-diagonal element is the one with $\lambda = 1$.
In order to obtain all possible graphs in FIG. 5.1, we have to take into account the following rules:

- According to $l \in \tilde{N}$ and thus $l \neq n$ in (3.62), the state we start in and the state we end in mustn't be reached in between.

- Since out interaction operator $\hat{V}$ is linear in $\hat{a}$ and $\hat{a}^\dagger$ (2.22), we can only get from one state to its nearest neighbouring states.

- Because the effective Hamiltonian $\hat{H}_{\text{eff}}$ (3.36) contains only the projection operator $\hat{Q}$, but is sandwiched by the projection operator $\hat{P}$ according to (3.35), it is only allowed that the first and the last state is within $\hat{P}$. This rule actually only occurs for the terms in the diagonal matrix elements.

We interpret each graph according to the following rules:

- For every graph we draw, the starting point corresponds to

$$S(\eta) = E_n - \mathcal{E}_\eta^{(0)}, \tag{5.1}$$

  with η denoting the state we start the graph with.

- For every line we draw, we get the following terms. For an ascending line, we get

$$L_A(\nu) = -\lambda J z \Psi \frac{\sqrt{\nu+1}}{E_n - \mathcal{E}_\nu^{(0)}}, \tag{5.2}$$

  with ν representing the state the line started in. For every descending line we draw, we get

$$L_D(\nu) = -\lambda J z \Psi^* \frac{\sqrt{\nu}}{E_n - \mathcal{E}_\nu^{(0)}}, \tag{5.3}$$

  with ν standing for the state the line started in.

- For the whole correction term, we must now multiply $S(\eta)$ with all the $L_A(\nu)$ and $L_D(\nu)$ we draw in our graph. The number of lines we draw gives us the exponent of λ, which has to stand in front of our correction term.

In order to illustrate the applicability of these graphical rules we start in the column for λ with the interaction from $n+1$ to n, which yields the matrix element $\langle n+1 | \hat{H}_{\text{eff}} | n \rangle$. We can now apply $\hat{a}$ on $n+1$, which leads us directly to n and finishes our diagram. If we now apply instead $\hat{a}^\dagger$ on $n+1$, we would end up in $n+2$, but in order to end up in n, we would reach in between $n+1$, which isn't allowed. So we can directly see that this is the only term for the matrix element $\langle n+1 | \hat{H}_{\text{eff}} | n \rangle$ which occurs.
We translate now the graph into a formula as follows:

$$S(n+1)\, L_D(n+1) = \left(E_n - \mathcal{E}_{n+1}^{(0)}\right) \left(-\lambda J z \Psi^* \frac{\sqrt{n+1}}{E_n - \mathcal{E}_{n+1}^{(0)}}\right) = -\lambda J z \Psi^* \sqrt{n+1}, \tag{5.4}$$

which is exactly the same result as the explicit calculation yields.
For the other graph in the column for λ, we get correspondingly

$$S(n)\,L_A(n) = \left(E_n - \mathcal{E}_n^{(0)}\right)\left(-\lambda J z \Psi \frac{\sqrt{n+1}}{E_n - \mathcal{E}_n^{(0)}}\right) = -\lambda J z \Psi \sqrt{n+1}\,. \tag{5.5}$$

The column with the graphs for λ^2 has to be read as follows: The graph starting in n, going downwards, gives us the correction terms for the matrix element $\langle\, n\,|\hat{H}_{\text{eff}}|\,n\,\rangle$, the formula is then

$$\begin{aligned} S(n)\,L_D(n)\,L_A(n-1) =& \left(E_n - \mathcal{E}_n^{(0)}\right)\left(-\lambda J z \Psi^* \frac{\sqrt{n}}{E_n - \mathcal{E}_n^{(0)}}\right)\left(-\lambda J z \Psi \frac{\sqrt{n}}{E_n - \mathcal{E}_{n-1}^{(0)}}\right) \\ =& \lambda^2 \frac{J^2 z^2 \Psi^* \Psi n}{E_n - \mathcal{E}_{n-1}^{(0)}}\,. \end{aligned} \tag{5.6}$$

The graph starting in $n+1$, going upwards, gives us the correction terms for the matrix element $\langle\, n+1\,|\hat{H}_{\text{eff}}|\,n+1\,\rangle$, the formula is then

$$\begin{aligned} S(n+1)\,L_A(n+1)\,L_D(n+2) =& \left(E_n - \mathcal{E}_{n+1}^{(0)}\right)\left(-\lambda J z \Psi \frac{\sqrt{n+2}}{E_n - \mathcal{E}_{n+1}^{(0)}}\right)\left(-\lambda J z \Psi^* \frac{\sqrt{n+2}}{E_n - \mathcal{E}_{n+2}^{(0)}}\right) \\ =& \lambda^2 \frac{J^2 z^2 \Psi^* \Psi\,(n+2)}{E_n - \mathcal{E}_{n+2}^{(0)}}\,. \end{aligned} \tag{5.7}$$

Correspondingly the column with the graphs for λ^4 yields the formulas

$$\begin{aligned} & S(n)\,L_D(n)\,L_D(n-1)\,L_A(n-2)\,L_A(n-1) \\ =& \left(E_n - \mathcal{E}_n^{(0)}\right)\left(-\lambda J z \Psi^* \frac{\sqrt{n}}{E_n - \mathcal{E}_n^{(0)}}\right)\left(-\lambda J z \Psi^* \frac{\sqrt{n-1}}{E_n - \mathcal{E}_{n-1}^{(0)}}\right) \\ & \left(-\lambda J z \Psi \frac{\sqrt{n-1}}{E_n - \mathcal{E}_{n-2}^{(0)}}\right)\left(-\lambda J z \Psi \frac{\sqrt{n}}{E_n - \mathcal{E}_{n-1}^{(0)}}\right) \\ =& \lambda^4 \frac{J^4 z^4 \Psi^{*2} \Psi^2\,(n-1)\,n}{\left(E_n - \mathcal{E}_{n-1}^{(0)}\right)^2\left(E_n - \mathcal{E}_{n-2}^{(0)}\right)} \end{aligned} \tag{5.8}$$

and

$$
\begin{aligned}
&S\,(n+1)\,L_A\,(n+1)\,L_A\,(n+2)\,L_D\,(n+3)\,L_D\,(n+2)\\
=&\left(E_n-\mathcal{E}^{(0)}_{n+1}\right)\left(-\lambda J z\Psi\frac{\sqrt{n+2}}{E_n-\mathcal{E}^{(0)}_{n+1}}\right)\left(-\lambda J z\Psi\frac{\sqrt{n+3}}{E_n-\mathcal{E}^{(0)}_{n+2}}\right)\\
&\left(-\lambda J z\Psi^*\frac{\sqrt{n+3}}{E_n-\mathcal{E}^{(0)}_{n+3}}\right)\left(-\lambda J z\Psi^*\frac{\sqrt{n+2}}{E_n-\mathcal{E}^{(0)}_{n+2}}\right)\\
=&\lambda^4\frac{J^4z^4\Psi^{*2}\Psi^2\,(n+2)\,(n+3)}{\left(E_n-\mathcal{E}^{(0)}_{n+2}\right)^2\left(E_n-\mathcal{E}^{(0)}_{n+3}\right)}\,.
\end{aligned}
\tag{5.9}
$$

It is easy to see from this graphical point of view, that every correction term with λ to an odd power cannot give a contribution to the diagonal matrix elements.
In the column with the graphs for λ^6, we have two different graphs for the matrix element $\langle\, n\,|\hat{H}_{\text{eff}}|\,n\,\rangle$. In order to get the corresponding λ^6 correction term correctly, we must translate both graphs into a formula and just add both formulas then, yielding

$$
\begin{aligned}
&S\,(n)\,L_D\,(n)\,L_D\,(n-1)\,L_D\,(n-2)\,L_A\,(n-3)\,L_A\,(n-2)\,L_A\,(n-1)\\
&+S\,(n)\,L_D\,(n)\,L_D\,(n-1)\,L_A\,(n-2)\,L_D\,(n-1)\,L_A\,(n-2)\,L_A\,(n-1)\\
=&S\,(n)\,L_D\,(n)\,L_D\,(n-1)\\
&[L_D\,(n-2)\,L_A\,(n-3)+L_A\,(n-2)\,L_D\,(n-1)]\\
&L_A\,(n-2)\,L_A\,(n-1)\\
=&\lambda^6\frac{J^6z^6\Psi^{*3}\Psi^3n\,(n-1)\,(n-2)}{\left(E_n-\mathcal{E}^{(0)}_{n-1}\right)^2\left(E_n-\mathcal{E}^{(0)}_{n-2}\right)^2\left(E_n-\mathcal{E}^{(0)}_{n-3}\right)}+\lambda^6\frac{J^6z^6\Psi^{*3}\Psi^3n\,(n-1)^2}{\left(E_n-\mathcal{E}^{(0)}_{n-1}\right)^3\left(E_n-\mathcal{E}^{(0)}_{n-2}\right)^2}\,.
\end{aligned}
\tag{5.10}
$$

In the same way we get the λ^6 term for the matrix element $\langle\, n+1\,|\hat{H}_{\text{eff}}|\,n+1\,\rangle$ as

$$
\begin{aligned}
&S\,(n+1)\,L_A\,(n+1)\,L_A\,(n+2)\,L_A\,(n+3)\,L_D\,(n+4)\,L_D\,(n+3)\,L_D\,(n+2)\\
&+S\,(n+1)\,L_A\,(n+1)\,L_A\,(n+2)\,L_D\,(n+3)\,L_A\,(n+2)\,L_D\,(n+3)\,L_D\,(n+2)\\
=&S\,(n+1)\,L_A\,(n+1)\,L_A\,(n+2)\\
&[L_A\,(n+3)\,L_D\,(n+4)+L_D\,(n+3)\,L_A\,(n+2)]\\
&L_D\,(n+3)\,L_D\,(n+2)\\
=&\lambda^6\frac{J^6z^6\Psi^{*3}\Psi^3\,(n+2)\,(n+3)\,(n+4)}{\left(E_n-\mathcal{E}^{(0)}_{n+2}\right)^2\left(E_n-\mathcal{E}^{(0)}_{n+3}\right)^2\left(E_n-\mathcal{E}^{(0)}_{n+4}\right)}+\lambda^6\frac{J^6z^6\Psi^{*3}\Psi^3\,(n+2)\,(n+3)^2}{\left(E_n-\mathcal{E}^{(0)}_{n+2}\right)^3\left(E_n-\mathcal{E}^{(0)}_{n+3}\right)^2}\,.
\end{aligned}
\tag{5.11}
$$

In the column with the graphs for the order λ^8, we have already five different diagrams, which we have to add up for the right λ^8 correction term. But due to symmetry reasons the third and

fourth graph turn out to be equivalent. Thus we can just translate one of them into a formula, and multiply the result by two.
For the correction term of the matrix element $\langle\, n\,|\hat{H}_{\text{eff}}|\, n\,\rangle$ we get

$$\begin{aligned}
&S\,(n)\,L_D\,(n)\,L_D\,(n-1)\,[L_D\,(n-2)\,L_D\,(n-3)\,L_A\,(n-4)\,L_A\,(n-3)\\
&+L_D\,(n-2)\,L_A\,(n-3)\,L_D\,(n-2)\,L_A\,(n-3)+L_A\,(n-2)\,L_D\,(n-1)\,L_D\,(n-2)\,L_A\,(n-3)\\
&+L_D\,(n-2)\,L_A\,(n-3)\,L_A\,(n-2)\,L_D\,(n-1)+L_A\,(n-2)\,L_D\,(n-1)\,L_A\,(n-2)\,L_D\,(n-1)]\\
&L_A\,(n-2)\,L_A\,(n-1)\\
=&S\,(n)\,L_D\,(n)\,L_D\,(n-1)\,[L_D\,(n-2)\,L_D\,(n-3)\,L_A\,(n-4)\,L_A\,(n-3)\\
&+L_D\,(n-2)\,L_A\,(n-3)\,L_D\,(n-2)\,L_A\,(n-3)+2L_A\,(n-2)\,L_D\,(n-1)\,L_D\,(n-2)\,L_A\,(n-3)\\
&+L_A\,(n-2)\,L_D\,(n-1)\,L_A\,(n-2)\,L_D\,(n-1)]\,L_A\,(n-2)\,L_A\,(n-1)\\
=&\lambda^8\frac{J^8z^8\Psi^{*4}\Psi^4n\,(n-1)\,(n-2)\,(n-3)}{\left(E_n-\mathcal{E}^{(0)}_{n-1}\right)^2\left(E_n-\mathcal{E}^{(0)}_{n-2}\right)^2\left(E_n-\mathcal{E}^{(0)}_{n-3}\right)^2\left(E_n-\mathcal{E}^{(0)}_{n-4}\right)}\\
&+\lambda^8\frac{J^8z^8\Psi^{*4}\Psi^4n\,(n-1)\,(n-2)^2}{\left(E_n-\mathcal{E}^{(0)}_{n-1}\right)^2\left(E_n-\mathcal{E}^{(0)}_{n-2}\right)^3\left(E_n-\mathcal{E}^{(0)}_{n-3}\right)^2}\\
&+2\lambda^8\frac{J^8z^8\Psi^{*4}\Psi^4n\,(n-1)^2\,(n-2)}{\left(E_n-\mathcal{E}^{(0)}_{n-1}\right)^3\left(E_n-\mathcal{E}^{(0)}_{n-2}\right)^3\left(E_n-\mathcal{E}^{(0)}_{n-3}\right)}+\lambda^8\frac{J^8z^8\Psi^{*4}\Psi^4n\,(n-1)^3}{\left(E_n-\mathcal{E}^{(0)}_{n-1}\right)^4\left(E_n-\mathcal{E}^{(0)}_{n-2}\right)^3}\,,
\end{aligned}\tag{5.12}$$

and for the correction term of the matrix element $\langle\, n+1\,|\hat{H}_{\text{eff}}|\, n+1\,\rangle$ we get

$$\begin{aligned}
&S\,(n+1)\,L_A\,(n+1)\,L_A\,(n+2)\,[L_A\,(n+3)\,L_A\,(n+4)\,L_D\,(n+5)\,L_D\,(n+4)\\
&+L_A\,(n+3)\,L_D\,(n+4)\,L_A\,(n+3)\,L_D\,(n+4)+L_D\,(n+3)\,L_A\,(n+2)\,L_A\,(n+3)\,L_D\,(n+4)\\
&+L_A\,(n+3)\,L_D\,(n+4)\,L_D\,(n+3)\,L_A\,(n+2)+L_D\,(n+3)\,L_A\,(n+2)\,L_D\,(n+3)\,L_A\,(n+2)]\\
&L_D\,(n+3)\,L_D\,(n+2)\\
=&S\,(n+1)\,L_A\,(n+1)\,L_A\,(n+2)\,[L_A\,(n+3)\,L_A\,(n+4)\,L_D\,(n+5)\,L_D\,(n+4)\\
&+L_A\,(n+3)\,L_D\,(n+4)\,L_A\,(n+3)\,L_D\,(n+4)+2L_D\,(n+3)\,L_A\,(n+2)\,L_A\,(n+3)\,L_D\,(n+4)\\
&+L_D\,(n+3)\,L_A\,(n+2)\,L_D\,(n+3)\,L_A\,(n+2)]\,L_D\,(n+3)\,L_D\,(n+2)\\
=&\lambda^8\frac{J^8z^8\Psi^{*4}\Psi^4\,(n+2)\,(n+3)\,(n+4)\,(n+5)}{\left(E_n-\mathcal{E}^{(0)}_{n+2}\right)^2\left(E_n-\mathcal{E}^{(0)}_{n+3}\right)^2\left(E_n-\mathcal{E}^{(0)}_{n+4}\right)^2\left(E_n-\mathcal{E}^{(0)}_{n+5}\right)}\\
&+\lambda^8\frac{J^8z^8\Psi^{*4}\Psi^4\,(n+2)\,(n+3)\,(n+4)^2}{\left(E_n-\mathcal{E}^{(0)}_{n+2}\right)^2\left(E_n-\mathcal{E}^{(0)}_{n+3}\right)^3\left(E_n-\mathcal{E}^{(0)}_{n+4}\right)^2}\\
&+2\lambda^8\frac{J^8z^8\Psi^{*4}\Psi^4\,(n+2)\,(n+3)^2\,(n+4)}{\left(E_n-\mathcal{E}^{(0)}_{n+2}\right)^3\left(E_n-\mathcal{E}^{(0)}_{n+3}\right)^3\left(E_n-\mathcal{E}^{(0)}_{n+4}\right)}+\lambda^8\frac{J^8z^8\,(n+2)\,(n+3)^3}{\left(E_n-\mathcal{E}^{(0)}_{n+2}\right)^4\left(E_n-\mathcal{E}^{(0)}_{n+3}\right)^3}\,.
\end{aligned}\tag{5.13}$$

Note that these high perturbative orders for the matrix elements are much faster obtained by

the graphical approach than by doing the actual analytical calculation. While this graphical approach has the advantage of yielding a relative small number of diagrams, the resulting formulas have the condensate density $\Psi^*\Psi$ in the denominator.

An alternative graphical approach is needed if the other primal split is used. FIG. 5.2 sketches the graphical approach to get the correction terms of higher λ in the matrix according to the primal split (2.22).

5.2 Explicit Case

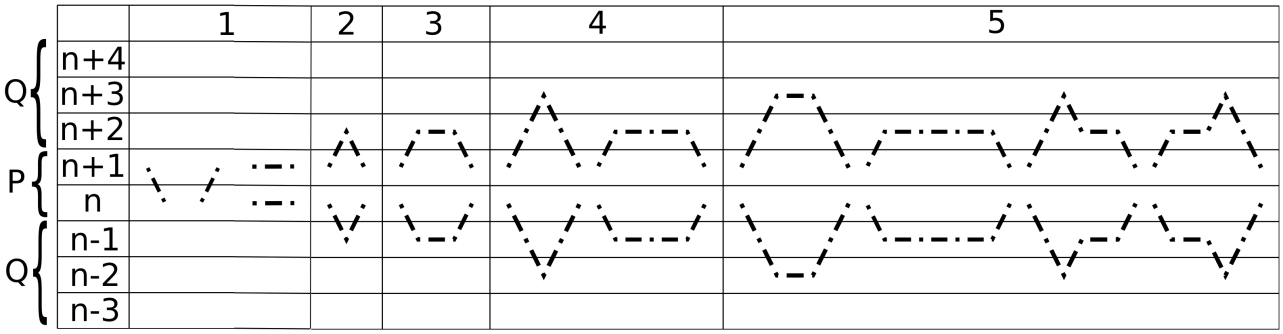

FIG. 5.2: This is the explicit graphical approach for the matix elements up to eighth order of the two-state approach. It uses the primal split (2.22).

In the first row of FIG. 5.2, we denote the orders of λ for our correction terms. In the first column, we have our different states, here from $n-3$ up to $n+4$. We choose $\hat{P}$ to be n and $n+1$, just as in the previous chapters. Basically, all the rules apply which we used in the previous graphical approach, just that we are now allowed to draw horizontal lines as well:

- For every graph we draw, the starting point corresponds to

$$S(\eta) = E_n - E_\eta^{(0)}\,, \tag{5.14}$$

  with η being the state we start the graph in.

- For every line we draw, we get the following terms. For an ascending line, we get

$$L_A(\nu) = -\lambda J z \Psi \frac{\sqrt{\nu+1}}{E_n - E_\nu^{(0)}}\,, \tag{5.15}$$

  with ν being the state the line started in. For every descending line we draw, we get

$$L_D(\nu) = -\lambda J z \Psi^* \frac{\sqrt{\nu}}{E_n - E_\nu^{(0)}}\,, \tag{5.16}$$

with ν being the state the line started in.

- For a horizontal line, we get

$$L_H(\nu) = \frac{\lambda J z \Psi^* \Psi}{E_n - E_\nu^{(0)}}\,, \tag{5.17}$$

with ν being the state the line started in.

In the column for λ, we get for the off-diagonal matrix elements

$$S(n+1)L_D(n+1) = -\lambda J z \Psi^* \sqrt{n+1}\,, \tag{5.18}$$

$$S(n)L_A(n) = -\lambda J z \Psi \sqrt{n+1}\,. \tag{5.19}$$

In the column for λ, we get for the diagonal matrix elements

$$S(n+1)L_H(n+1) = \lambda J z \Psi^* \Psi\,, \tag{5.20}$$

$$S(n)L_H(n) = \lambda J z \Psi^* \Psi\,. \tag{5.21}$$

In the column for λ^2, we get

$$S(n+1)L_A(n+1)L_D(n+2) = \lambda^2 J^2 z^2 \Psi^* \Psi \frac{n+2}{E_n - E_{n+2}^{(0)}}\,, \tag{5.22}$$

$$S(n)L_D(n)L_A(n-1) = \lambda^2 J^2 z^2 \Psi^* \Psi \frac{n}{E_n - E_{n-1}^{(0)}}\,. \tag{5.23}$$

In the column for λ^3, we get

$$S(n+1)L_A(n+1)L_H(n+2)L_D(n+2) = \lambda^3 J^3 z^3 \Psi^{*2}\Psi^2 \frac{n+2}{\left(E_n - E^{(0)}_{n+2}\right)^2}\,, \tag{5.24}$$

$$S(n)L_D(n)L_H(n-1)L_A(n-1) = \lambda^3 J^3 z^3 \Psi^{*2}\Psi^2 \frac{n}{\left(E_n - E^{(0)}_{n-1}\right)^2}\,. \tag{5.25}$$

In the column for λ^4, we get

$$\begin{aligned}
&S(n+1)L_A(n+1)\left[L_A(n+2)L_D(n+3) + L_H(n+2)L_H(n+2)\right]L_D(n+2)\\
&= \lambda^4 J^4 z^4 \Psi^{*2}\Psi^2 \frac{(n+2)\,(n+3)}{\left(E_n - E^{(0)}_{n+2}\right)^2\left(E_n - E^{(0)}_{n+3}\right)} + \lambda^4 J^4 z^4 \Psi^{*3}\Psi^3 \frac{n+2}{\left(E_n - E^{(0)}_{n+2}\right)^3}\,,
\end{aligned} \tag{5.26}$$

$$\begin{aligned}
&S(n)L_D(n)\left[L_D(n-1)L_A(n-2) + L_H(n-1)L_H(n-1)\right]L_A(n-1)\\
&= \lambda^4 J^4 z^4 \Psi^{*2}\Psi^2 \frac{n\,(n-1)}{\left(E_n - E^{(0)}_{n-1}\right)^2\left(E_n - E^{(0)}_{n-2}\right)} + \lambda^4 J^4 z^4 \Psi^{*3}\Psi^3 \frac{n}{\left(E_n - E^{(0)}_{n-1}\right)^3}\,.
\end{aligned} \tag{5.27}$$

In the column for λ^5, we get

$$\begin{aligned}
&S(n+1)L_A(n+1)\left[L_A(n+2)L_H(n+3)L_D(n+3) + L_H(n+2)L_H(n+2)L_H(n+2)\right.\\
&\left. + 2L_A(n+2)L_D(n+3)L_H(n+2)\right]L_D(n+2)\\
&= \lambda^5 J^5 z^5 \Psi^{*3}\Psi^3 \frac{(n+2)\,(n+3)}{\left(E_n - E^{(0)}_{n+2}\right)^2\left(E_n - E^{(0)}_{n+3}\right)^2} + \lambda^5 J^5 z^5 \Psi^{*4}\Psi^4 \frac{n+2}{\left(E_n - E^{(0)}_{n+2}\right)^4}\\
&+ 2\lambda^5 J^5 z^5 \Psi^{*3}\Psi^3 \frac{(n+2)\,(n+3)}{\left(E_n - E^{(0)}_{n+2}\right)^3\left(E_n - E^{(0)}_{n+3}\right)}\,,
\end{aligned} \tag{5.28}$$

$$\begin{aligned}
&S(n)L_D(n)\left[L_D(n-1)L_H(n-2)L_A(n-2) + L_H(n-1)L_H(n-1)L_H(n-1)\right.\\
&\left. + 2L_D(n-1)L_A(n-2)L_H(n-1)\right]L_A(n-1)\\
&= \lambda^5 J^5 z^5 \Psi^{*3}\Psi^3 \frac{n\,(n-1)}{\left(E_n - E^{(0)}_{n-1}\right)^2\left(E_n - E^{(0)}_{n-2}\right)^2} + \lambda^5 J^5 z^5 \Psi^{*4}\Psi^4 \frac{n}{\left(E_n - E^{(0)}_{n-1}\right)^4}\\
&+ \lambda^5 J^5 z^5 \Psi^{*3}\Psi^3 \frac{n\,(n-1)}{\left(E_n - E^{(0)}_{n-1}\right)^3\left(E_n - E^{(0)}_{n-2}\right)}\,.
\end{aligned} \tag{5.29}$$

With the explicit graphical approach, we have more terms, but the denominator is independent of $\Psi^*\Psi$.

We now compare the results for the matrix entries calculated by the implicit and by the explicit graphical approach, respectively. If both approaches are executed up to the same order, they yield the same result. For instance, up to fourth order the implicit approach yields (5.4)–(5.9) which coincides with the results of the explicit approach (5.18)–(5.27), provided all denominators are expanded in λ by taking into account (2.21).

6 Mean-Field Phase Boundary

The mean-field phase boundary was already shown in FIG. 2.1 obtained from the Rayleigh-Schrödinger perturbation theory. Here we will reproduce this result within the Brillouin-Wigner perturbation theory. In principle, the mean-field phase boundary can be obtained out of the one-state approach as well as the two-state approach. Here, we restrict ourselves to the two-state approach. In order to calculate the mean-field phase boundary, we start with the determinant of the matrix (3.76) with $m = n$

$$\begin{aligned}\mathrm{Det}\left(\Gamma^{(4)}\right) = &\left[E_n^{(0)} + \lambda J z \Psi^*\Psi - E_n + \lambda^2 \frac{J^2 z^2 \Psi^*\Psi n}{E_n - E_{n-1}^{(0)} - \lambda J z \Psi^*\Psi}\right. \\ &\left. + \lambda^4 \frac{J^4 z^4 \Psi^{*2}\Psi^2 n\,(n-1)}{\left(E_n - E_{n-1}^{(0)} - \lambda J z \Psi^*\Psi\right)^2 \left(E_n - E_{n-2}^{(0)} - \lambda J z \Psi^*\Psi\right)}\right] \\ &\times \left[E_{n+1}^{(0)} + \lambda J z \Psi^*\Psi - E_n + \lambda^2 \frac{J^2 z^2 \Psi^*\Psi\,(n+2)}{E_n - E_{n+2}^{(0)} - \lambda J z \Psi^*\Psi}\right. \\ &\left. + \lambda^4 \frac{J^4 z^4 \Psi^{*2}\Psi^2\,(n+2)\,(n+3)}{\left(E_n - E_{n+2}^{(0)} - \lambda J z \Psi^*\Psi\right)^2 \left(E_n - E_{n+3}^{(0)} - \lambda J z \Psi^*\Psi\right)}\right] \\ &- \lambda^2 J^2 z^2 \Psi^*\Psi\,(n+1) + \ldots . \end{aligned} \tag{6.1}$$

In order to get the phase boundary, we calculate the function

$$f\left(\Psi^*\Psi\right) = \frac{1}{\Psi}\frac{\partial}{\partial \Psi^*}\mathrm{Det}\left(\Gamma^{(4)}\right) , \tag{6.2}$$

which depends on the condensate density $\Psi^*\Psi$ and evaluate this at $\Psi^*\Psi = 0$. We show now in a general way that we can neglect all terms with λ of the order 3 or higher. To do so, we use the exemplary formula $\varphi\left(\Psi^*\Psi\right)$, which has the same structure as $f\left(\Psi^*\Psi\right)$:

$$\varphi\left(\Psi^*\Psi\right) = \frac{1}{\Psi}\frac{\partial}{\partial \Psi^*}\left[\alpha + \Psi^*\Psi\beta + \frac{\Psi^*\Psi\gamma_0}{\gamma_1 + \Psi^*\Psi\gamma_2} + \sum_{m\geq 2}^{\infty} \frac{\left(\Psi^*\Psi\right)^m k_m}{P\left(\Psi^*\Psi\right)}\right] . \tag{6.3}$$

The coefficients α, β, γ_1, γ_2, γ_3, and k_m are independent of $\Psi^*\Psi$, while m is a natural number and P is a polynomial in $\Psi^*\Psi$. All terms in (6.1) independent of $\Psi^*\Psi$ are represented by α, the terms linear in $\Psi^*\Psi$ by β, and so on. Performing the differentiation in(6.3) yields

$$\begin{aligned}\varphi\left(\Psi^*\Psi\right) =& \beta + \frac{\gamma_0\gamma_1}{\left(\gamma_1 + \Psi^*\Psi\gamma_2\right)^2} \\ &+ \sum_{m\geq 2}^{\infty} \frac{m\left(\Psi^*\Psi\right)^{m-1} k_m P\left(\Psi^*\Psi\right) - \left(\Psi^*\Psi\right)^m k_m \frac{1}{\Psi}\frac{\partial}{\partial\Psi^*} P\left(\Psi^*\Psi\right)}{P\left(\Psi^*\Psi\right)^2}\,, \end{aligned} \tag{6.4}$$

with

$$\varphi\left(0\right) = \beta + \frac{\gamma_0}{\gamma_1}\,. \tag{6.5}$$

Because of the similar structure in $\varphi\left(\Psi^*\Psi\right)$ and $f\left(\Psi^*\Psi\right)$, we read off the result from (6.5) and obtain

$$\begin{aligned} f\left(0\right) =& \lambda J z\left[\left(E_n^{(0)} - E_n\right) + \left(E_{n+1}^{(0)} - E_n\right) - \lambda J z\left(n+1\right)\right] \\ &+ \lambda^2 J^2 z^2 \left[\frac{\left(n+2\right)\left(E_n^{(0)} - E_n\right)}{E_n - E_{n+2}^{(0)}} + \frac{n\left(E_{n+1}^{(0)} - E_n\right)}{E_n - E_{n-1}^{(0)}}\right]\,. \end{aligned} \tag{6.6}$$

We put $f\left(0\right) = 0$, solve with respect to $\frac{Jz}{U}$, and get

$$\frac{Jz}{U} = \frac{-\left(2E_n - E_n^{(0)} - E_{n+1}^{(0)}\right)\left(E_n - E_{n+2}^{(0)}\right)\left(E_n - E_{n-1}^{(0)}\right)}{\lambda n U\left(E_n - E_{n+1}^{(0)}\right)\left(E_n - E_{n+2}^{(0)}\right) + \lambda U\left[\left(n+1\right)\left(E_n - E_{n+2}^{(0)}\right) + \left(n+2\right)\left(E_n - E_n^{(0)}\right)\right]}\,. \tag{6.7}$$

This is the mean-field phase boundary. All higher order corrections drop out of the formula if we set $\Psi^*\Psi = 0$. Thus, the phase boundary does not change even if higher orders in λ are taken into account. To determine E_n in (6.7), we take (6.1) and set $\Psi^*\Psi = 0$, which results effectively in calculating the matrix up to zeroth order. We set this equal to zero and get

$$\mathrm{Det}\left(\Gamma^{(0)}\right) = \left(E_n^{(0)} - E_n\right)\left(E_{n+1}^{(0)} - E_n\right) = 0\,. \tag{6.8}$$

This gives two solutions for E_n, namely $E_{n,1} = E_n^{(0)}$ and $E_{n,2} = E_{n+1}^{(0)}$.
Thus, the mean-field phase boundary (6.7) agrees with the previous result (2.34). By using

$$E_n^{(0)} = \frac{1}{2} U n\,(n-1) - \mu n \tag{6.9}$$

and

$$E_{n+1}^{(0)} = \frac{1}{2} U n\,(n+1) - \mu\,(n+1) \tag{6.10}$$

together with $\mu = Un + \varepsilon$ gives for $n = 1$

$$E_1 = (-1 - \varepsilon)\, U \tag{6.11}$$

and

$$E_2 = (-1 - 2\varepsilon)\, U\,. \tag{6.12}$$

These two energies are depicted in FIG. 6.1 and yield the lowest energies, corresponding to the two Mott lobes. For $-1 < \frac{\varepsilon}{U} < 0$, E_1 is the minimal energy, while for $0 < \frac{\varepsilon}{U} < 1$ it is E_2.

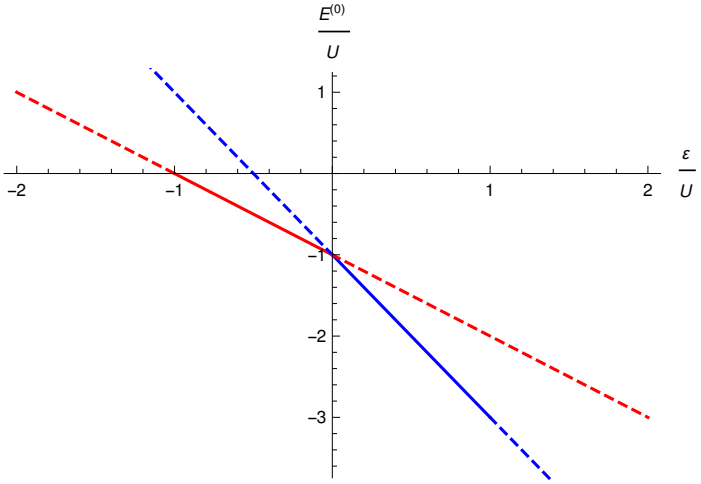

FIG. 6.1: The red line corresponds to E_1 in (6.11), and the blue line corresponds to E_2 in (6.12). The solid parts present the lowest energy.

To get the phase boundary, we insert E_1 in (6.11) and E_2 in (6.12) into (6.7). According to FIG. 6.1, E_1 gives rise to the first lobe, and E_2 to the second. Therefore, we obtain the Mott lobes in FIG. 6.2, which were already discussed via FIG. 2.1.

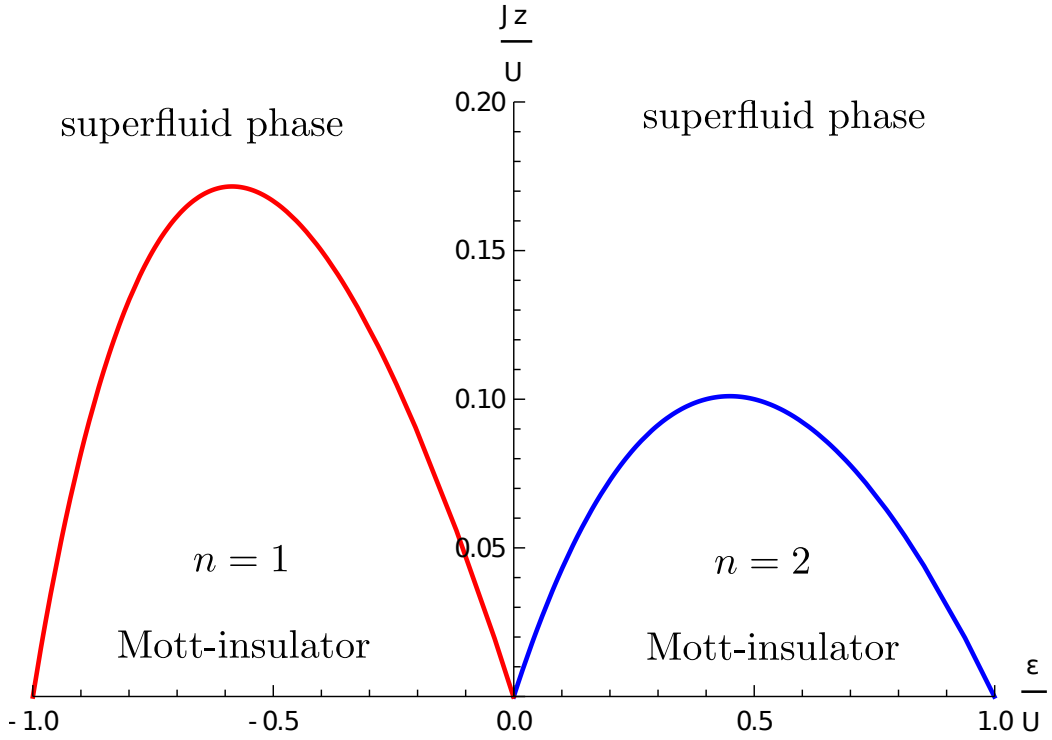

FIG. 6.2: Mott lobes which represent the mean-field phase boundary.

7 Order Parameter

In this chapter, we calculate explicitly the order parameter, whose absolute square defines the condensate density $\Psi^*\Psi$. While the one-state approach (3.52) gives a discontinuous order parameter, the two-state approach yields a continuous order parameter. Nevertheless, both give the right mean-field phase boundary and are non-zero at the degeneracy $\mu = Un$, unlike the order parameter obtained out of the Rayleigh-Schrödinger perturbation theory, depicted in FIG. 2.3. For both approaches, we have to extremalize the perturbed energy E_n with respect to the order parameter Ψ^*, Ψ.

7.1 General Considerations

Generally, the Brillouin-Wigner perturbation theory enables us to obtain a polynomial representation of the unperturbed ground-state energy E_n and the condensate density $\Psi^*\Psi$ in orders of λ, which is of the following form:

$$\begin{aligned} 0 =& A_0(E_n) + A_1(E_n, \Psi^*\Psi)\lambda + A_2(E_n, \Psi^*\Psi)\lambda^2 + A_3(E_n, \Psi^*\Psi)\lambda^3 \\ &+ A_4(E_n, \Psi^*\Psi)\lambda^4 + A_5(E_n, \Psi^*\Psi)\lambda^5 + \dots . \end{aligned} \tag{7.1}$$

By applying $\frac{1}{\Psi}\frac{\partial}{\partial\Psi^*}$ to (7.1) and using the condition $\frac{\partial E_n}{\partial\Psi^*} = 0$, another polynomial is obtained

$$\begin{aligned} 0 =& B_1(E_n, \Psi^*\Psi) + B_2(E_n, \Psi^*\Psi)\lambda + B_3(E_n, \Psi^*\Psi)\lambda^2 \\ &+ B_4(E_n, \Psi^*\Psi)\lambda^3 + B_5(E_n, \Psi^*\Psi)\lambda^4 + \dots , \end{aligned} \tag{7.2}$$

with

$$B_i(E_n, \Psi^*\Psi) = \frac{1}{\Psi}\frac{\partial A_i(E_n, \Psi^*\Psi)}{\partial\Psi^*} . \tag{7.3}$$

Now we evaluate both equations (7.1) and (7.2) up to second order in λ and get

$$0 = A_0(E_n) + A_1(E_n, \Psi^*\Psi)\lambda + A_2(E_n, \Psi^*\Psi)\lambda^2 \tag{7.4}$$

as well as

$$0 = B_1(E_n, \Psi^*\Psi) + B_2(E_n, \Psi^*\Psi)\lambda + B_3(E_n, \Psi^*\Psi)\lambda^2 \,. \tag{7.5}$$

Note that due to the derivative with respect to Ψ^*, the third-order coefficient B_3 appears in the second order of λ. The two equations (7.4) and (7.5) define the two variables, i. e. the perturbed ground-state energy E_n and the condensate density $\Psi^*\Psi$. Generically we have to solve them numerically by iteration. In the next two sections, this is done for the one-state approach and for the two-state approach, respectively.

7.2 One-State Approach

We consider the subspace of the Hilbert space which is just spanned by one eigenstate $|\,\Psi_n^{(0)}\,\rangle$ of the unperturbed Hamiltonian $\hat{H}^{(0)}$. Any state vector is projected into that subspace by the projector

$$\hat{P} = |\,\Psi_n^{(0)}\,\rangle\langle\,\Psi_n^{(0)}\,| \,. \tag{7.6}$$

Therefore, according to (3.52) we calculate the expectation value of the ground-state energy $E_n = \langle\,\Psi_n^{(0)}\,|\hat{H}_{\text{eff}}|\,\Psi_n^{(0)}\,\rangle$ up to third order in λ:

$$\begin{aligned} E_n =& \langle\,\Psi_n^{(0)}\,|\hat{H}^{(0)}|\,\Psi_n^{(0)}\,\rangle + \lambda\langle\,\Psi_n^{(0)}\,|\hat{V}|\,\Psi_n^{(0)}\,\rangle + \lambda^2 \sum_{l\neq n} \frac{\langle\,\Psi_n^{(0)}\,|\hat{V}|\,\Psi_l^{(0)}\,\rangle\langle\,\Psi_l^{(0)}\,|\hat{V}|\,\Psi_n^{(0)}\,\rangle}{E_n - E_l^{(0)}} \\ &+ \lambda^3 \sum_{l,l'\neq n} \frac{\langle\,\Psi_n^{(0)}\,|\hat{V}|\,\Psi_l^{(0)}\,\rangle\langle\,\Psi_l^{(0)}\,|\hat{V}|\,\Psi_{l'}^{(0)}\,\rangle\langle\,\Psi_{l'}^{(0)}\,|\hat{V}|\,\Psi_n^{(0)}\,\rangle}{\left(E_n - E_l^{(0)}\right)\left(E_n - E_{l'}^{(0)}\right)} \,, \end{aligned} \tag{7.7}$$

where the restriction $l, l' \in \tilde{N}$ allows to sum over all $l, l' \neq n$. Inserting $\hat{H}^{(0)}$ and $\hat{V}$ from (2.22) yields

$$\begin{aligned} E_n =& E_n^{(0)} + \lambda J z \Psi^*\Psi + \lambda^2 J^2 z^2 \Psi^*\Psi \left(\frac{n}{E_n - E_{n-1}^{(0)}} + \frac{n+1}{E_n - E_{n+1}^{(0)}} \right) \\ &+ \lambda^3 J^3 z^3 \left(\Psi^*\Psi\right)^2 \left[\frac{n}{\left(E_n - E_{n-1}^{(0)}\right)^2} + \frac{n+1}{\left(E_n - E_{n+1}^{(0)}\right)^2} \right] \,, \end{aligned} \tag{7.8}$$

with the unperturbed ground-state energy $E_n^{(0)}$ from (2.23) being independent of $\Psi^*\Psi$.
Note that the non-perturbative result (7.8) contains up to second order in λ two important special cases, which have been previously discussed in the literature. On the one hand, by approximating the ground-state energy E_n on the right-hand side of (7.8) with the unperturbed ground state energy $E_n \approx E_n^{(0)}$, we reobtain (2.30) [23, 30] up to second order in λ, which is compatible with the mean-field phase boundary. On the other hand, by considering $\frac{n}{E_n - E_{n-1}^{(0)}}$ to be negligible, we get directly (4.8), and thus all results of Ref. [24].

To get the condensate density within the one-state approach, we determine $\frac{1}{\Psi}\frac{\partial E_n}{\partial \Psi^*} = 0$ from (7.8) after dividing by $\lambda J z$:

$$\begin{aligned} 0 =& 1 + \lambda J z \left(\frac{n}{E_n - E_{n-1}^{(0)}} + \frac{n+1}{E_n - E_{n+1}^{(0)}} \right) \\ &+ \lambda^2 2 J^2 z^2 \Psi^*\Psi \left[\frac{n}{\left(E_n - E_{n-1}^{(0)}\right)^2} + \frac{n+1}{\left(E_n - E_{n+1}^{(0)}\right)^2} \right], \end{aligned} \tag{7.9}$$

which corresponds to (7.5). Furthermore, by evaluating (7.8) up to second order in λ, we get

$$0 = E_n^{(0)} - E_n + \lambda J z \Psi^*\Psi + \lambda^2 J^2 z^2 \Psi^*\Psi \left(\frac{n}{E_n - E_{n-1}^{(0)}} + \frac{n+1}{E_n - E_{n+1}^{(0)}} \right), \tag{7.10}$$

which corresponds to (7.4). Multiplying (7.9) with $\left(E_n - E_{n-1}^{(0)}\right)^2 \left(E_n - E_{n+1}^{(0)}\right)^2$ and (7.10) with $\left(E_n - E_{n-1}^{(0)}\right)\left(E_n - E_{n+1}^{(0)}\right)$ yields

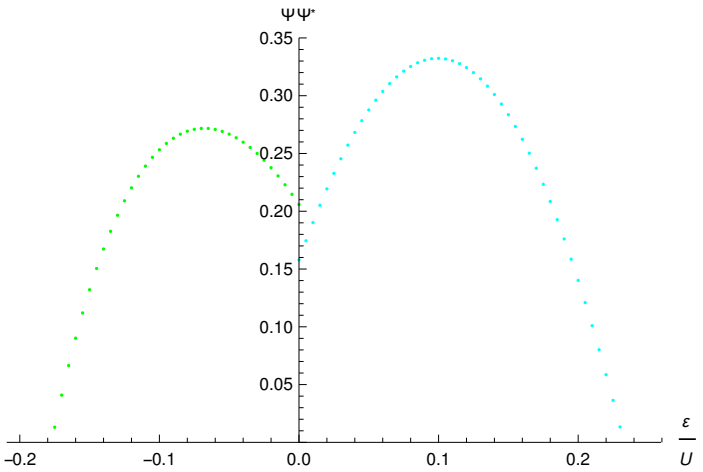

FIG. 7.1: Condensate density from one-state approach for $n = 1$ (green) and $n = 2$ (cyan). The green part origins from $n = 1$ and the cyan part from $n = 2$.

$$
\begin{aligned}
0 = &\left(E_n - E_{n-1}^{(0)}\right)^2 \left(E_n - E_{n+1}^{(0)}\right)^2 + \lambda J z \left[n \left(E_n - E_{n-1}^{(0)}\right) \left(E_n - E_{n+1}^{(0)}\right)^2 \right. \\
&\left. + (n+1) \left(E_n - E_{n-1}^{(0)}\right)^2 \left(E_n - E_{n+1}^{(0)}\right) \right] \\
&+ \lambda^2 2 J^2 z^2 \Psi^* \Psi \left[n \left(E_n - E_{n+1}^{(0)}\right)^2 + (n+1) \left(E_n - E_{n-1}^{(0)}\right)^2 \right]
\end{aligned} \tag{7.11}
$$

and

$$
\begin{aligned}
0 = &\left(E_n - E_{n-1}^{(0)}\right) \left(E_n - E_{n+1}^{(0)}\right) \left(E_n^{(0)} - E_n + \lambda J z \Psi^* \Psi\right) \\
&+ \lambda^2 J^2 z^2 \Psi^* \Psi \left[n \left(E_n - E_{n+1}^{(0)}\right) + (n+1) \left(E_n - E_{n-1}^{(0)}\right) \right] .
\end{aligned} \tag{7.12}
$$

Both equations (7.11) and (7.12) are now used to calculate the ground-state energy E_n and the condensate density $\Psi^*\Psi$. They are numerically solved by iteration and the condensate density is plotted in FIG. 7.1 for $\mu = Un + \varepsilon$, $\lambda = 1$ and $\frac{Jz}{U} = 0.08$. The order parameter obtained by Brillouin-Wigner perturbation theory from the one-state approach according to FIG. 7.1 is better than the one obtained by Rayleigh-Schrödinger perturbation theory, where the order parameter vanishes at the degeneracy as seen in FIG. 2.3. Nevertheless, the order parameter plotted in FIG. 7.1 still is unphysically discontinuous at $\frac{\varepsilon}{U} = 0$.

7.3 Two-State Approach

In the previous section it was shown that the Brillouin-Wigner perturbation theory in the one-state approach up to second order in λ cannot provide a proper condensate density. Therefore, the Brillouin-Wigner two-state approach is used now. In order to do so, we consider the subspace of the Hilbert space which is just spanned by two eigenstates $|\,\Psi_n^{(0)}\,\rangle$ and $|\,\Psi_{n+1}^{(0)}\,\rangle$ of the unperturbed Hamiltonian $\hat{H}^{(0)}$. Any state vector is projected into that subspace by the projector

$$
\hat{P} = |\,\Psi_n^{(0)}\,\rangle\langle\,\Psi_n^{(0)}\,| + |\,\Psi_{n+1}^{(0)}\,\rangle\langle\,\Psi_{n+1}^{(0)}\,| \,. \tag{7.13}
$$

Therefore, according to (3.75) we calculate the expectation value of the perturbed ground-state energy $E_m = E_n$ similar to the previous section from the condition

$$
\mathrm{Det}\left(\Gamma^{(2)}\right) = 0 \,, \tag{7.14}
$$

where the matrix entries are evaluated up to third order in λ

$$\Gamma^{(2)} = \begin{pmatrix} \mathcal{E}_n^{(0)} - E_n + \lambda^2 \frac{J^2 z^2 \Psi^* \Psi n}{E_n - \mathcal{E}_{n-1}^{(0)}} & -\lambda J z \Psi^* \sqrt{n+1} \\ -\lambda J z \Psi \sqrt{n+1} & \mathcal{E}_{n+1}^{(0)} - E_n + \lambda^2 \frac{J^2 z^2 \Psi^* \Psi (n+2)}{E_n - \mathcal{E}_{n+2}^{(0)}} \end{pmatrix} . \tag{7.15}$$

We multiply (7.14) with the denominators $E_n - \mathcal{E}_{n-1}^{(0)}$ and $E_n - \mathcal{E}_{n+2}^{(0)}$, then we apply $\frac{1}{\Psi}\frac{\partial}{\partial \Psi^*}$, divide by $\lambda J z$ and neglect then all orders in λ higher than 2. With this we get

$$\begin{aligned} & E_n^{(0)} E_{n+1}^{(0)} \left(E_{n+2}^{(0)} + E_{n-1}^{(0)} \right) + E_{n+2}^{(0)} E_{n-1}^{(0)} \left(E_n^{(0)} + E_{n+1}^{(0)} \right) - 2E_n \left[\left(E_n^{(0)} + E_{n+1}^{(0)} \right) \left(E_{n+2}^{(0)} \right. \right. \\ & \left. + \left. E_{n-1}^{(0)} \right) + E_n^{(0)} E_{n+1}^{(0)} + E_{n+2}^{(0)} E_{n-1}^{(0)} \right] + 3E_n^2 \left(E_n^{(0)} + E_{n+1}^{(0)} + E_{n+2}^{(0)} + E_{n-1}^{(0)} \right) - 4E_n^3 \\ & + \lambda J z \left(\left\{ 2\Psi^* \Psi \left[\left(E_n^{(0)} + E_{n+1}^{(0)} \right) \left(E_{n+2}^{(0)} + E_{n-1}^{(0)} \right) + E_n^{(0)} E_{n+1}^{(0)} + E_{n+2}^{(0)} E_{n-1}^{(0)} \right] \right. \right. \\ & - E_{n-1}^{(0)} \left[E_n^{(0)} (n+2) + E_{n+2}^{(0)} (n+1) \right] - n E_{n+1}^{(0)} E_{n+2}^{(0)} \Big\} + E_n \Big[-6\Psi^* \Psi \left(E_n^{(0)} + E_{n+1}^{(0)} \right. \\ & \left. + E_{n+2}^{(0)} + E_{n-1}^{(0)} \right) + E_n^{(0)} (n+2) + E_{n+1}^{(0)} n + E_{n+2}^{(0)} (2n+1) + E_{n-1}^{(0)} (2n+3) \Big] - 3E_n^2 [n \\ & \left. -4\Psi^* \Psi + 1]) + \lambda^2 J^2 z^2 \left\{ 3\Psi^{*2} \Psi^2 \left(E_n^{(0)} + E_{n+1}^{(0)} + E_{n+2}^{(0)} + E_{n-1}^{(0)} \right) - 2\Psi^* \Psi \left[E_n^{(0)} (n+2) \right. \right. \\ & \left. \left. + E_{n+1}^{(0)} n + E_{n+2}^{(0)} (2n+1) + E_{n-1}^{(0)} (2n+3) \right] + 12 E_n \left[(n+1)\Psi^* \Psi - \Psi^{*2} \Psi^2 \right] \right\} = 0 , \end{aligned} \tag{7.16}$$

which corresponds to (7.5). Furthermore, we multiply (7.14) with the denominators $E_n - \mathcal{E}_{n-1}^{(0)}$ and $E_n - \mathcal{E}_{n+2}^{(0)}$ and neglect then all orders in λ higher than 2, which yields

$$\begin{aligned} & E_n^4 + E_n^{(0)} E_{n+1}^{(0)} E_{n+2}^{(0)} E_{n-1}^{(0)} - E_n \left[E_n^{(0)} E_{n+1}^{(0)} E_{n+2}^{(0)} + E_{n+1}^{(0)} E_{n+2}^{(0)} E_{n-1}^{(0)} + E_n^{(0)} E_{n-1}^{(0)} \left(E_{n+1}^{(0)} + E_{n+2}^{(0)} \right) \right] \\ & + J z \lambda \Psi^* \Psi \left(E_n^{(0)} E_{n+1}^{(0)} E_{n+2}^{(0)} + E_n^{(0)} E_{n+1}^{(0)} E_{n-1}^{(0)} + E_n^{(0)} E_{n-1}^{(0)} E_{n+2}^{(0)} + E_{n-1}^{(0)} E_{n+1}^{(0)} E_{n+2}^{(0)} \right. \\ & \left. - J z \lambda \left\{ n E_{n+1}^{(0)} E_{n+2}^{(0)} + \left[(2+n) E_n^{(0)} + E_{n+2}^{(0)} + n E_{n+2}^{(0)} \right] \right\} \right) + J z \lambda E_n \Psi^* \Psi \left(-2 \left[E_{n+1}^{(0)} E_{n+2}^{(0)} \right. \right. \\ & + \left(E_{n+1}^{(0)} + E_{n+2}^{(0)} \right) E_{n-1}^{(0)} + E_n^{(0)} \left(E_{n+1}^{(0)} + E_{n+2}^{(0)} + E_{n-1}^{(0)} \right) \Big] + J z \Big\{ (2+n) E_n^{(0)} + E_{n+2}^{(0)} \\ & \left. \left. + 3E_{n-1}^{(0)} + n \left[E_{n+1}^{(0)} + 2 \left(E_{n+2}^{(0)} + E_{n-1}^{(0)} \right) \right] \right\} \right) - 3J^2 z^2 \lambda^2 E_n \Psi^{*2} \Psi^2 \left(E_n^{(0)} + E_{n+1}^{(0)} + E_{n+2}^{(0)} + E_{n-1}^{(0)} \right) \\ & + J^2 z^2 \lambda^2 \Psi^{*2} \Psi^2 \left[E_{n+1}^{(0)} E_{n+2}^{(0)} + E_{n-1}^{(0)} \left(E_{n+1}^{(0)} + E_{n+2}^{(0)} \right) + E_n^{(0)} \left(E_{n+1}^{(0)} + E_{n+2}^{(0)} + E_{n-1}^{(0)} \right) \right] \\ & - E_n^3 \left(E_n^{(0)} + E_{n+1}^{(0)} + E_{n+2}^{(0)} + E_{n-1}^{(0)} + 4 J z \lambda \Psi^* \Psi \right) + E_n^2 \left\{ E_n^{(0)} E_{n+1}^{(0)} + E_n^{(0)} E_{n+2}^{(0)} + E_{n+1}^{(0)} E_{n+2}^{(0)} \right. \\ & + E_n^{(0)} E_{n-1}^{(0)} + E_{n+1}^{(0)} E_{n-1}^{(0)} + E_{n+2}^{(0)} E_{n-1}^{(0)} + 3 J z \lambda \Psi^* \Psi \left[E_n^{(0)} + E_{n+1}^{(0)} + E_{n+2}^{(0)} + E_{n-1}^{(0)} - J z \lambda (n+1) \right] \\ & \left. + 6 J^2 z^2 \lambda^2 \Psi^{*2} \Psi^2 \right\} = 0 , \end{aligned} \tag{7.17}$$

which corresponds to (7.4). Both the condensate density $\Psi^* \Psi$ and the perturbed ground-state energy E_n are determined by solving (7.16) and (7.17) iteratively. The same procedure can be

done while taking λ into account up to other orders than just 2. For the plots FIG. 7.2–7.4, we set $\mu = Un + \varepsilon$, $\lambda = 1$ and $n = 1$. Between two points is always the distance $\frac{\varepsilon}{U} = 0.005$. The graphs for the condensate density have always a maximum at $\frac{\varepsilon}{U} > 0$, and they always go from the phase boundary of the Mott lobe with $n = 1$ up to the phase boundary of the Mott lobe with $n = 2$. Note that these different values for n are already taken into account by the structure of the matrix, therefore we evaluate the whole matrix with the numerical value $n = 1$, but get the physical result for the right half of the Mott lobe $n = 1$ and for the left half of the Mott lobe $n = 2$.
FIG. 7.2 shows for different plots of the condensate density $\Psi^*\Psi$ over $\frac{\varepsilon}{U}$. It is depicted in a graphical way that the results converge for higher orders in λ. This is shown numerically in TAB. 7.1. There we see that the two-state approach converges faster than the one-state approach. Furthermore, the difference of the condensate density from the two-state approach in λ^4 to λ^6 is about 0.0016%, which justifies to truncate the perturbative series at fourth order in λ.
In FIG. 7.3 the ground-state energy E_n is depicted against $\frac{\varepsilon}{U}$, but only for the superfluid regions between the Mott-lobes. Since this region is more shallow for small values of $\frac{Jz}{U}$, the energy plot is shorter for these values. The energy E_n decreases with increasing $\frac{\varepsilon}{U}$.
FIG. 7.4 illustrates the condensate density $\Psi^*\Psi$ over $\frac{\varepsilon}{U}$ for 20 different values of $\frac{Jz}{U}$. For $\frac{Jz}{U} = 0$, we get the black point at $\Psi^*\Psi = 0.5$. For $\frac{Jz}{U} = 0.01$ (pink) up to $\frac{Jz}{U} = 0.09$ (purple) we get an approximately parabola shaped graph. For $\frac{Jz}{U} = 5-2\sqrt{6} \approx 0.101$ (blue), we hit the second Mott lobe at its tip, and the graph touches the $\frac{\varepsilon}{U}$-axis in just one point for positive $\frac{\varepsilon}{U}$. For $\frac{Jz}{U} = 0.11$ (pink) up to $\frac{Jz}{U} = 0.16$, the part of the graph with positive $\frac{\varepsilon}{U}$ has still a minimum, while the negative parts intersect the $\frac{\varepsilon}{U}$-axis. For $\frac{Jz}{U} = 3 - 2\sqrt{2} \approx 0.172$ (orange), which is the tip of the first lobe, the part for negative $\frac{\varepsilon}{U}$ touches the $\frac{\varepsilon}{U}$-axis. For $\frac{Jz}{U} = 0.18$ (red) up to $\frac{Jz}{U} = 0.20$ (blue), which is just in the superfluid phase without touching any phase boundary, the whole graph is monotonically increasing. Note that this is a representation of the condensate density $\Psi^*\Psi$ which gives a non-zero, continuous result at the degeneracy, which was neither obtained by the Rayleigh-Schrödinger perturbation theory (see FIG. 2.3) [23] nor by the Brillouin-Wigner one-state approach (see FIG. 7.1) [24]. Therefore, for all future calculations, the condensate density out of the Brillouin-Wigner two-state matrix approach should be used.

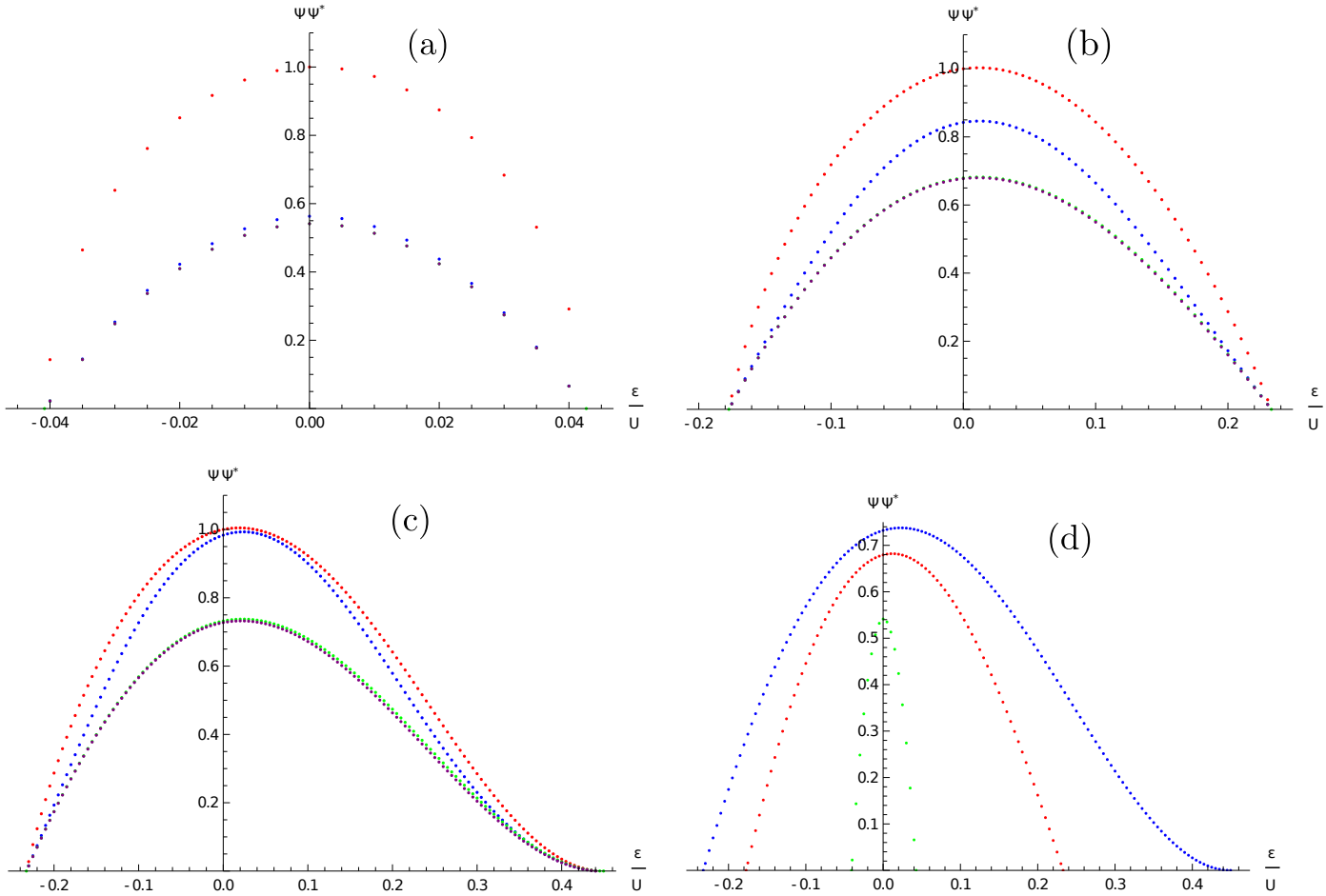

FIG. 7.2: Condensate density $\Psi\Psi^*$ as a function of $\frac{\varepsilon}{U}$ for $\frac{Jz}{U} = 0.02$ (a), $\frac{Jz}{U} = 0.08$ (b), and $\frac{Jz}{U} = 0.101$ (c) up to the order λ (red), λ^2 (blue), λ^3 (green), and λ^4 (purple). For small values of $\frac{Jz}{U}$ and thus close to the degeneracy, like in (a), the green and purple dots coincide. The three purple plots from (a)–(d) are depicted in (d), thus all 3 plots are up to λ^4 with $\frac{Jz}{U} = 0.02$ (green), $\frac{Jz}{U} = 0.08$ (red) and $\frac{Jz}{U} = 5 - 2\sqrt{6} \approx 0.101$ (blue), where at the latter case the second lobe hits exactly its tip.

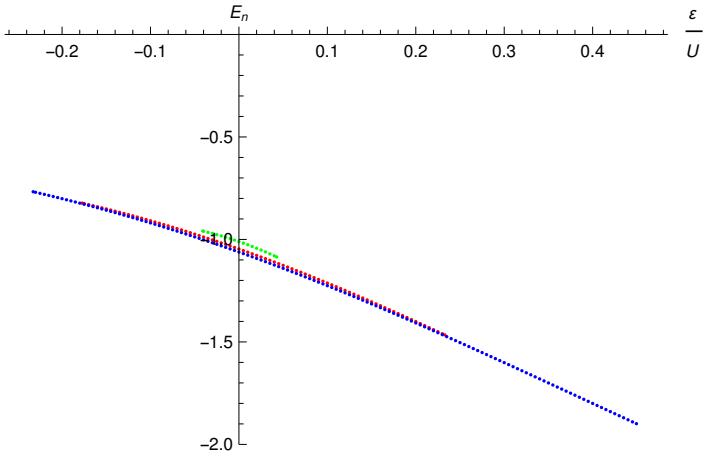

FIG. 7.3: Perturbed ground-state energies E_n up to λ^4 between the Mott lobes for different values of $\frac{Jz}{U}$: $\frac{Jz}{U} = 0.02$ (green), $\frac{Jz}{U} = 0.08$ (red) and $\frac{Jz}{U} = 5 - 2\sqrt{6} \approx 0.101$ (blue). At $\frac{Jz}{U} = 5 - 2\sqrt{6}$ the second lobe hits exactly its tip.

		Powers in λ		
		λ^2	λ^4	λ^6
One-State Approach	$\frac{E_1}{U}$	-1.0108081	-1.0102528	-1.0090297
	$\Psi^*\Psi$	0.19862639	0.24896610	0.25601384
Two-State Approach	$\frac{E_2}{U}$	-1.0100015	-1.0104087	-1.0104088
	$\Psi^*\Psi$	0.56303521	0.54132128	0.54131277

Table 7.1: Values for ground-state energy E_n and condensate density $\Psi^*\Psi$ at the degeneracy, i. e. $\mu = Un + \varepsilon$, $\varepsilon = 0$, $\lambda = 1$ and $\frac{Jz}{U} = 0.02$. The first two rows are obtained through the one-state approach, while the last two rows originate from the two-state matrix approach. Columns give values for formulas evaluated up to second, fourth, and sixth order in λ.

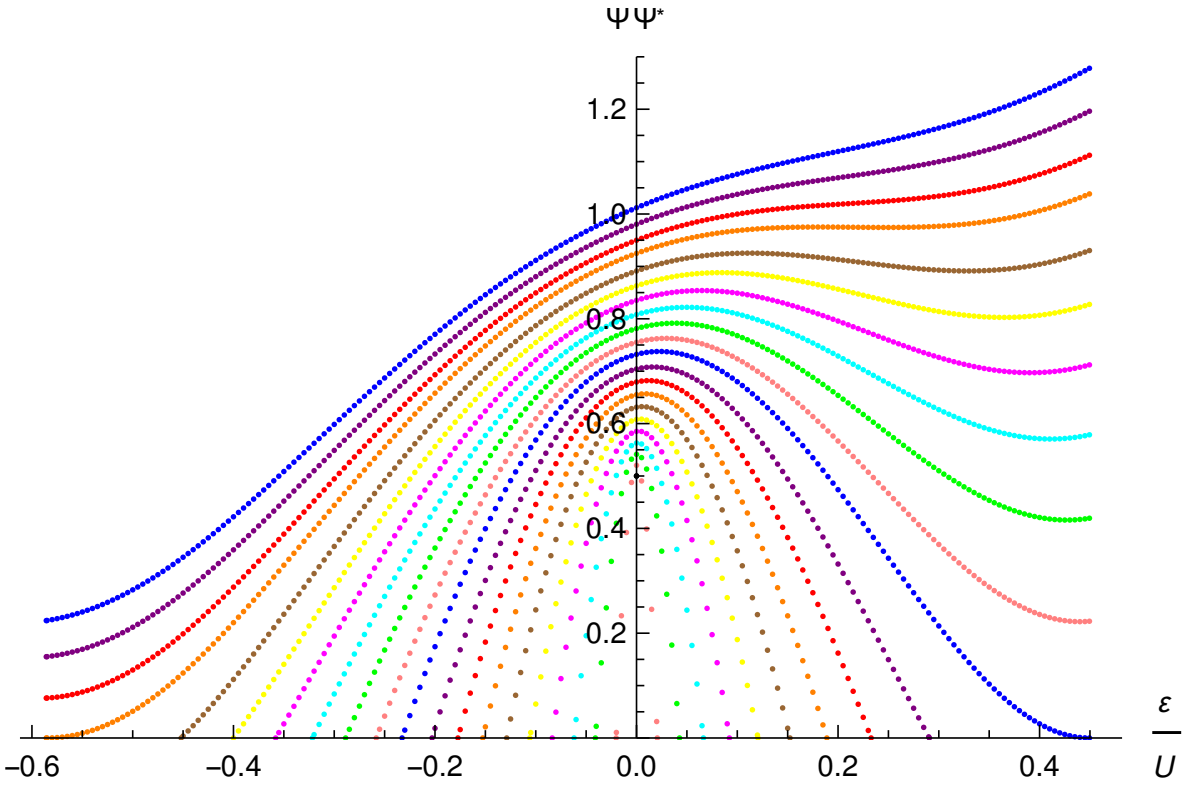

FIG. 7.4: Condensate density $\Psi^*\Psi$ up to λ^4 between the Mott lobes for different values of $\frac{Jz}{U}$, between $\frac{Jz}{U} = 0$ and $\frac{Jz}{U} = 0.20$ with a step size of 0.01 for $\frac{Jz}{U}$.

8 Conclusion and Outlook

This diploma thesis deals with the problem how to determine the condensate density for a homogeneous Bose gas in an optical lattice within mean-field theory. As in the vicinity of the mean-field phase boundary the condensate density is supposedly small, the standard approach starts with the mean-field Hamiltonian (2.19) and determines the ground-state-energy with non-degenerate perturbation theory [23]. However, the resulting Landau expansion (2.30) yields a condensate density, which turns out to vanish between two adjacent Mott lobes according to FIG. 2.3 and has, therefore, to be considered as unphysical. The origin for this unphysical result stems from the fact that between adjacent Mott lobes, i. e. at $\mu = Un$, a degeneracy occurs, so that there the non-degenerate perturbation theory is no longer valid. This deficiency was recognized, for instance, in Ref. [24] and solved tentatively by determining the condensate density with degenerate perturbation theory. Although this allowed to obtain a non-vanishing condensate density between two adjacent Mott lobes, the result is inconsistent insofar as the condensate density does not vanish at the mean-field phase boundary. Thus, the fundamental problem remained how to combine the results from non-degenerate [23] and degenerate [24] perturbation theory in order to obtain a consistent mean-field result for the condensate density.
The present diploma thesis solves this problem by using the Brillouin-Wigner perturbation theory [33]. It is based on a projector formalism, which allows to eliminate a larger fraction of the Hilbert space in order to obtain an effective eigenvalue problem for the remaining smaller subspace. The resulting effective Hamiltonian (3.36) can then be systematically expanded in a power series of the perturbation. In this way it turns out that the Brillouin-Wigner perturbation theory formally interpolates between the non-degenerate and the degenerate perturbation theory, see section 3.4. In the context of the Bose-Hubbard mean-field theory, chapter 4 shows that the results of Ref. [23] are reproduced by evaluating the effective Hamiltonian (3.36) up to fourth order in the one-state approach, whereas the results of Ref. [24] follow from restricting the effective Hamiltonian (3.36) to first order in the two-state approach. In chapter 7, however, we even demonstrate that evaluating the effective Hamiltonian (3.36) systematically to higher perturbative orders in the two-state approach yields fast converging results for the mean-field condensate density, see TAB. 7.1. In addition, the fourth perturbative order FIG. 7.4 shows a consistent mean-field condensate density as it vanishes at the mean-field phase boundary.
This new availability of the condensate density, above the mean-field phase boundary of FIG. 2.1 offers various possibilities of further insights into the physics of bosons in an optical lattice. For instance, in an experiment an additional harmonic trapping potential occurs, which gives rise to a wedding-cake like structure for the particle density [18, 34, 35]. In order to understand this theoretically, the Bose-Hubbard Hamiltonian has to be extended with such a harmonic confinement, making the chemical potential local within the Thomas-Fermi approximation. Although an initial crude calculation was performed for vanishing hopping $J = 0$ in Refs. [23, 24], the results of this diploma thesis allow to tackle the generic case of finite hopping. But in view of analyzing experimental results quantitatively, also the temperature has to be implemented into the calculation [23, 36]. Since both a finite temperature and the harmonic trapping potential

have the tendency to smoothen the Mott-lobes within the wedding-cake like density distribution, one needs to take both effects into consideration. In principle it should be possible to deduce the temperature from the experimentally observed smoothness of the density distribution. Thus, the implementation of temperature in addition to the confining trap would provide experimentalists with the required theory in order to establish a thermometer for bosons in optical lattices.
Another well-known problem is the quantitative inaccuracy of the mean-field approximation. For instance, the mean-field phase boundary differs from the result of extensive Quantum Monte-Carlo simulations up to 25% in three dimensions [37]. This discrepancy can be reduced by extending the mean-field theory to a full Landau theory according to Refs. [16, 28]. A systematic hopping expansion of the Landau theory allows to calculate the phase boundary to an accuracy which is comparable to the Quantum-Monte Carlo results [38, 39, 40, 41, 42]. The accuracy is so high that it is even possible to determine critical exponents from the hopping expansions [43]. Therefore, it is plausible to predict that also the condensate density could be calculated with a similar accuracy by applying the Brillouin-Wigner perturbation theory to this Landau theory.

9 Acknowledgement

First of all I want to thank Prof. Dr. Sebastian Eggert for giving me the possibility to do my diploma thesis in the group "theory of condensed matter and many body systems" although I did my studies in biophysics. Furthermore, I want to thank Prof. Dr. Michael Fleischhauer for being the second reviewer of my thesis.
In addition, I want to show my gratitude towards Priv. Doz. Dr. Axel Pelster for all the support and patience over the years, for all the scientific discussions, and all the numerous corrections which made it into this thesis. Without him, this thesis would not be the way it is now, and neither would I have seen the world during my studies.
In good memory I will keep the team of Prof. Dr. Antun Balaz from the institute of physics in Belgrade, as well as Prof Dr. Francisco Ednilson Alves dos Santos from the universidade federal de São Carlos in Brazil.
The following people should not go unmentioned, as they contributed to the daily life at the university: Denis Morath and Dominik Straßel for vital assistance with Latex and Mathematica. Kevin Jägering to help me with all the small and large questions arising in the daily life of a physicist. And last but not least, Martin Bonkhoff who went with me through all the ups and downs of being a student.
Finally, I want to thank for all the backup from the people outside of university: My mother and my father, my sister and her boyfriend, and my friends.

Bibliography

[1] A. Trabesinger, "Quantum simulation," *Nature Physics* **8**, 263, 2012.

[2] R. P. Feynman, "Simulating physics with computers," *International Journal of Theoretical Physics* **21**, 486, 1982.

[3] J. Klaers, J. Schmitt, F. Vewinger, and M. Weitz, "Bose–Einstein condensation of photons in an optical microcavity," *Nature* **468**, 545, 2010.

[4] W. Ketterle, "Nobel lecture: When atoms behave as waves: Bose-Einstein condensation and the atom laser," *Reviews of Modern Physics* **74**, 1131, 2002.

[5] A. Einstein, "Quantentheorie des einatomigen idealen Gases (Zweite Abhandlung)," *Sitzungsberichte der preussischen Akademie der Wissenschaften* **I**, 1925.

[6] S. N. Bose, "Plancks Gesetz und Lichtquantenhypothese," *Zeitschrift für Physik* **26**, 178, 1924.

[7] M. H. Anderson, J. R. Ensher, M. R. Matthews, C. E. Wieman, and E. A. Cornell, "Observation of Bose-Einstein Condensation in a Dilute Atomic Vapor," *Science* **269**, 198, 1995.

[8] K. B. Davis, M. O. Mewes, M. R. Andrews, N. J. van Druten, D. S. Durfee, D. M. Kurn, and W. Ketterle, "Bose-Einstein Condensation in a Gas of Sodium Atoms," *Physical Review Letters* **75**, 3969, 1995.

[9] S. Chu, L. Hollberg, J. E. Bjorkholm, A. Cable, and A. Ashkin, "Three-dimensional viscous confinement and cooling of atoms by resonance radiation pressure," *Physical Review Letters* **55**, 48, 1985.

[10] C. N. Cohen-Tannoudji and W. D. Phillips, "New Mechanisms for Laser Cooling," *Physics Today* **43**, 33, 1990.

[11] S. Stellmer, B. Pasquiou, R. Grimm, and F. Schreck, "Laser cooling to quantum degeneracy," *Physical Review Letters* **110**, 263003, 2013.

[12] L. Pitaevskii and S. Stringari, *Bose-Einstein Condensation and Superfluidity.* Second Edition, University Press, Oxford, 2016.

[13] A. Ashkin, J. M. Dziedzic, J. E. Bjorkholm, and S. Chu, "Observation of a single-beam gradient force optical trap for dielectric particles," *Optics Letters* **11**, 288, 1986.

[14] C. Becker, P. Soltan-Panahi, J. Kronjäger, S. Dörscher, K. Bongs, and K. Sengstock, "Ul-

tracold quantum gases in triangular optical lattices," *New Journal of Physics* **12**, 065025, 2010.

[15] J. Gyu-Boong, J. Guzman, C. K. Thomas, P. Hosur, A. Vishwanath, and D. M. Stamper-Kurn, "Ultracold atoms in a tunable optical kagome lattice," *Physical Review Letters* **108**, 045305, 2012.

[16] F. E. A. dos Santos, "Ginzburg-Landau Theory for Bosonic Gases in Optical Lattices", dissertation, Freie Universität Berlin, Germany, 2011, http://users.physik.fu-berlin.de/∼pelster/Theses/santos.pdf.

[17] V. G. Ivancevic and T. T. Ivancevic, *Complex Nonlinearity - Chaos, Phase Transitions, Topology Change and Path Integrals.* Springer, Berlin, 2008.

[18] F. Gerbier, A. Widera, S. Fölling, O. Mandel, T. Gericke, and I. Bloch, "Phase coherence of an atomic mott insulatore," *Physical Review Letters* **95**, 050404, 2005.

[19] W. Heisenberg, "Über den anschaulichen Inhalt der quantentheoretischen Kinematik und Mechanik," *Zeitschrift für Physik* **17**, 1927.

[20] J. Zinn-Justin, *Quantum Field Theory and Critical Phenomena.* Fourth Edition, Clarendon Press, Oxford, 2002.

[21] H. Kleinert and V. Schulte-Frohlinde, *Critical Properties of* Φ^4*-Theories.* World Scientific, Singapore, 2001.

[22] S. Sachdev, *Quantum Phase Transitions.* Second Edition, Cambridge University Press, Cambridge, 2011.

[23] A. Hoffmann, "Bosonen im optischen Gitter", diploma thesis, Freie Universität Berlin, Germany, 2007, http://www.physik.fu-berlin.de/∼pelster/Theses/hoffmann.pdf.

[24] K. Mitra, C. J. Williams, and C. A. R. Sá de Melo, "Superfluid and Mott-insulating shells of bosons in harmonically confined optical lattices," *Physical Review A* **77**, 033607, 2008.

[25] H. A. Gersch and G. C. Knollman, "Quantum cell model for bosons," *Physical Review Letters* **129**, 959, 1963.

[26] J. Hubbard, "Electron correlations in narrow energy bands," *Proceedings of the Royal Society* **276**, 238, 1963.

[27] L. D. Landau and E. M. Lifschitz, *Lehrbuch der theoretischen Physik V, Statistische Physik, Teil 1.* Verlag Harri Deutsch, 1991.

[28] F. E. A. dos Santos and A. Pelster, "Quantum phase diagram of bosons in optical lattices," *Physical Review A* **79**, 013614, 2009.

[29] W. Nolting, *Grundkurs theoretische Physik 5/2 Quantenmechanik - Methoden und Anwendungen.* Springer, Berlin, 2012.

[30] M. P. A. Fisher, P. B. Weichman, G. Grinstein, and D. S. Fisher, "Boson localization and the superfluid-insulator transition," *Physical Review B* **40**, 546, 1989.

[31] H. Kleinert, *Path Integrals in Quantum Mechanics, Statistics, Polymer Physics, and Financial Markets*. 5th Edition, World Scientific, Singapore, 2009.

[32] https://en.wikipedia.org/wiki/Perturbation_theory_(quantum_mechanics).

[33] I. Hubač and S. Wilson, *Brillouin-Wigner Methods for Many-Body Systems*. Springer, Berlin, 2010.

[34] S. Fölling, A. Widera, T. Müller, F. Gerbier, and I. Bloch, "Formation of Spatial Shell Structure in the Superfluid to Mott Insulator Transition," *Physical Review Letters* **97**, 060403, 2006.

[35] F. Gerbier, A. Widera, S. Fölling, O. Mandel, T. Gericke, and I. Bloch, "Interference pattern and visibility of a Mott insulator," *Physical Review A* **72**, 053606.

[36] F. Gerbier, "Boson Mott Insulators at Finite Temperatures," *Physical Review Letters* **99**, 120405, 2007.

[37] B. Capogrosso-Sansone, N. V. Prokof'ev, and B. V. Svistunov, "Phase diagram and thermodynamics of the three-dimensional Bose-Hubbard model," *Physical Review B* **75**, 134302, 2007.

[38] A. Eckardt, "Process-chain approach to high-order perturbation calculus for quantum lattice models," *Physical Review B* **79**, 195131, 2009.

[39] N. Teichmann, D. Hinrichs, and M. Holthaus, "Process-chain approach to the Bose-Hubbard model: Ground-state properties and phase diagram," *Physical Review B* **79**, 224515, 2009.

[40] N. Teichmann, D. Hinrichs, and M. Holthaus, "Bose-Hubbard phase diagram with arbitrary integer filling," *Physical Review B* **79**, 100503, 2009.

[41] N. Teichmann and D. Hinrichs, "Scaling property of the critical hopping parameters for the Bose-Hubbard model," *European Physical Journal B* **71**, 219, 2009.

[42] N. Teichmann, D. Hinrichs, and M. Holthaus, "Reference data for phase diagrams of triangular and hexagonal bosonic lattices," *Europhysics Letters* **91**, 10004, 2010.

[43] D. Hinrichs, A. Pelster, and M. Holthaus, "Perturbative calculation of critical exponents for the Bose–Hubbard model," *Applied Physics B* 113, 57, 2013.

Name: Martin Kübler Datum: 04. 10. 2016

Erklärung gem. § 16 Abs. 7 Diplomsprüfungsordnung (DPO) Biophysik

Die Diplomarbeit mit dem Thema
Improving Mean Field Theory for Bosons in Optical Lattices via Degenerate Perturbation Theory
abgegeben am 30. 09. 2016 wurde am 03. 01. 2016
von Herrn Prof. Dr. Sebastian Eggert an mich ausgegeben und betreut.

Ich versichere, dass ich die Arbeit selbstständig verfasst und keine anderen als die angegebenen Quellen und Hilfsmittel benutzt habe.

Zum zweiten Gutachter gem. § 17 Abs. 2 DPO bitte ich
Herrn Prof. Dr. Michael Fleischhauer zu bestimmen.

Unterschrift: